2020

Reconstructing Hydrologic Conditions and Metals Supplied by the Peace River to the Peace-Athabasca Delta

Jelle André Faber
fabe1950@mylaurier.ca

RECONSTRUCTING HYDROLOGIC CONDITIONS AND METALS SUPPLIED BY THE PEACE RIVER TO THE PEACE-ATHABASCA DELTA

by

Jelle André Faber

BA Geography, Wilfrid Laurier University, 2016

THESIS

Submitted to the Department of Geography and Environmental Studies

in partial fulfilment of the requirements for

Master of Science in Geography

Wilfrid Laurier University

Abstract

The Peace-Athabasca Delta (PAD) in northern Alberta, Canada, is recognized internationally for its ecological, historical, and cultural significance. The delta is mostly within Wood Buffalo National Park, a UNESCO World Heritage Site, and is a Ramsar Wetland of International Importance. The construction of the WAC Bennett Dam (1967) and the Site C Dam (ongoing, 2024) on the Peace River, and expansion of the Alberta Oil Sands industry along the Athabasca River have raised concerns over water quantity and quality in the delta. When industry operations began, effective monitoring had not been implemented. Consequently, pre-industrial reference conditions are unknown and can be difficult to define. Paleolimnological techniques provide means to assess current environmental conditions of the PAD in the context of a pre-industrial baseline. Research focuses on lakes very near to the Peace River to reconstruct past hydrological conditions and to characterize sediment metal deposition derived from Peace River floodwaters.

Results from sediment core analysis at lakes 'PAD 65' and 'PAD 52' show that organic matter content and $\delta^{13}C_{org}$ increase while C/N ratios decrease after 1970, suggesting a decrease in flood frequency. The timing of this stratigraphic shift aligns with changes in the Peace River hydrograph caused by river regulation as a result of the construction of the Bennett Dam. Notably, these are the first lakes (of >30 in the PAD) with paleolimnological evidence to attribute hydroecological change in the PAD to the Bennett Dam, which suggests these effects are evident in very close proximity to the Peace River. These two lakes lie in regions and perhaps at elevations that are highly sensitive to changes in the Peace River hydrograph that have occurred during the open-water season. Other lake sediment stratigraphic records examined in this study from the northern part of the PAD, and just downstream along the Slave River, show drying trends since the early twentieth century, likely due to climate change, consistent with previously published paleolimnological records. Sediment metal concentrations were analyzed at two lakes in the Peace River sector of the PAD, lakes 'PAD 65' and 'PAD 67', where metal-normalizer

relationships and enrichment factors show no evidence of anthropogenic influence, although post-1920 metals at PAD 67, especially cadmium, copper, nickel, and zinc, did have an enrichment factor of up to 1.4. However, these concentrations fall below the minimum threshold of influence of 1.5 (Birch 2017) and are closely correlated with percent organic matter. This suggests the influence of metals scavenging by primary producers, as aquatic productivity increased. These findings will be of interest to multiple stakeholders, and will inform stewardship and lake ecosystem monitoring of the delta.

Acknowledgements

My experiences as part of the Wolfe/Hall lab have been very positive. Many thanks especially, first and foremost, to my supervisors, Dr. Brent Wolfe and Dr. Roland Hall. I am eternally grateful for your instruction, guidance, encouragement, and patience throughout the years. You have given me many incredible opportunities, more than I imagined when this project began. I am sure that what I have learned from you will be very valuable in the years ahead.

Many thanks to my friends and colleagues in the Wolfe/Hall lab group. It has been wonderful to see this group grow through the years. Thanks to my colleagues at the beginning, Casey Remmer, Mitchell Kay, and Wynona Klemt at UW, and James Telford and eventually Tanner Owca at Laurier. I look back fondly at these first months/years, when we spent many days in the field, in the lab, and in the office. Thanks for working alongside me over the years, being so hard-working, dedicated, and passionate about your research. This applies also to the current members of the Wolfe/Hall lab. Thank you all, too, for your friendliness. I have received many comments throughout the years noting how close our group is, despite the competitive nature of academia! Thank you for making my time in this lab so enjoyable. You make it hard to leave!

Many thanks to the post-doctoral fellows of the lab group, especially to Research Associate Dr. Johan Wiklund, who have all been very helpful. Johan, your extensive knowledge and expertise of specialty topics, and your scientific curiosity, make you very much appreciated as part of our lab. We've had some excellent conversations over the years, and I hope we might work together again someday.

Thanks to my fellow grad students in the office at Laurier, especially Jeremy, Catherine, Kaitlin, Rachel, Jordyn, and Mackenzie, for helping me stay on task or providing emotional relief… It has been a pleasure getting to know you all, and I am sure we will stay in touch!

Thanks also to my long-time friend, Garnet van Weerden. You have encouraged me to pursue my research and stay focussed, but also provided many opportunities for relaxation. This is what a good friend should do!

A special thanks to my family. Dad and Mom, your support and encouragement through the years has been very much appreciated, even if I didn't always show it. You are both examples of who I strive to be. Thanks to my siblings, as well: my brother Jakob and his wife Ruth, and my sister Christine. Thank you for always believing in me, and for being excited about what I do. I'm sure I wouldn't have made it to this point without you all!

I would also like to acknowledge the sources of financial support for this project. Thanks to the Northern Scientific Training Program, NSERC, and the Polar Continental Shelf Program. Without the funding for this project, none of this would have been possible.

Contents

List of Figures:

List of Tables:

Chapter 1: Introduction

The Peace-Athabasca Delta (PAD), located in northern Alberta, Canada, is one of the world's largest inland freshwater deltas (Timoney 2013). Two of Canada's largest rivers, the Peace and the Athabasca, create a vast deltaic landscape adjacent to Lake Athabasca. This landscape, containing hundreds of shallow lakes, provides fertile soil and a seemingly endless supply of water, creating a unique habitat for an abundance of biota. The delta consists of boreal forest, muskeg, and shallow lakes that are a valuable source of clean water and support a vast trophic network, which the local First Nation communities have depended upon for generations (Peace-Athabasca Delta Ecological Monitoring Program; Athabasca Chipewyan First Nation 2003; Timoney 2013; Mikisew Cree First Nation 2014; WHC/IUCN 2017). The wetland habitat draws large numbers of waterfowl to the region, including the endangered Whooping Crane (WBNP 2016). The highly productive environment provides a significant source of food and income for members of the local community. Large and small mammals, such as Wood Bison and Western Moose, provide a source of food, while fur-bearing beaver and muskrat provide a source of income. To publicly recognize the ecological, historical, and cultural significance of the region, the delta is protected within Canada's largest national park, Wood Buffalo National Park (WBNP) (44 741 km^2, greater in area than The Netherlands). Internationally, the park is recognized by UNESCO (World Heritage Site #256, inscribed in 1983), and the delta is a Ramsar Wetland of International Importance (Site #241, designated in 1982).

Environmental Stressors

The Peace-Athabasca Delta is threatened by two industries: pollution from the refinement of bituminous oil sands and river regulation for the generation of hydroelectricity. Canada's bitumen is mainly refined in the region of the Athabasca Oil Sands, one of the largest deposits in the world, located along the Athabasca River, which flows from the Columbia Icefield to the Athabasca Delta where it enters Lake Athabasca. The Alberta Oil Sands Region is several hundred kilometres upstream of the PAD.

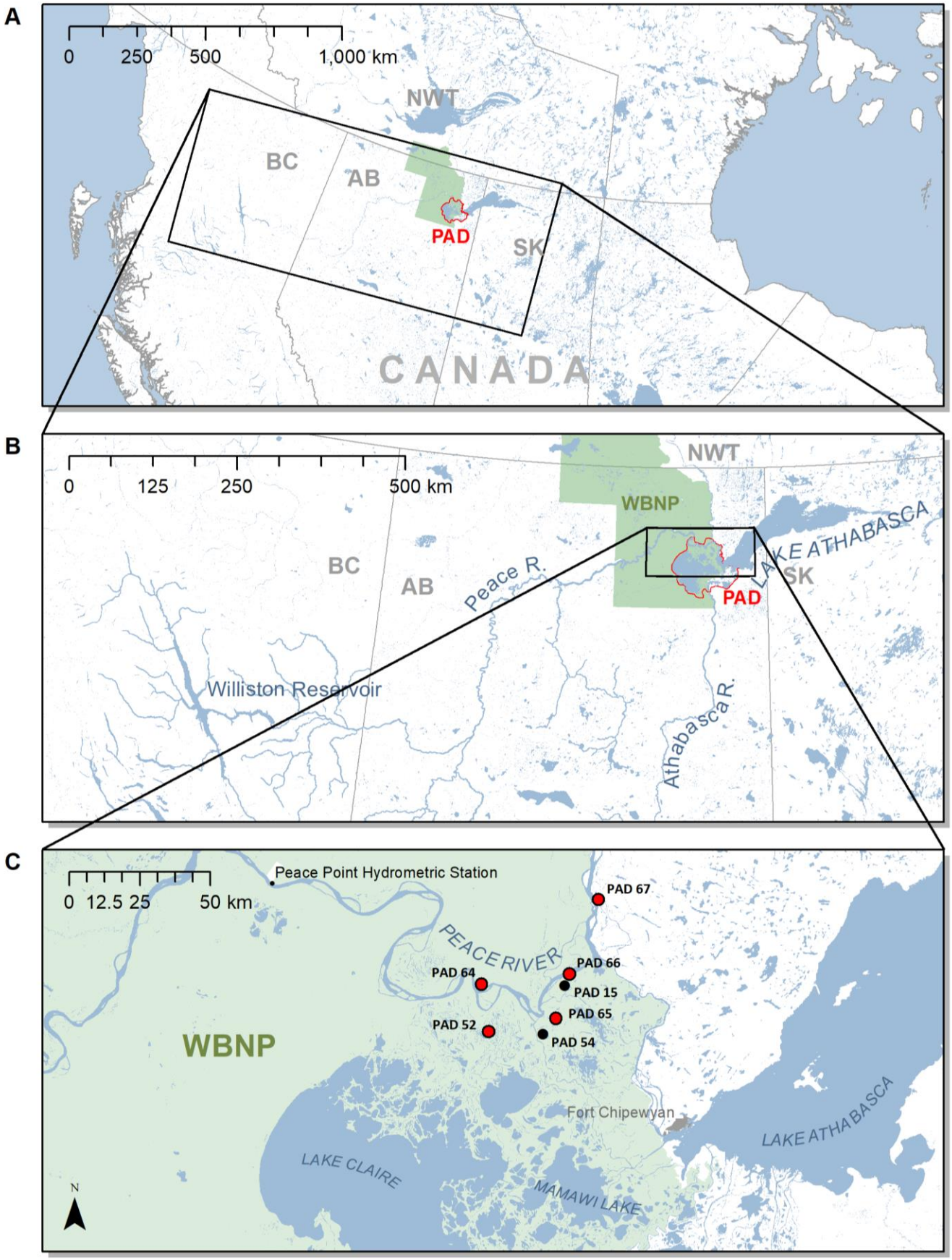

Figure 1: The location of the Peace-Athabasca Delta, and significant landforms and points of interest.

The hydroelectric power industry in the west also threatens the delta, including the W.A.C. Bennett Dam (constructed in the late 1960s; Beltaos 2018a) and the current development of the Site C Hydroelectric Dam. Both dams are located on the Peace River, which flows from the northern Rocky Mountains into the Slave River, near Lake Athabasca, where it forms the Peace Delta (54).

During the past century, the oil sands and hydroelectricity industries have grown significantly. As these industries have been developing, there has been increasing concern regarding their effects on the hydrology and contaminants in downstream ecosystems, and the lack of monitoring and poor management in the region (Mikisew Cree First Nation 2014; Cronmiller & Noble 2018; Parks Canada 2019). Observed changes in water quality and the drying of lakes in the delta have, consequently, been a source of concern for local stakeholders (Mikisew Cree First Nation 2014).

Developing an Understanding of Flooding and Contaminant Deposition in Lakes of the PAD

Over the course of the 50 years since the construction of the Bennett Dam, a significant amount of peer-reviewed research has been conducted to address these concerns of water quality and quantity. Both government-funded projects and university-based researchers have worked to better understand the mechanisms at play in the PAD and to characterize the reference conditions, conditions that represent the water and sediment quality of the PAD before the potential effects of the oil sands industry. The following pages summarize the journey followed by researchers to better understand A) the mechanisms and frequency of flooding of the Peace Delta, and B) the deposition of contaminants in the Peace-Athabasca Delta.

A) Mechanisms and frequency of flooding of the Peace River Delta

The Peace River bypasses the delta and forms the Slave River at its confluence with the Rivière des Rochers. The Peace Delta is a relict delta – flooding occurs less frequently than in the active Athabasca Delta. Much research has sought to understand the mechanisms and frequency of flooding of

the Peace and Athabasca sectors of the delta, and how these mechanisms, and therefore flood frequency, are affected by the WAC Bennett Dam regulation of the Peace River (Peace-Athabasca Delta Project Group 1973; Peace-Athabasca Delta Implementation Committee 1987; Peace-Athabasca Delta Technical Studies 1996; Prowse & Lalonde 1996; Prowse & Conly 1998; Peters & Prowse 2001; Prowse et al. 2002; Timoney 2002; Wolfe et al. 2005; Peters, Prowse, Marsh, et al. 2006; Wolfe et al. 2006; Peters, Prowse, Pietroniro, et al. 2006; Wolfe et al. 2007; Wolfe et al. 2008; Wolfe et al. 2011; Wiklund, Hall, & Wolfe 2012; Wolfe et al. 2012; Beltaos 2018b; Beltaos 2018a; Timoney et al. 2018; Hall et al. 2019; Remmer et al. 2020).

Widespread flooding of perched basins in the Peace River Delta is dependent on ice-jam flood events. Researchers in the 1970s and 1980s were not aware of this (Peace-Athabasca Delta Project Group 1972; Peace-Athabasca Delta Implementation Committee 1987). Early projects to mitigate the effects of river regulation focussed on finding immediate, short-term solutions to solve the problem of low water levels in the PAD. In 1971, as part of the PAD Project Group (Peace-Athabasca Delta Project Group 1973), a temporary rockfill dam was constructed at the outlet of Mamawi Lake on the Chenal des Quatre Fourches to increase water levels of Lake Claire and Lake Mamawi. It was removed in 1975 since it disrupted the natural water regime, prevented flushing of the lakes (required to maintain water quality), and prevented fish spawning migration. Weirs were constructed on the Rivière des Rochers (1975) and the Revillon Coupé (1976) at the recommendation of the Peace-Athabasca Delta Implementation Committee (established in 1974 by the Saskatchewan, Alberta, and federal governments). They were found to restore summer peak water levels, but also raised the summer minimum water level and did not result in recharging of the perched basins (Peace-Athabasca Delta Implementation Committee 1987). Lakes that were already flood-prone were affected, but the lakes where drying was occurring were not being recharged. The failure of these projects supported the

developing knowledge that the perched basins in the PAD are flooded by ice jams in the early spring, and not simply by high lake water levels in the interior of the PAD.

The PAD Technical Studies (1993-1996, "PAD-TS") built on this knowledge and examined river ice (Peace-Athabasca Delta Technical Studies 1996). One of the major findings and recommendations was that the increased winter discharge of the Peace River (due to regulation by the W.A.C. Bennett Dam) was raising the ice levels of the river, requiring higher spring discharges to break the river ice, resulting in a decline in ice-jam floods. The study concluded that:

> The effects of regulation could be mitigated by modifying Bennett Dam operations. Maintaining increased winter releases through the breakup period would complement tributary run-off effects. However, the timing and magnitude of releases may be constrained by the risk of flooding to communities downstream of the dam. (Peace-Athabasca Delta Technical Studies 1996, p. 2)

This presents a complicated situation where river regulation protects upstream communities at the apparent cost of flood frequency and timing in the PAD. This does not even consider the supply and demand of electricity at different times of the year for BC Hydro. Consequently, the PAD-TS provided some key information regarding the mechanisms of ice-jam flooding, but did not result in any major changes in either the operations of the dam or the flood frequency of the PAD.

To support these findings, the Peace River experienced exceptionally high levels of open-water river discharge in 1990, the highest since 1962, with more than twice as much discharge as the previous record in 1964 (Prowse & Conly, 1998; Figure 2). However, since this was an open-water event in absence of ice jams, this extreme discharge did not recharge the perched basins in the Peace sector. This suggests that "the other obvious source of potential flooding is that produced by ice-jam backwater" (Prowse & Lalonde 1996, p. 92). Evidently, high rates of open-water flow, whether natural or from the Bennett Dam, do not recharge the perched basins in the PAD.

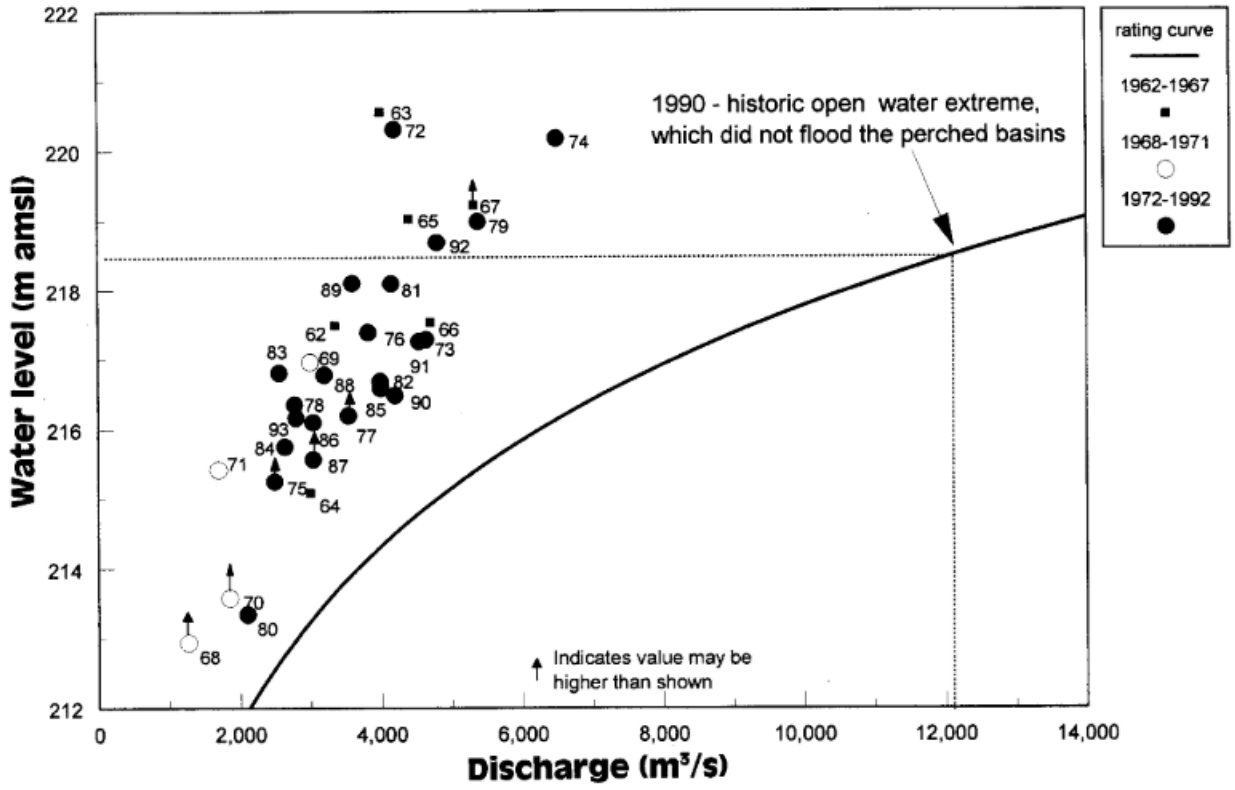

Figure 2: Open water rating curve for Peace Point hydrometric station and peak water levels produced by ice jams. Dotted line indicates historical maximum water level achieved under open water conditions. Taken from Prowse and Conly (1998), p. 1591.

Because these perched lakes are dependent on ice-jam floods, climate has a strong impact on the likelihood and magnitude of these flood events. Changes in climate affect snow water equivalent, ice strength and thickness, ice elevation, heat flux, and number of days above freezing, which all affect the likelihood of an ice-jam flood (Prowse & Conly 1998; Prowse et al. 2002; Peters, Prowse, Marsh, et al. 2006; Peters, Prowse, Pietroniro, et al. 2006). Additionally, the floods are dependent on low ice elevation, followed by increases in spring discharge to cause ice breakup, which in turn result in ice jams (Prowse & Conly 1998; Prowse & Conly 2000; Prowse et al. 2002; Prowse et al. 2006; Beltaos et al. 2009). However, research shows that river regulation has actually increased river discharge during the narrow window of time during which ice jams occur, the spring freshet, as the dam released snowmelt water stored up during the winter (See Figure 3, below, modified from Peters & Prowse 2001, and

Beltaos & Peters 2020). Prowse and Conly (1998; 2000) concluded that apparent reduction in flood frequency was due to both river regulation and climate variability.

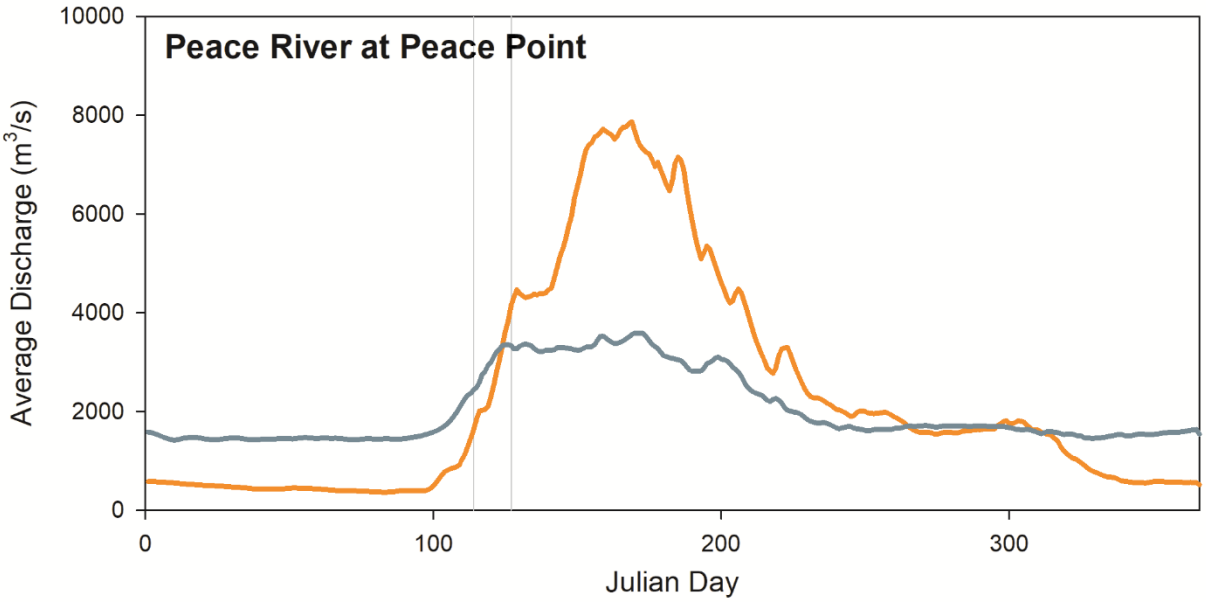

Figure 3: Average daily discharge for the Peace River at Peace Point, modified from Peters and Prowse (2001) (orange: pre-regulation 1960-1967, teal: post-regulation 1967-2019). The two-week period during which ice jam floods typically occur is indicated by grey lines – day 114 through 127, the last week of April and the first week of May. Data sourced from wateroffice.ec.gc.ca.

Further studies of lake water levels also support these findings. A study by Timoney (2002) compared the water levels of Lake Athabasca and Lesser Slave Lake. Despite differences in hydrologic influence, Timoney (2002) found that the water levels of the two lakes were both low at the time that the Williston reservoir was being filled. Lake Athabasca receives input from the Peace River during spring flood events, when river channels in the PAD can experience a reversal of flows (Bennett et al. 1973; PAD-PG 1973; Prowse & Lalonde 1996; Prowse et al. 2006; Peters et al. 2006; Jasek 2019); while Lesser Slave Lake, upstream of Lake Athabasca in the Athabasca River drainage basin, and is not influenced by the Bennett Dam. The water levels of the two lakes appear to be closely correlated, suggesting that these findings are likely due to changes in regional climate rather than solely influenced by the filling of the Williston reservoir.

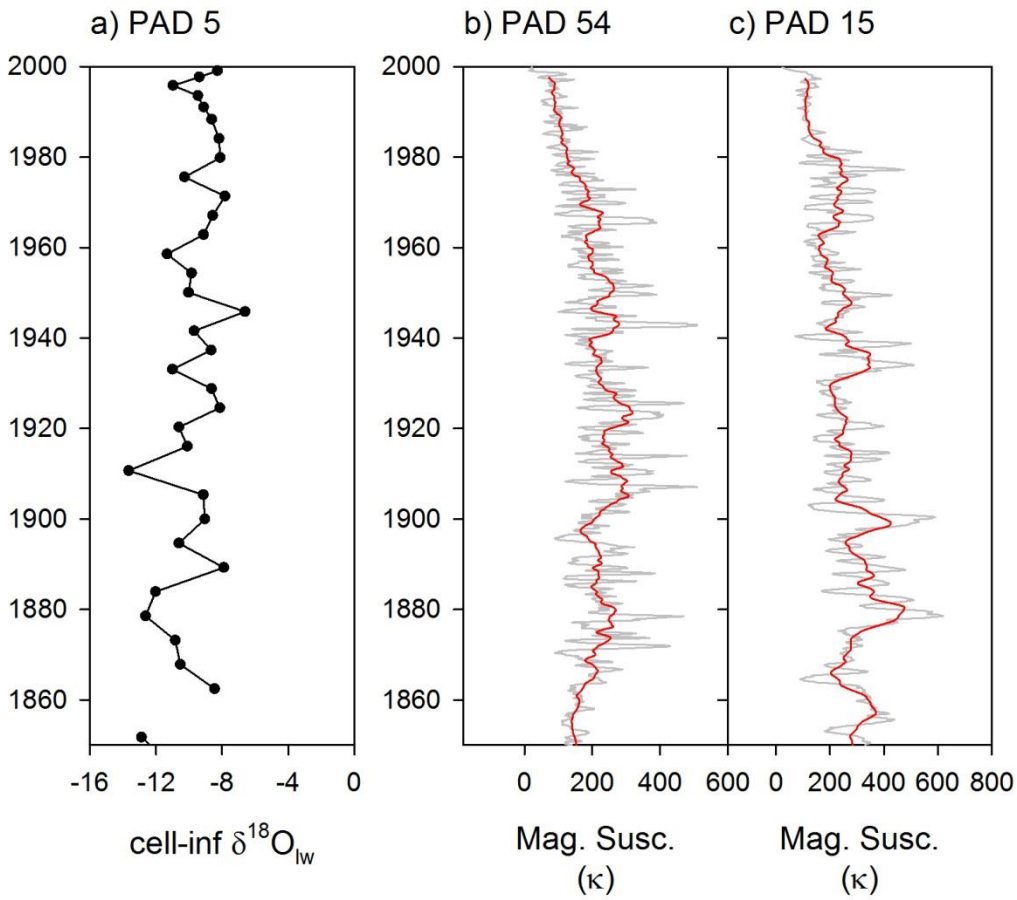

Figure 4: a) PAD 5 cellulose-inferred lakewater $\delta^{18}O$ record from Wolfe et al. (2005); b) PAD 54 and c) PAD 15 magnetic susceptibility records from Wolfe et al. (2006).

Evidence of climatic warming in the Delta is also demonstrated by dendrochronological and paleolimnological research, which shows a gradual drying trend during the past century, especially in the Peace sector, and a decrease in water levels of Lake Athabasca since the end of the Little Ice Age (Meko 2006; Edwards et al. 2008; Wolfe et al. 2008; Johnston et al. 2010; Sinnatamby et al. 2010; Wolfe et al. 2011). Lake sediment cores from the northeastern portion of the Delta have been analyzed for cellulose $\delta^{18}O$ (PAD 5, "Spruce Island"; Wolfe et al. 2005) and magnetic susceptibility (PAD 15, 54; Wolfe et al. 2006; Figure 4). At PAD 5, cellulose-inferred lakewater $\delta^{18}O$ is low in the mid-1800s, evidence of a wet period between 1780 and 1940. From 1940 to present, cellulose-inferred lakewater $\delta^{18}O$ gradually increases, indicating an increase in evaporation. At sites PAD 15 and PAD 54, there has been a gradual

decrease in magnetic susceptibility since the late 1800s and early 1900s, respectively, indicating a decrease in flood frequency. Additionally, the paleohydrologic records of PAD 15 and 54 correlate with the traditional knowledge of flood history examined by Timoney et al. (1997), as shown by Wolfe et al. (2006).

However, some of the academic community believe that the regulation of the Peace River has had a significant effect on the flood frequency of the PAD. A recent analysis of the Traditional Knowledge and historical flood frequency record compared the cumulative number of floods between 1880 and 1968 with the cumulative number of floods after 1968, and concluded that change has occurred at 1968 (Beltaos 2018a). However, Beltaos' methods of statistical analysis may not have been appropriate, given that a linear regression was used for the post-1968 data and a polynomial regression for 1880-1968 (Hall et al. 2019; Wolfe et al. 2020). Though all agree that there is drying in the PAD, there still remains controversy in the role of the extent of river regulation on recent lake drying. Thus, additional paleolimnological research in the Peace sector is warranted to further distinguish the roles of river regulation and climate change on the hydrological conditions of perched lakes.

B) Deposition of sediment contaminants in the PAD

Many studies have been conducted to assess for evidence of contamination of the PAD from the industrial activity of the Alberta Oil Sands. The airborne transport of contaminants has been shown to have little to no effect on the PAD (Kelly et al. 2010; Wiklund, Hall, Wolfe, et al. 2012), with some contaminants peaking between 1950 and 1970, corresponding with continent-wide air quality (Wiklund et al. 2014). However, the transport of contaminants to the PAD via the Athabasca River remains a concern (Kelly et al. 2009; Kelly et al. 2010; Mikisew Cree First Nation 2014), although this has recently been addressed in the comparison of contemporary and pre-industrial lake sediments (Kay et al. 2020; Owca et al. 2020). Due to a lack of monitoring in the PAD prior to and at the beginning of oil sands operations (Dowdeswell et al. 2010; Gosselin et al. 2010; Kelly et al. 2010; Cronmiller & Noble 2018),

there has been little understanding of baseline, “natural”, pre-oil-sands metals concentrations (WHC/IUCN 2017; Wrona 2017).

The perched lakes in the PAD collect river-borne sediment carried to these lakes via ice-jam floodwaters (Peterson 1995; Wolfe et al. 2006; Wiklund, Hall, Wolfe, et al. 2012; Wiklund et al. 2014). The sediment in deltaic lakes has been used as a natural archive of river sediment through time, due to the vertical accumulation of sediment from each flood event (Wiklund, Hall, Wolfe, et al. 2012; Wiklund et al. 2014; MacDonald et al. 2016). Wiklund et al. (2014) examined the concentration of metals known to be associated with oil sands activity by comparing river sediment sampled by the Regional Aquatic Monitoring Program to deltaic lake sediment dated pre-1920, to determine whether there was evidence of external, anthropogenic sources of these metals. These methods are useful in comparing pre-industrial metal concentrations to post-industrial metal concentrations to assess the input of these metals by the oil sands industry.

These methods have been applied to lakes in the Athabasca sector of the PAD along the river and at the terminus to better understand the deposition of contaminants by the Athabasca River and its role in the distribution of oil sands contaminants across the southern portion of the delta (Kay et al. 2020). These methods are now applied in this study to the Peace Sector of the PAD, where sediment cores have been collected with the aim to provide this record of baseline metal concentrations - the unaffected natural supply of metals to the PAD via the Peace River, to examine whether there has been enrichment since industrial development began (post-1920). From these studies, baseline metal-normalizer relationships have been developed for a range of lakes across the PAD. This knowledge of baseline concentrations has already been used to compare contemporary surface sediments to pre-industrial sediment, to assess for the distribution of anthropogenic contaminants across the Delta (Owca et al. 2020).

Research Objectives

As outlined in the preceding pages, prior research has utilized hydrometric records on the Peace River and historical records of flood events to attribute recent drying of lakes in the Peace-Athabasca Delta in part, or largely to, river regulation (Peace-Athabasca Delta Technical Studies 1996; Prowse & Lalonde 1996; Timoney et al. 1997; Prowse & Conly 1998; Peters & Prowse 2001; Beltaos et al. 2009; Timoney 2013; Beltaos 2018a). On the other hand, paleohydrological records from lakes in the Peace sector of the delta indicate that flood frequency (PAD 15, 54) and increased influence of evaporation on perched basins (PAD 5, 9, 12) began decades prior to river regulation as a consequence of climate change (Wolfe et al. 2005; Wolfe et al. 2006; Wolfe et al. 2008; Sinnatamby et al. 2010; Wolfe et al. 2012; Wolfe et al. 2020). Here, sediment records from a new suite of lakes located close to the Peace and Slave rivers are utilized to further assess the relative influence of river regulation and climate variability on hydrological conditions of lakes located in the Peace sector of the delta and vicinity.

Concerns regarding metal pollution in the PAD, stemming from oil sands mining, continue to persist. In this study, the same suite of lake sediment cores mentioned above are analyzed for metal concentrations to establish baseline, reference concentrations of metals supplied to the delta by the Peace River, and to explore if there is evidence of changes in lake sediment metal concentrations during the post-industry era.

Paleolimnological approaches used in this research project focus on several short lake sediment cores collected along the Peace and Slave rivers to enhance knowledge of the natural hydrological regime of the Peace River, in advance of Site C Dam operation, and to characterize the supply of metals to the Peace-Athabasca Delta via the Peace River. With accurately dated cores, the time periods at which changes are observed can provide insight to the sources and mechanisms of change within the Delta.

Study Sites

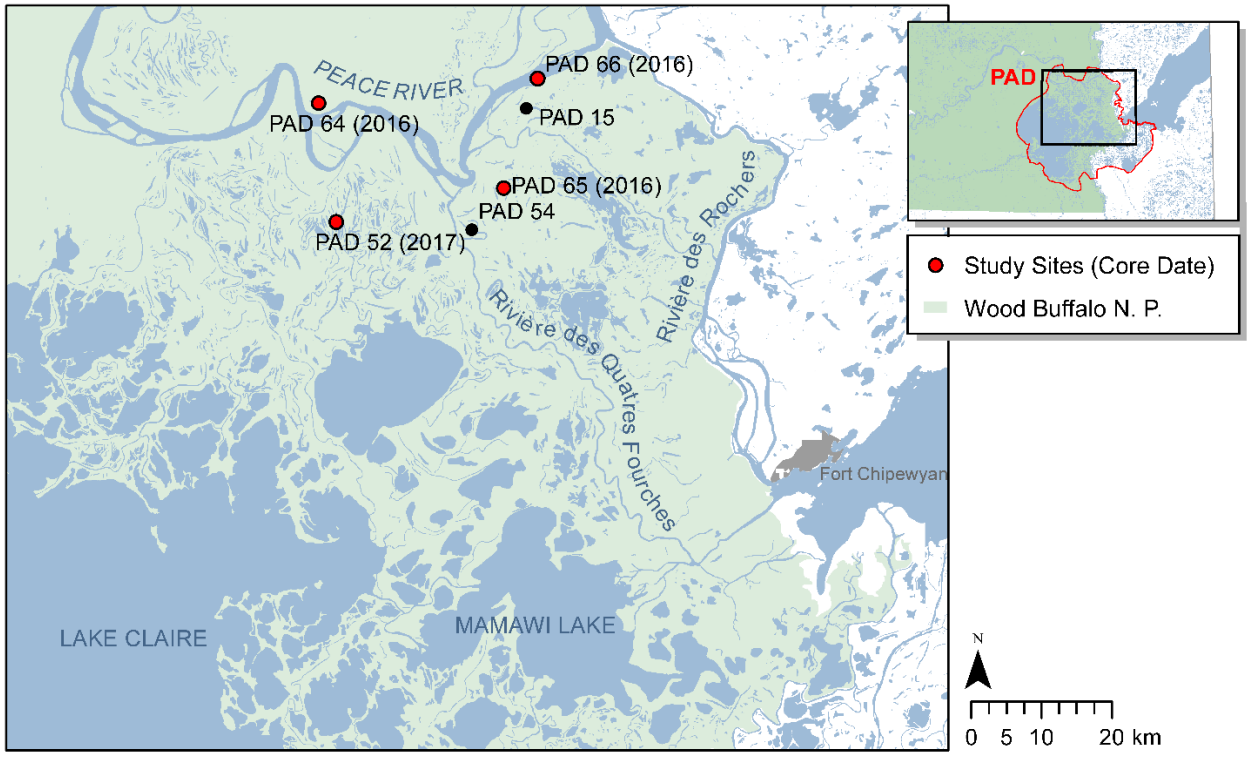

Figure 5: Study site locations within the Peace-Athabasca Delta, Alberta, Canada.

The five lakes that are the focus of this thesis are in and near the northern portion of the Peace-Athabasca Delta. Four are located along the Peace River and one is adjacent to the Slave River (Figure 5). Previous research at lakes PAD 15 and PAD 54 did not identify changes as a result of regulation of the Peace River (Wolfe et al. 2006), so lakes were included in this study in the same vicinity to test this finding.

As is typical of the PAD, the lakes of this study are quite small and shallow. The lake farthest upstream, 'PAD 52' (58.874761, -111.750013), is in the northwest of the PAD, 3.2 km from the Peace River. It is 0.5 m deep and at 212 m elevation, the same elevation as the nearby Peace River. It appears to be an ancient channel of a deltaic distributary of the Peace River. This lake was cored a year after the previous four lakes. While in the field in September 2017 and sorting through photos of lakes monitored for water quantity and quality, it was noted that the water levels of PAD 52 had decreased significantly

(Figure 6). An examination of the water isotope monitoring data from the past several years also showed that it was, at present time, a predominantly evaporation-dominated lake. This evidence suggested that the lake might be an excellent site to test whether the timing of drying coincides with regulation of the Peace River.

'PAD 64' (58.953290, -111.773086), by far the deepest lake, is approximately 4 m deep. It is circular with a diameter of approximately 150 m. Located 1 km north of the Peace River, it is in relatively close proximity to the river, although its elevation is 4 metres higher (217 m asl). There are no deep channels connecting the river and the lake, but the lake is nestled in the floodplain along a sharp bend in the Peace River, where large ice jams are likely to form.

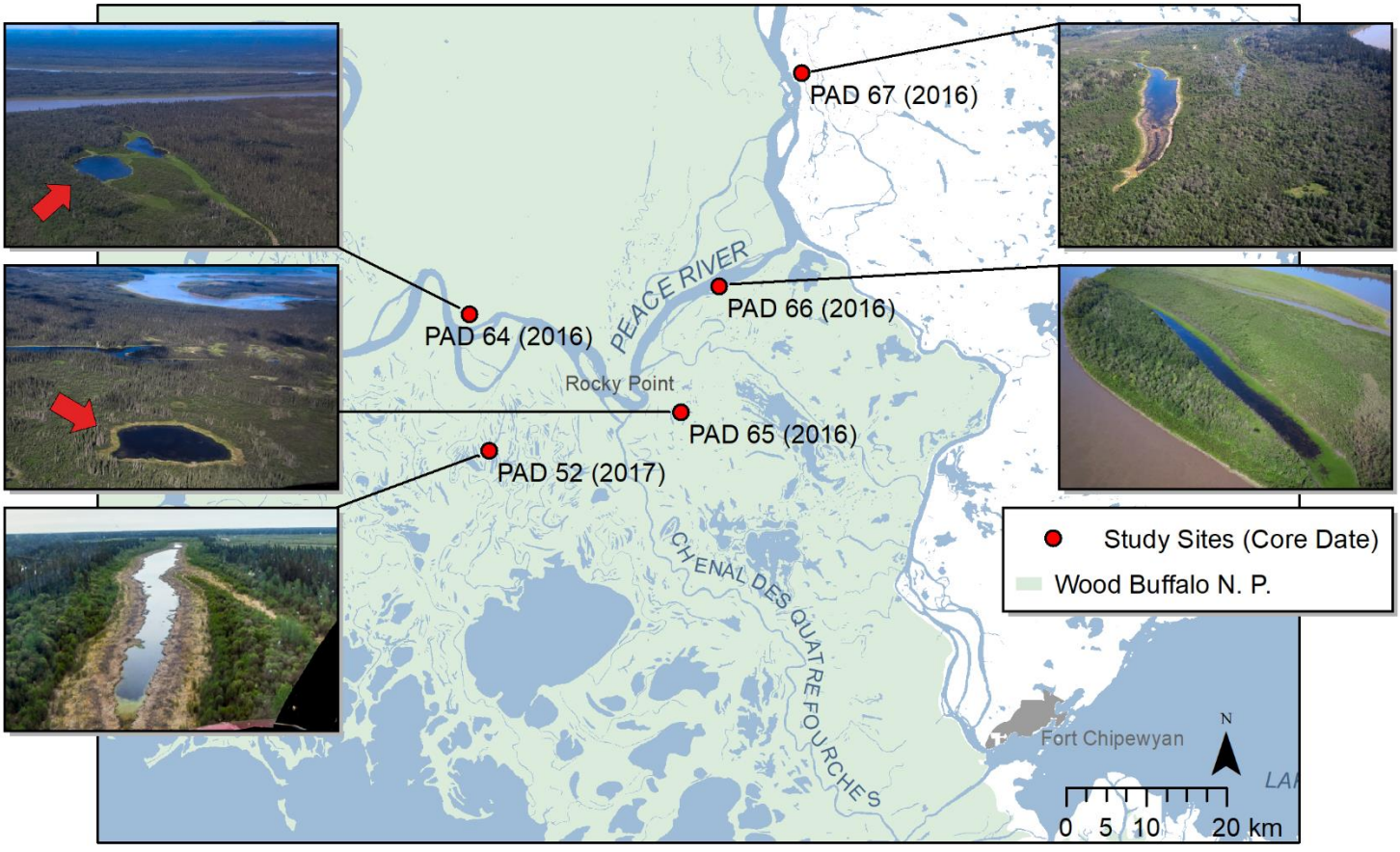

Figure 6: The five lakes of this research project, accompanied by photos of each lake.

'PAD 65' (58.896948, -111.535802) is 1.5 m deep and is also circular with a diameter of approximately 150 m, set 2.2 kilometres from the Peace River, east of Rocky Point (an exceptionally sharp bend in the Peace River), and within one metre of elevation from the Peace River (213 m asl). It is east of the Chenal des Quatre Fourches, which can carry water in both directions between the Peace River and Mamawi Lake depending on flow conditions.

'PAD 66' (58.969567, -111.493240) is located on an island in the Peace River, and is quite long and narrow, parallel to the Peace River. It is clearly a former channel of the river, and actively flooded by high spring discharge likely annually, since it is at the same elevation as the river. PAD 66 is 1 m deep, 100 m wide, and 400 m long. It is located 25 metres from the Peace River in the late summer, the dry season, but is connected to the river in the spring. Despite its proximity to the river, the island has elevated areas with some large trees and tall willow growth, so the lake was not expected to be too frequently flooded to impair paleolimnological reconstruction.

'PAD 67' (59.090748, -111.401042), 700 metres from the eastern bank of the Slave River, is 1.5 m deep, 200 m wide, and 400 m long, and is within a metre of elevation of the river. It is located on the floodplain of the Slave River, but is flanked on the east by upland bedrock. Despite being located along the Slave River, this lake is expected to receive sediment derived from the Peace River. The reversal of flows in the PAD during ice jam flood events prevents water from the Athabasca River reaching the Slave River (Bennett et al. 1973; Peace-Athabasca Delta Project Group 1973; Prowse & Lalonde 1996; Prowse et al. 2006; Peters, Prowse, Pietroniro, et al. 2006; Jasek 2019).

Chapter 2: Methods

Fieldwork

Sediment cores were collected from five lakes along the Peace and Slave river floodplains in the vicinity of the PAD (Figure 5, Figure 6). A hammer-driven gravity corer was used. Since the lakes were shallow (approximately 1 m in depth), cores were collected by standing in the water with the corer in hand, to increase weight and lift on the core. Two sediment cores were collected at each lake and they vary in length from 36 to 59 cm (Table 1). After collection, the cores were transported to Fort Chipewyan by helicopter, where they were described and sectioned at 1-cm intervals into WhirlPak™ bags. Samples were shipped to the University of Waterloo for subsequent analysis. Coolers and freezer packs were used during transportation to keep the sediment cool prior to analysis.

Lake	Date	UTM (Zone 12V)	Lake Depth (cm)	Core 1 length (cm)	Core 2 length (cm)	Working core
PAD 64	29-Jun-16	0455430m E 6535236m N	280	59	59	Core 2
PAD 65	29-Jun-16	0469090m E 6528703m N	80	54	57	Core 1
PAD 66	30-Jun-16	0471685m E 6536792m N	54	36	39	Core 2
PAD 67	30-Jun-16	0476973m E 6550287m N	100	57	56	Core 2
PAD 52	15-Sep-17	0456712m E 6526395m N	47	36	36	Core 1

Table 1. Lake sediment core sampling sites including location (NAD 83), water depth, core lengths, and which core was selected as the working core.

Laboratory Analyses

Sediment sub-samples were varyingly analysed to reconstruct past hydrological conditions and metal deposition (Table 2). Radiometric analyses (^{137}Cs, ^{210}Pb) were completed to establish a sediment core chronology where possible. Loss-on-ignition was performed to document changes in organic and

inorganic matter content. Organic carbon and nitrogen elemental and isotope composition analysis was used to reconstruct past changes in the origin of organic matter delivered to the lakes (as a proxy for past hydrological conditions) and nutrient cycling. Metal concentrations were analyzed to reconstruct deposition of metals.

PAD Lake	LOI	Chronology	C&N	Metals
64	Complete	Not datable		
65	Complete	Complete	Complete	Complete
66	Complete	Not datable		Complete
67	Complete	Complete	Complete	Complete
52	Complete	Complete		

Table 2: Overview of analyses conducted for each lake

Loss-on-ignition

Loss-on-ignition uses combustion at varying temperatures to measure water content, organic matter, carbonate content, and non-carbonate mineral content. These methods provide an understanding of the general compositional characteristics of the sediment core, where the results are reported as percent sample mass. Loss-on-ignition was completed on both cores collected from each lake. Half a gram of subsample from each section of the cores was put in a small crucible, placed in a drying oven at 90°C for at least 24 hours, and weighed again to measure the amount of water lost. Next, each crucible of subsample was placed in a muffle furnace and burned at 550°C for two hours, and then weighed to measure the loss of organic matter. Finally, each crucible was placed in the furnace at 950°C for two hours and weighed again to measure the amount of carbonate lost. The remaining mass in the crucible constitutes the non-carbonate mineral matter of the original half-gram of sediment. The protocol followed here has been developed by Dean (1974) and re-assessed by Hieri et al.(2001). Based

on the results of loss-on-ignition, a 'working core', the most promising core upon which further analyses were conducted, was chosen for each lake, which was used for subsequent analyses.

Radiometric analysis

Sediment samples were dated using radioactive isotopes ^{210}Pb and ^{137}Cs to develop a stratigraphic chronological record based on their decay. ^{210}Pb is part of the natural decay series for ^{238}U to the stable isotope ^{206}Pb. Within the series, the gaseous isotope ^{226}Ra is formed, and enters the atmosphere. This ^{226}Ra decays to ^{222}Rn, which falls from the atmosphere and decays with a half-life of 3.8 days to ^{210}Pb (Oldfield & Appleby 1984). The ^{210}Pb is washed to the bottom of the lake and becomes immobilized within the sediment deposits (Appleby 2001). This ^{210}Pb formed from atmospheric ^{226}Ra is considered "unsupported ^{210}Pb".

At the same time, ^{238}U, present in the lithogenic material that has been deposited in the lake, also produces ^{226}Ra. Within the sediment sample, the ^{226}Ra also decays to ^{210}Pb (via ^{222}Rn). The ^{210}Pb that forms from ^{226}Ra is considered "supported ^{210}Pb". This supported ^{210}Pb is created from the sediment present in the sample, at a constant rate, and is not of atmospheric origin (Appleby & Oldfield 1978). Supported ^{210}Pb is assumed to be equal to the amount of ^{226}Ra, ^{214}Bi, or ^{214}Pb, since these are present equally in the decay series between ^{226}Ra and ^{210}Pb. Therefore, to calculate the supported ^{210}Pb, the total ^{210}Pb present within a sample is measured, and supported ^{210}Pb is assumed to be equal to the average of the measured values of ^{214}Bi and ^{214}Pb (Appleby & Oldfield 1978; Appleby 2001).

Unsupported ^{210}Pb is the dominant source of ^{210}Pb to lakes, but naturally decays with a half-life of 22.26 years. Since the supply of atmospherically-sourced ^{210}Pb within the lake sediment profile is not being replenished, the presence of unsupported ^{210}Pb in the sample decreases over time. When the total amount of ^{210}Pb in a sample is equal to the production of supported ^{210}Pb (i.e., no unsupported

^{210}Pb is being created, and total ^{210}Pb is equal to supported ^{210}Pb), then background ^{210}Pb has been reached and approximately 150 years have passed (Appleby & Oldfield 1978).

The rate at which ^{210}Pb decreases through the depth of the core is an indication of sedimentation rates. The ^{210}Pb is diluted by the deposition of other materials, both organic and inorganic. Changes in the ^{210}Pb curve by depth can be interpreted as changes in sedimentation rate (Appleby & Oldfield 1978). A major assumption here, however, is that there is a constant rate of supply of ^{210}Pb from the atmosphere through the duration of the deposition of the entire core. This is referred to as the Constant Rate of Supply model (Appleby & Oldfield 1978; Appleby 2001). It is appropriately chosen in this study since the sedimentation rates within the PAD typically are highly variable and the atmospheric supply of ^{210}Pb is more likely to have remained relatively constant, since the watershed of each individual lake is very small, and ^{210}Pb carried in to these lakes from the river via flood events is negligible. A linear extrapolation (based on cumulative dry mass) was used in the depths below the presence of unsupported ^{210}Pb, which assumes a constant sedimentation rate. This is an approximation in a deltaic landscape, but no simple alternatives exist, and these depths are older than the time period of primary interest in this study (1900 to present).

In addition, the measurement of ^{137}Cs can be used via the identification of peak nuclear fallout from the testing of bombs which reached a maximum in 1963. With a significant peak in ^{137}Cs activity within the core, the date of 1963 can be identified, and thus contribute to the accuracy of the developed chronology (Appleby 2001). However, it can, in some situations, especially in sediments rich in organic matter, be mobile within the sediment (Foster et al. 2006).

^{210}Pb and ^{137}Cs analysis was completed by Dr. Johan Wiklund at the University of Waterloo using an Ortec Coaxial HPGe Digital Gamma Ray Spectrometer. A weighed amount of approximately three grams of freeze-dried sediment from every second 1.0-cm section of core were sealed into Sarstedt test

tubes with a teflon septum and epoxy. Sealed tubes were left for 21 days to allow atmospherically-sourced (unsupported) ^{222}Rn to decay before the measurement of ^{210}Pb activity. Samples were then placed in the gamma ray spectrometer, and measured for up to five days, depending on their radioactivity. Unfortunately, sediment cores from PAD 64 and PAD 66 could not be dated because they contained low concentrations of ^{210}Pb. It is suspected that these lakes are too flood-prone and contain high inorganic sedimentation rates, which dilute the unsupported ^{210}Pb concentrations.

Organic carbon and nitrogen elemental and isotope composition

Measurement of organic carbon and nitrogen elemental and isotope composition provides knowledge about the origin of organic matter, either terrestrial- or aquatic-derived, and insight about past nutrient cycling and levels of aquatic productivity (Meyers 1994; Wolfe et al. 2001). Only a small portion of organic matter produced within a lake is preserved after sedimentation, avoiding decomposition, but the remaining C/N and $\delta^{13}C_{org}$ values of total organic matter survive within the sediment (Meyers 1994).

C/N ratios are used here to generally infer flood frequency using ratios to differentiate aquatic and terrestrial organic matter in lake sediments (Meyers & Teranes 2001; Talbot 2001). These ratios are calculated using %C and %N by mass of sample. In general, terrestrial vegetation (vascular plants) have higher C/N ratios, since compounds such as lignin form tight fibres and matrices, which are required to support the plant, and have larger percentage of carbon than aquatic plants which are supported in a lower-gravity environment. Aquatic vegetation has access to readily available dissolved nitrogen compounds within the water column, and therefore through incorporation of nitrogen compounds this leads to a lower C/N ratio (Meyers & Teranes 2001; Wolfe et al. 2001). Terrestrial organic matter, the source of allochthonous organic matter delivered to these lakes, generally has C/N ratios of >20, while aquatic algal matter typically possess ratios between 4 and 10 (Meyers 1994). In terrestrial soils, the C/N

ratio can be affected by microbial activity, but the ratio is generally preserved in aquatic sediments (Meyers 1994). The weight C/N ratio is commonly calculated from total percent C and total percent N by dry weight of the sample.

The measurement of carbon isotope composition in organic matter can also be effective in understanding the source of the organic material and nutrient cycling in lakes. The metabolic pathway of photosynthesis in aquatic primary producers preferentially uses ^{12}C relative to ^{13}C due to the kinetic effects of each metabolic process, as well as the partial pressure of CO_2 (CO_2 concentration). The mechanism by which plants metabolize CO_2 (C3, C4, CAM) alters the carbon isotope ratio, also known as isotopic fractionation. For example, in the metabolic pathway of photosynthesis, the carboxylation reaction via the RuBisCO enzyme preferentially uses ^{12}C rather than ^{13}C, as a result of the mass-differences between the two isotopes and the energy associated with breaking molecular bonds (Meyers 1994). This preference results in aquatic organic matter with varying $^{13}C/^{12}C$ ratios, which reflect how much primary productivity occurred during the cumulative open-water season within a particular water body. Atmospheric CO_2 has a $\delta^{13}C$ value of approximately -7 per mil (although this is becoming more negative due to the combustion of fossil fuels, the "Suess Effect", currently -8.5 per mil). The fractionation by photosynthesis in C3 plants typically results in a $\delta^{13}C_{org}$ shift of -20 per mil by preferential use of ^{12}C in the Calvin cycle relative to the inorganic source. Since lacustrine algae perform C3 photosynthesis, $\delta^{13}C_{org}$ cannot normally be used distinguish terrestrial from aquatic C3 plants because of their overlapping $\delta^{13}C_{org}$ values, but the combined use of C/N ratios and $\delta^{13}C_{org}$ values can distinguish the sources of organic matter in lake sediments (Meyers 1994). Carbon isotope composition is reported in delta notation in units per mil, where $\delta^{13}C_{org}$ is the isotope ratio of the sample relative to the isotope ratio of a reference standard. In aquatic environments, the working standard is derived from the Pee Dee Belemnite formation (which has a known and constant $^{13}C/^{12}C$ ratio), referred to as the Vienna Pee Dee Belemnite reference standard. Precision of $\delta^{13}C_{org}$ is 0.2 per mil.

Nitrogen cycle and related isotopic processes appear to be significantly more complex and consequently less well understood than metabolic C fractionation (Talbot 2001). Plant metabolic processes result in nitrogen fractionation, but the widely varying sources of N in aquatic systems can make $\delta^{15}N$ interpretation difficult (surface and groundwater, cyanobacterial fixation, fertilizers, manure and solid waste, terrestrial plants, aquatic macrophytes and algae; Leng et al. 2005). Often, $\delta^{15}N$ must be supplemented with other proxies, for example diatoms and algal pigments, to differentiate between N sources. $\delta^{15}N$ is reported in per mil relative to the atmospheric N_2 ratio of ^{15}N to ^{14}N.

Subsamples of wet sediment from each 1.0-cm interval were pre-treated with 10% HCl to remove carbonates and rinsed with de-ionized water, repeatedly, until neutralized, and then freeze-dried, as developed-by Wolfe et al. (2001). The subsamples were then sieved (at 250 μm) and the fine fraction sub-sampled into tin capsules and submitted to the University of Waterloo - Environmental Isotope Laboratory (UW-EIL). Analysis was completed by UW-EIL using a 4010 Elemental Analyzer (Costech Instruments) interfaced with a Delta Plus XL (Thermo-Finnigan) continuous flow isotope ratio mass spectrometer (CFIRMS), using a modification of method EPA 2002.2/6020A. Precision of $\delta^{15}N$ is 0.5 per mil, and precision of $\delta^{13}C$ is 1 per mil.

Metals analysis

Vanadium is a metal pollutant commonly associated with the refinement of bitumen and the production of oil (Khalaf et al. 1982; Galloway et al. 1985; Juichang et al. 1995), where its source is a vanadyl porphyrin. The oil sands in Alberta have exceptionally high concentrations of vanadium (Gosselin et al. 2010), making it the metal of key concern in wetland regions, where it is taken up by flora and fauna (Baker et al. 2012). Thirteen other metals considered metals of priority pollutants are considered here and include Sb, As, Be, Cd, Cr, Cu, Pb, Hg, Ni, Se, Ag, Tl, and Zn. Wiklund et al. (2014) has studied Be, Cd, Cr, Cu, Pb, Ni, and Zn as the main metals of concern in the Alberta Oil Sands Region for

paleolimnological research, since these metals were found to be elevated in the snowpack around the Alberta Oil Sands Region by Kelly et al. (2010) and are relatively immobile within lake sediments.

Unfortunately, the raw measurement of these metals of concern is not a reliable measurement of industrial activity. Within the deltaic environment of the PAD, hydrologic energy can fluctuate greatly, resulting in the deposition of sediment in a wide range of grain sizes. During transport, metals and metalloids dissolved in the river water adsorb to the surface of these grains, due to the low solubility of the metals (Loring 1991; Kersten & Smedes 2002). As a consequence, the concentration of adsorbed metals in the sediment is influenced by the surface area, and therefore diameter, of the grains.

Both natural and anthropogenically-sourced metals adsorb to the sediment, are carried by the rivers that supply the PAD, and are deposited in the lakes of the delta via flooding. Therefore, changes in the raw concentration of metals of concern is an expected observation and these raw metal concentrations are not a reliable measurement of pollution. Fortunately, some metals naturally present in the river due to the weathering of the geologic material within the river catchment (including rock, sedimentary material, and bitumen deposits) will maintain a relatively constant relationship with each other (Loring 1991; Kersten & Smedes 2002; Wiklund et al. 2014). Measuring these relationships is, indirectly, a measure of the adsorptive ability of the sediment within a core sample. If the raw concentration of a metal of concern deviates from its observed (measured) natural relationship to the raw concentration of an exclusively lithogenic metal (or to sediment grain size), then there are processes besides weathering that are supplying this metal to the river. The measurement of these relationships is "normalization", and is a way to standardize the data to account for confounding factors (Loring 1991). Normalization against a lithogenic metal accounts for changes in the adsorptive capacity of the sediment through the core, so that the presence of elevated levels of contaminant metals can be assessed (Loring 1991; Kersten & Smedes 2002).

There are three metals considered to be most suitable for use as lithogenic normalizing agents: lithium, titanium, and aluminum (Loring 1991; Kersten & Smedes 2002), though occasionally zirconium and organic matter have been used. For a metal to be an effective normalizing agent, it must have several criteria. 1) It cannot be mobile within the sediment (Gobeil et al. 1997). 2) It cannot become concentrated through industrial activity or other anthropogenic sources (its concentration will be the same in polluted and clean samples). The concentration of titanium is often associated with bitumen refinement, but lithium and aluminum are both potentially useful normalizing agents in the PAD. 3) It must be consistently found in the geologic material of the river catchment, so that its source does not provide fluctuating concentrations, and must be consistently physically and chemically eroded and deposited. 4) Its extraction and analysis in the laboratory must be reliable. And 5) if possible, it should be able to be used in the normalization of metals in other regions and at other study sites, to ease communication and maintain consistency within the scientific community. Aluminum is most commonly used in literature, especially in estuarine and coastal environments, and thus is the most desirable normaliser to be used in this study.

To statistically confirm the suitability of the normalizing agent, an Akaike Information Criterion (AIC) test was used to compare the linear relationships of the different potential normalizing agents: aluminum, lithium, titanium, zirconium, and organic matter. The metals concentrations and organic matter values from both PAD 65 and PAD 67 that were dated as pre-1920 are used in the test, since a baseline for the Peace sector of the delta was sought. The year 1920 is considered the divide between pre- and post-industrial activity, used by Wiklund et al. (2014), since atmospherically-sourced metals pollution has been identified in one lake in the PAD beginning the 1920s (Wiklund, Hall, Wolfe, et al. 2012), and well before development of the Alberta Oil Sands industry beginning in the 1960s (Chastko 2004).

Approximately one gram of freeze-dried sediment from every 1.0-cm of the core was subsampled and crushed with a glass crucible to expose all adsorptive surfaces of the sediment. Subsamples were then sent to ALS Environmental, where a modified version of method EPA 200.2/6020A is used. In this method, the sediment undergoes a partial acid digestion (HNO_3 and HCL and heat) to liberate metals that may be environmentally available. This is an appropriate method, since the environmentally available metals are the metals of interest at the PAD.

As explained above, a cross-plot is used to develop the relationship between a primary pollutant metal versus and a lithogenic metal (Loring 1991; Kersten & Smedes 2002; Wiklund et al. 2014). By comparing these relationships pre-industry and post-industry, the presence of contamination can be identified. A 95% prediction interval is used to establish a range of reasonable natural variation in the sediment core (Loring 1991; Wiklund et al. 2014), based on the data from the pre-industry samples. Thus, 95% of the sample should fall between the prediction interval lines, with an expected 2.5% above and 2.5% below the lines. In the case of metal pollution, more than 2.5% of the data would fall above the 95% prediction interval, a significant deviation from the natural relationship between that metal and the normalizing agent. Through this analysis, the raw measurements of sediment metals can be valuable in the detection of industrial pollution of metals through the sediment layers of a lake.

An examination of the enrichment factor, by time, assists in identifying at which time periods elevated metal concentrations occur. The enrichment factor is calculated as the ratio of the metal of interest (X) to the normalizing agent, aluminum (Al), in a given sample (i), over the ratio of the expected concentration of the metal of interest as calculated by the linear regression of baseline concentrations (X_r) at the aluminum concentration of that same sample (Equation 1):

$$EF = \frac{X_i / Al_i}{X_r / Al_i} \quad (1)$$

Because it is calculated using the pre-1920 baseline, the data pre-1920 will average to an EF of 1.0. Both PAD 65 and PAD 67 were used to develop the pre-1920 EF calculation, since one of the objectives of this research project is to develop a baseline of metals supply from the Peace River to the delta, as a whole, and not on a per-lake basis.

Chapter 3: Results

Radiometric Dating

Radiometric analyses were performed on sediment cores from PAD 52, 65, 67, and 64 to generate data needed for establishing core chronologies (Figure 7). Results for PAD 52, 65, and 67 demonstrated down-core decline in total ^{210}Pb, which permitted Constant Rate of Supply (CRS) age calculations to be performed (Figure 7a-c). In contrast, the total ^{210}Pb profile for PAD 64 does not display expected down-core decline. Only samples from the top 4 cm and at 12 cm depth display total ^{210}Pb activity in excess of the supported (i.e., background; ^{226}Ra concentration as estimated from the weighted mean of ^{214}Bi and ^{214}Pb concentrations) ^{210}Pb (Figure 7d). Radiometric results for PAD 64 likely reflect exceedingly high sedimentation rates and dilution of total ^{210}Pb and, therefore, a core chronology could not be constructed for this sediment record. Similar profiles of total ^{210}Pb have been obtained for nearby oxbow lakes, PAD 15 and 54, which are also subject to high sedimentation rates (Wolfe et al. 2006). For PAD 66, because the organic matter content was extremely low throughout the sediment core, likely also indicative of very high sedimentation rates, radiometric analysis was not attempted. Given that sediment core chronologies could not be determined for PAD 64 and 66, they were not subject to further analysis.

At PAD 52, total ^{210}Pb activity is ~146 Bq/kg in the upper 5 cm of the core and declines to 46 Bq/kg at 16.5 cm depth, where it reaches background ^{210}Pb activity (average = 37 Bq/kg; Figure 7a). Using the CRS model, the estimated date at the base of the unsupported ^{210}Pb profile is 1953. Linear extrapolation, based on the average sedimentation rate determined for the unsupported ^{210}Pb interval, was used to estimate the chronology of the remainder of the core, which dates to ~1770 (36 cm). The CRS chronology is supported by the ^{137}Cs profile and the calculated sedimentation rate. Maximum ^{137}Cs activity occurs between 16 and 13 cm depth corresponding to the CRS dates 1946-1964, which

encompasses peak fallout concentrations in 1963 (Appleby 2001). A prominent increase in sedimentation rate occurs in the mid-1970s (peak at 12.5 cm depth, dated 1977), of exclusively inorganic material, likely corresponding with the major flood event of 1974 (Peters & Prowse 2001).

At PAD 65, the total ^{210}Pb activity is 179 Bq/kg in the top 2 cm of the core and declines with some fluctuations until reaching background ^{210}Pb activity (average = 39 Bq/kg) at 24.5 cm depth (Figure 7b). The CRS model estimates the date at the base of the unsupported ^{210}Pb at 1930. Linear extrapolation of the average sedimentation rate dates the bottom of the 55 cm core at 1722. In support of the CRS dating model, a major peak in inorganic sedimentation rate occurs in the early 1970s, likely corresponding to the known large flood event of 1974. The small peak in ^{137}Cs at 14.5-16.5 cm depth corresponds to CRS dates of 1974-1978, rather than the expected date of 1963. This offset may be due to the mobilization of ^{137}Cs.

At PAD 67, the total ^{210}Pb activity is 128 Bq/kg at the top of the core and decreases to background ^{210}Pb activity at 17 cm depth (average = 46 Bq/kg, Figure 7c). The base of the unsupported ^{210}Pb interval is dated at 1945 using the CRS model. Linear extrapolation of the average sedimentation rate dates the bottom of the 57 cm sediment core at 1516. Several peaks in inorganic sedimentation rate are evident, including the 1974 flood event, but also at ca. 1961, 1987, and 2012. There is no distinct peak in ^{137}Cs, so it cannot be used to assist in developing the sediment core chronology.

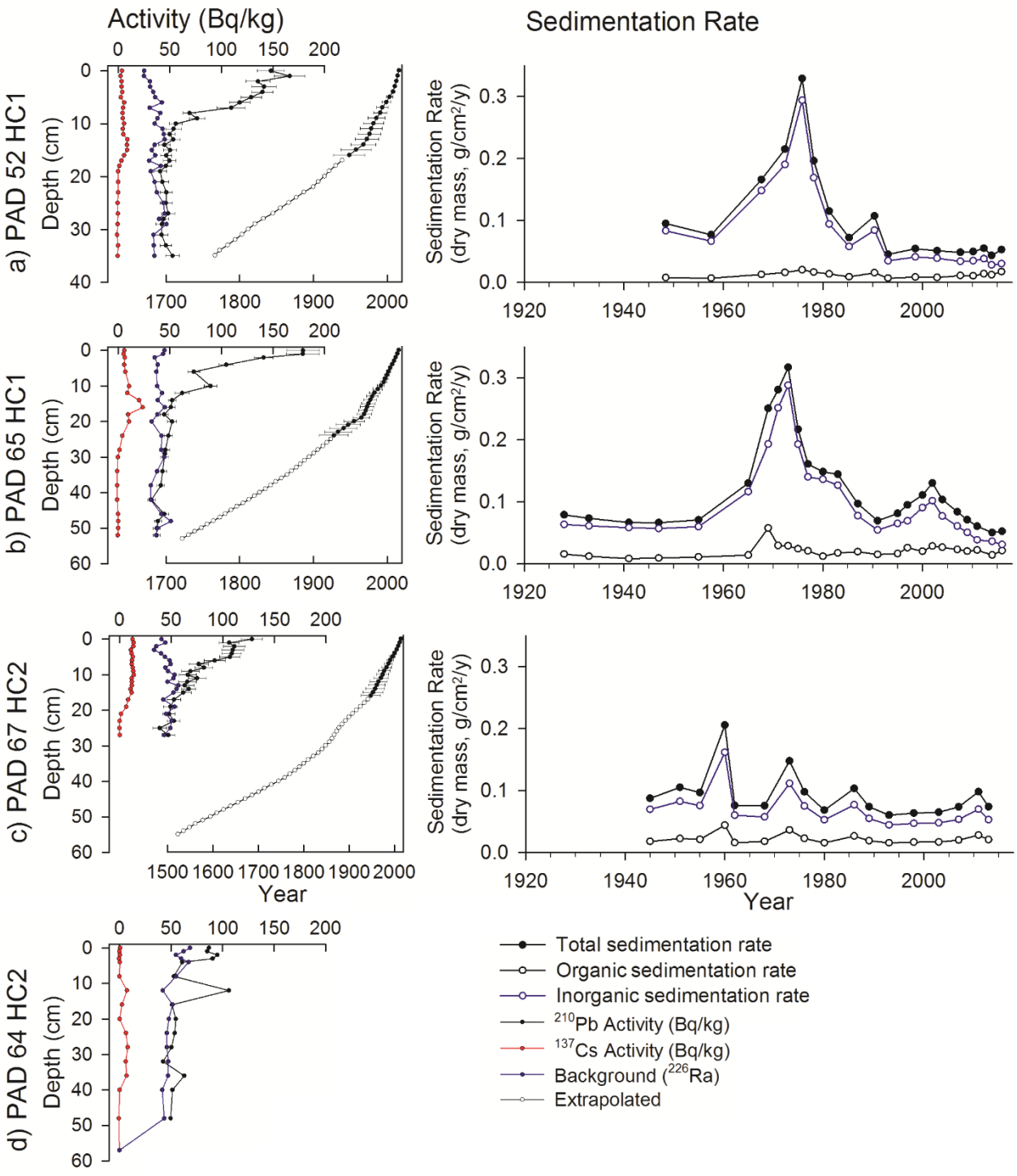

Figure 7: Results of radiometric dating, showing radioactivity of ^{210}Pb and ^{137}Cs, age-depth models (where developed), and sedimentation rates for a) PAD 52, b) PAD 65, c) PAD 67, and d) PAD 64. Error bars represent 1 standard deviation.

LOI and Organic Carbon and Nitrogen Elemental and Stable Isotope Composition

PAD 52

Two distinct phases have been visually identified in the loss-on-ignition (LOI) record of PAD 52 (Figure 8). Phase 1 extends from the bottom of the core (1766) to 1976, and Phase 2 occurs from 1976 to the top of the core (2016). Phase 1 consists of mainly low water content (H_2O; average = 46%) and low organic matter (OM; average = 10%), high mineral matter (MM; average = 85%), and low $CaCO_3$ (average = 11%) content. At 1900 and 1915, there are peaks in H_2O (54% and 66%, respectively), OM (15% and 22%, respectively) and $CaCO_3$ content (20% and 14%, respectively), accompanied by decreases in MM content (76% and 72%, respectively). Overall, the low OM content during Phase 1 suggests low aquatic productivity as a result of frequent influx of inorganic sediment supplied by river floodwater. Exceptions to these conditions at 1900 and 1915 may represent brief intervals of reduced flooding and higher aquatic productivity.

Phase 2 (1976-2016) is characterised by distinct trends in the LOI parameters. Water content increases from 45% to 98%, OM increases from 6% to 33%, MM decreases from 89% to 57%, and $CaCO_3$ increases with some fluctuations from 7% to 23%. Notably, the lowest %OM and highest %MM in the core occurs at the base of Phase 2, at ca. 1976, and may correspond to the 1974 flood event. After this event, the substantial increase in %OM and decrease in %MM are indicative of lake conditions that promote aquatic productivity – clear, warm water and low inorganic sedimentation rates. A decline in organic matter content down from the surface of the core is expected due to sediment decomposition, but such a steep decline, accompanied by an increase in carbonates-suggests that there are more processes occurring than simply organic matter decay.

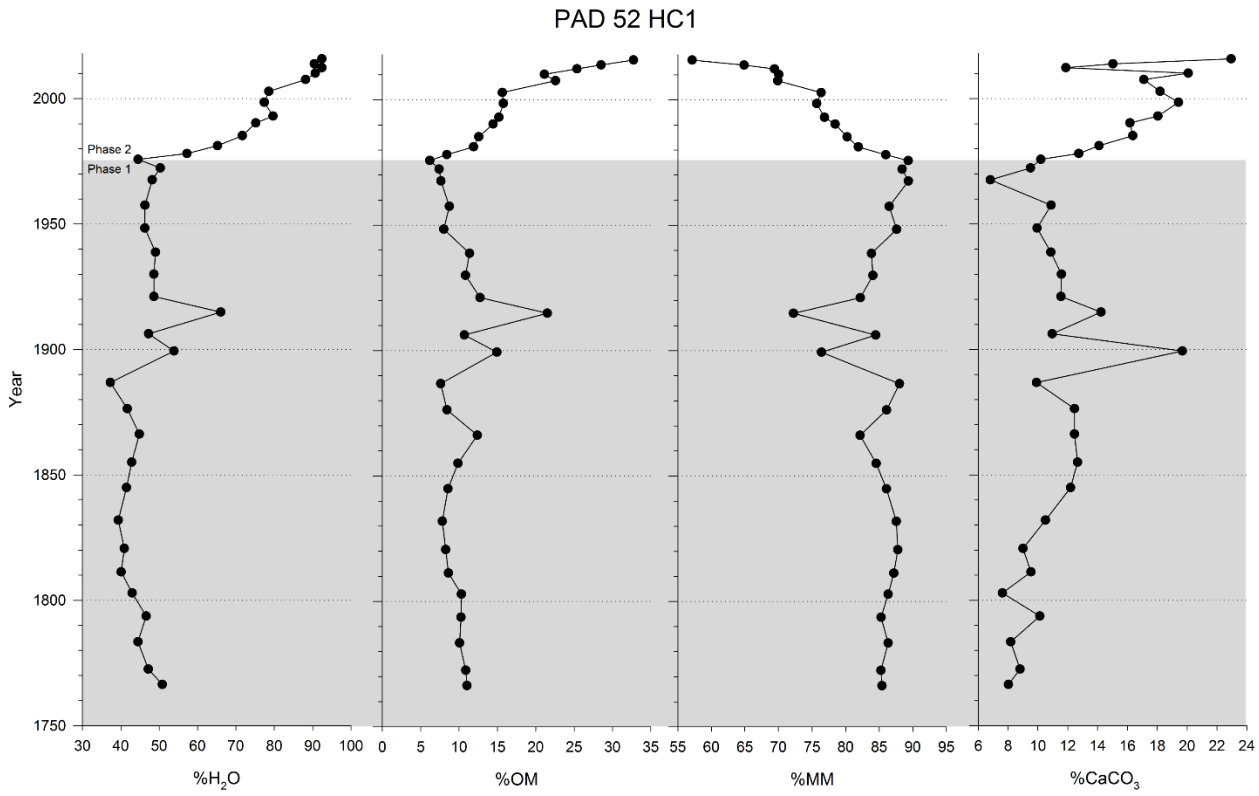

Figure 8: Results from loss on ignition for PAD 52 by CRS year.

PAD 65

The LOI and organic carbon and nitrogen elemental and isotope stratigraphic record from PAD 65 can be described in two phases (Figure 9). Phase 1, extending from 1721 to 1968, is characterised by low OM (average = 15%), relatively high C/N ratio (average = 12), low $\delta^{13}C_{org}$ (average = -27.0‰), and high $\delta^{15}N$ (average = -0.2‰). %C and %N are low, but increase and are marked by some fluctuations in the late 19th and early 20th centuries. A low C/N ratio is understood to be sourced from aquatic productivity, while higher C/N ratios originate from allochthonous organic matter (Meyers et al. 1984; Meyers & Ishiwatari 1993; Meyers 1994; Leng et al. 2005). This is because terrestrial, vascular plants have higher concentrations of cellulose and lignin, which possess high concentrations of C. The low OM and high C/N ratio are an indication of frequent inundation of inorganic sediment supplied by river floodwater, depositing inorganic material and terrestrial organic matter in the lake.

Phase 2 of PAD 65 (1968 to present) is characterised by variation in all parameters and directional trends. OM increases from an average of 16% in Phase 1 to 41% at the top of the core, accompanied by nearly identical trends in %C and %N (from 4% to 8%C and 0.4% to 1.8%N), though these increases do not occur until after a period of low values between 1968 and 1987, likely resulting from large flood events in the 1970s. There is a decrease in C/N ratio from an average of 12 in Phase 1 to an average of 10 in Phase 2. $\delta^{13}C_{org}$ increases from an average ~-27‰ in Phase 1 to an average ~-26 ‰ in Phase 2, marked by a steep transition between 1971 and 1983. $\delta^{15}N$ increases toward 0‰ in the 1970s and 1980s, but decreases after 1989 to -2.0‰ at the top of the core. These trends, including increasing %OM, %C, and %N, and decreasing C/N ratios, are indicative of a shift to less flood-prone conditions and higher aquatic productivity (Meyers et al. 1984; Meyers & Ishiwatari 1993; Meyers 1994; Leng et al. 2005). CO_2 becomes limited in highly productive conditions, allowing less fractionation of C, resulting in a higher $\delta^{13}C$ (Fogel & Cifuentes 1993; Smyntek et al. 2012). Alternatively, in these highly productive, low dissolved CO_2 conditions, algae generally use bicarbonate as a source of carbon (~8‰ higher than dissolved CO_2; Mizutani & Wada 1982). Meanwhile, N concentrations may increase due to the stimulation of aquatic plant growth (Wiklund, Hall, & Wolfe 2012), which would allow primary producers to fractionate more against ^{15}N, resulting in decreasing $\delta^{15}N$ (Fogel & Cifuentes 1993).

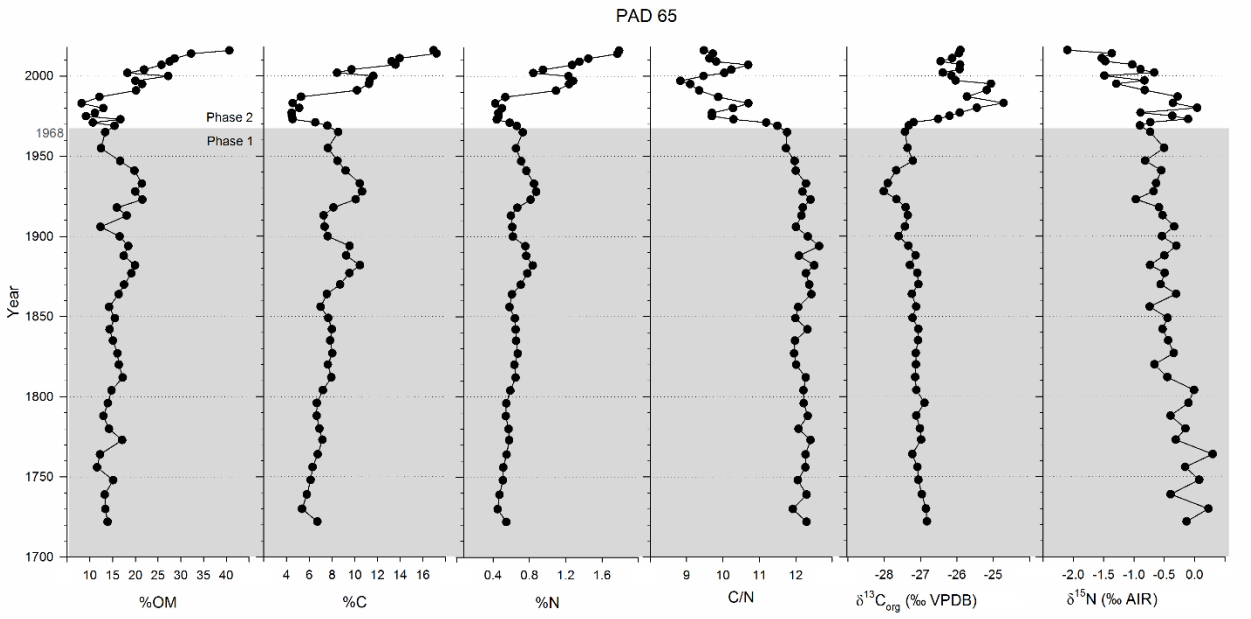

Figure 9: Results of organic matter content from LOI and carbon and nitrogen data for PAD 65, displaying two distinct phases separated at 1968.

PAD 67

Three phases can be identified in the LOI and organic carbon and nitrogen elemental and isotope stratigraphic record from PAD 67: Phase 1, from the bottom of the core (1516) to 1760, Phase 2, from 1760 to 1880, and Phase 3, from 1880 to present (Figure 10). Phase 1 is marked by low %OM (average = 10%), %C (average = 4%), and %N (average = 0.4%), high C/N ratios (average = 12), high $\delta^{13}C_{org}$ (average = -26.6‰), and high, varying $\delta^{15}N$ (between -0.1‰ and 1.2‰, average = 0.4‰). These conditions suggest highly flood-prone conditions, in which terrestrial organic material and high volumes of inorganic suspended river sediment are delivered to the lake, and aquatic productivity is limited, resulting in low %OM.

Phase 2, from 1760 to 1880, is characterised by high variation and peaks in OM (between 15% and 35%), high C/N ratio (between 11.5 and 14.5), low $\delta^{13}C_{org}$ (-29.8‰ and -27.9‰), and high $\delta^{15}N$ (between -0.1‰ and 0.5‰). The notable peak in OM at ~1870 to 35% is accompanied by increases in %C (to 17.3%), %N (to 1.5%), C/N (to 14), $\delta^{15}N$ (to ~0.5), and a decrease in $\delta^{13}C_{org}$ (to -29.9‰). The

increases in %OM, %C, and %N are indicative of an increase in productivity, suggesting low flood frequency at this time. A high C/N ratio is usually interpreted as influence of terrestrial OM, but in this case likely resulting from increased growth of emergent vegetation in this shallow lake during a dry phase (Meyers et al. 1984; Meyers & Ishiwatari 1993; Meyers 1994; Leng et al. 2005).The C and N isotope values permit this interpretation, as the $\delta^{13}C_{org}$ and $\delta^{15}N$ values are within the range of vascular C3 plants (O'Leary 1981). The decrease in the $\delta^{13}C_{org}$ record may be due to the influence of the emergent vegetation, which are able to discriminate more against ^{13}C in the CO_2-rich atmosphere (O'Leary 1981; Farquhar et al. 1989; Meyers & Teranes 2001). Overall, Phase 2 appears to be characterized by severely dry, low-flood conditions. It is worth noting that, at the end of Phase 2, lake conditions abruptly change, returning to conditions similar to Phase 1, with low aquatic productivity. This may be the result of a change in local geomorphology, where a strong flood event eroded a levee, exposing the lake to less extreme flood events and increasing the flood susceptibility of the lake at the beginning of Phase 3.

During Phase 3, %OM decreases from 18% in 1880 to 16% in 1930, and then increases to 29% at the top of the core. Trends in %C and %N are nearly identical, at 8%C and 0.62%N in 1880, and 7%C and 0.6%N in 1930, and then increasing to 14%C and 1.5%N at the top of the core. Throughout Phase 3, C/N ratios and $\delta^{15}N$ values decrease (to 9 and -1.0‰, respectively), while $\delta^{13}C_{org}$ increases to -26.3‰. The period from 1880-1930 appears to be a return to higher flood frequency, suggested by the decrease in OM% as water depth increased and waters became cloudy. Increased floodwaters brought nutrients to the lake, promoting the growth of algae during that time as water became clear (evidenced by sharp decrease in C/N), but also the deposition of inorganic material. The decrease in C/N suggests a rapid shift from emergent vegetation to algae-dominated productivity. It is likely that the inorganic material of the floodwaters dilute the organic matter, resulting in a low %OM – perhaps the floodwaters are great enough to discourage the growth of emergent vegetation, causing a transition from predominantly emergent to algal-dominated productivity. The increase in organic matter content (and increase in %C

and %N) and enrichment of ^{13}C is the result of a transition to a more productive lake as flood frequency declined from 1930 to present.

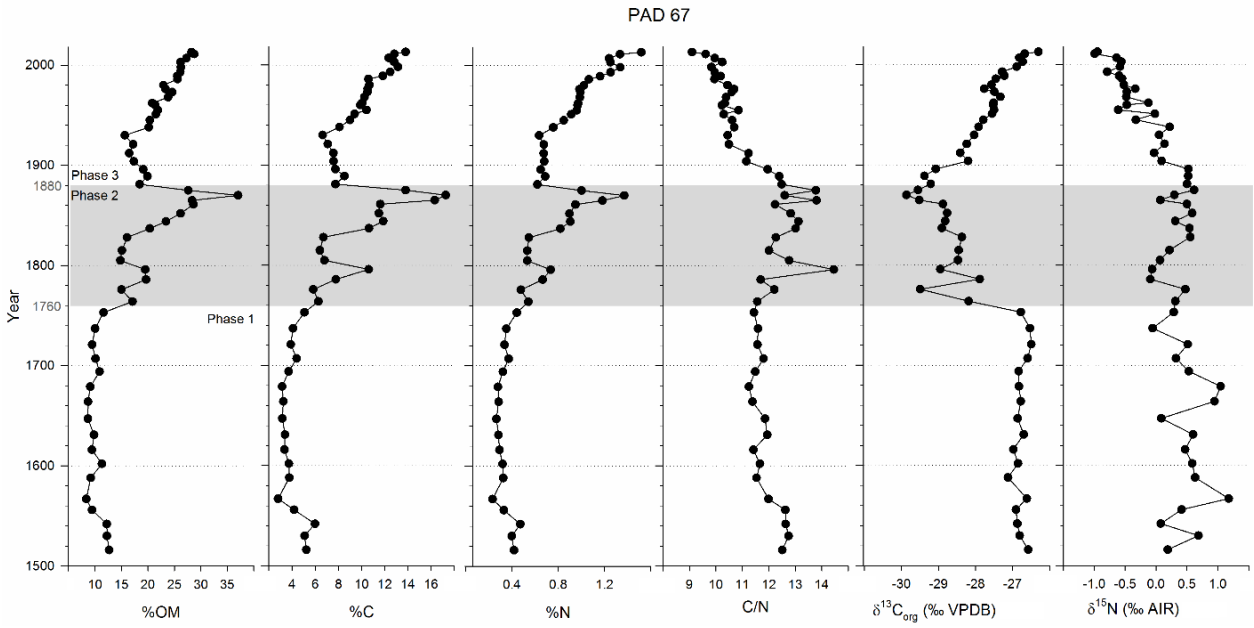

Figure 10: Results of organic matter content from LOI and carbon and nitrogen data from isotopic and elemental analysis for PAD 67, displaying three phases, from the bottom of the core to 1760, from 1760-1880, and from 1880 to present.

Regressions and Correlation Analysis of Sediment Metal Concentrations

Results from the Akaike Information Criterion test

Results from the AIC test for all eight metals of concern indicate that aluminum is the best normalizing agent for all metals except beryllium and lead, for which lithium is the best normalizer (see Table 3). However, aluminum is shown to be the second-best normalizing agent for beryllium and lead. It is most efficient to use the same normalizing agent across the suite of metals for comparability, especially with concurrent studies in the PAD, where aluminum-normalized baselines have been used for the Athabasca sector to assess for evidence of pollution (Kay et al. 2020; Owca et al. 2020). For these reasons, aluminum was selected as the most suitable normalizer for this study.

Table 3: Normalizing agent AICc results for all 8 metals of concern.

	Model	AICc	ΔAIC	AIC weight	Cumulative weight
Vanadium	Al	280.618	0	1	1
	Li	344.8625	64.24457	1.12E-14	1.12E-14
	Zr	436.7884	156.1704	1.22E-34	1.22E-34
	Ti	455.1171	174.4992	1.28E-38	1.28E-38
	OM	475.7754	195.1574	4.19E-43	4.19E-43
Beryllium	Li	-255.258	0	1	1
	Al	-177.328	77.93011	1.20E-17	1.20E-17
	Zr	-98.7436	156.5146	1.03E-34	1.03E-34
	Ti	-59.9762	195.2819	3.94E-43	3.94E-43
	OM	-46.7509	208.5073	5.29E-46	5.29E-46
Cadmium	Al	-213.019	0	0.9998252	1
	Li	-195.716	17.30327	0.0001748	0.0001748
	Zr	-120.558	92.46109	8.36E-21	8.39E-21
	Ti	-109.154	103.8645	2.79E-23	2.88E-23
	OM	-102.114	110.9053	8.26E-25	8.26E-25
Chromium	Al	122.8169	0	1	1
	Li	252.1387	129.3218	8.28E-29	8.28E-29
	Zr	352.8972	230.0803	1.09E-50	1.09E-50
	Ti	373.7033	250.8863	3.32E-55	3.32E-55
	OM	390.1956	267.3786	8.70E-59	8.70E-59
Copper	Al	195.6049	0	1	1
	Li	263.6882	68.08332	1.64E-15	1.64E-15
	Zr	350.6677	155.0628	2.13E-34	2.13E-34
	Ti	378.5462	182.9413	1.88E-40	1.94E-40
	OM	385.4825	189.8776	5.87E-42	5.87E-42
Lead	Li	170.8444	0	0.999999	1
	Al	198.4352	27.59082	1.02E-06	1.02E-06
	Zr	232.828	61.98362	3.47E-14	3.47E-14
	Ti	278.7717	107.9273	3.66E-24	4.05E-24
	OM	283.2612	112.4168	3.88E-25	3.88E-25
Nickel	Al	299.9726	0	0.9999938	1
	Li	323.9603	23.98766	6.18E-06	6.18E-06
	Zr	392.5817	92.60904	7.77E-21	7.77E-21
	Ti	417.2645	117.2918	3.39E-26	3.40E-26
	OM	429.4038	129.4312	7.84E-29	7.84E-29
Zinc	Al	407.2074	0	1	1
	Li	450.7297	43.52223	3.54E-10	3.54E-10
	Zr	547.0623	139.8548	4.27E-31	4.27E-31
	Ti	570.0306	162.8232	4.40E-36	4.44E-36
	OM	579.2037	171.9962	4.48E-38	4.48E-38

Development of pre-1920 metals concentrations baselines

Metal-normalizer crossplots for lakes PAD 65 and PAD 67 are plotted together on one linear regression for each metal of concern for pre-1920 data (Figure 11), and the resulting R^2 values are high, ranging between 0.78 and 0.99 (Table 4), supporting the use of aluminum as a normalizer. Results demonstrate that both lakes can be used together to develop each regression, and thus more robust baseline relations emerge. This strongly suggests that both lakes have a common source of metals, improving the value and credibility of a regional baseline. Aluminum ranges from 9000 to 20500 ug/g. The metals of concern also span a broad range, with maximum concentrations about double the minimum concentrations of each metal. Overall, the metal concentrations from PAD 65 are more tightly clustered and are lower in concentration than PAD 67, which span a broader range. For example, the PAD 65 sediment aluminum concentration ranges from 9000 to 13000 ug/g, while PAD 67 ranges from 10000 to 20500 ug/g. This range could indicate that higher aluminum concentrations may result from smaller grain sizes, suggesting that PAD 65 captures higher-energy conditions, while PAD 67 captures lower-energy conditions, presenting a suitable range of hydrologic conditions in the assessment of post-industrial samples that may also reflect a range of hydrological conditions. It should be noted that some baseline concentrations of cadmium, copper, and zinc exceed the interim sediment quality guideline (ISQG) as defined by the Canadian Council of Ministers of the Environment (CCME's Water Quality Guidelines and Soil Quality Guidelines Task Groups 2015).

Table 4: Regression statistics for Peace Sector (PAD 65 and PAD 67) metals vs Aluminum for samples dated pre-1920.

Metal(loid)	R^2	Y-intercept	Slope	p-value
Be	0.8756	0.124	4.985e-5	<2.2e-16
Cd	0.8387	0.227	3.242e-5	<2.2e-16
Cr	0.9863	1.412	1.661e-3	<2.2e-16
Cu	0.9541	8.242	1.579e-3	<2.2e-16
Pb	0.7798	4.541	6.660e-4	<2.2e-16
Ni	0.8681	9.108	2.007e-3	<2.2e-16
V	0.9549	2.921	3.095e-3	<2.2e-16
Zn	0.9344	0.194	6.823e-3	<2.2e-16

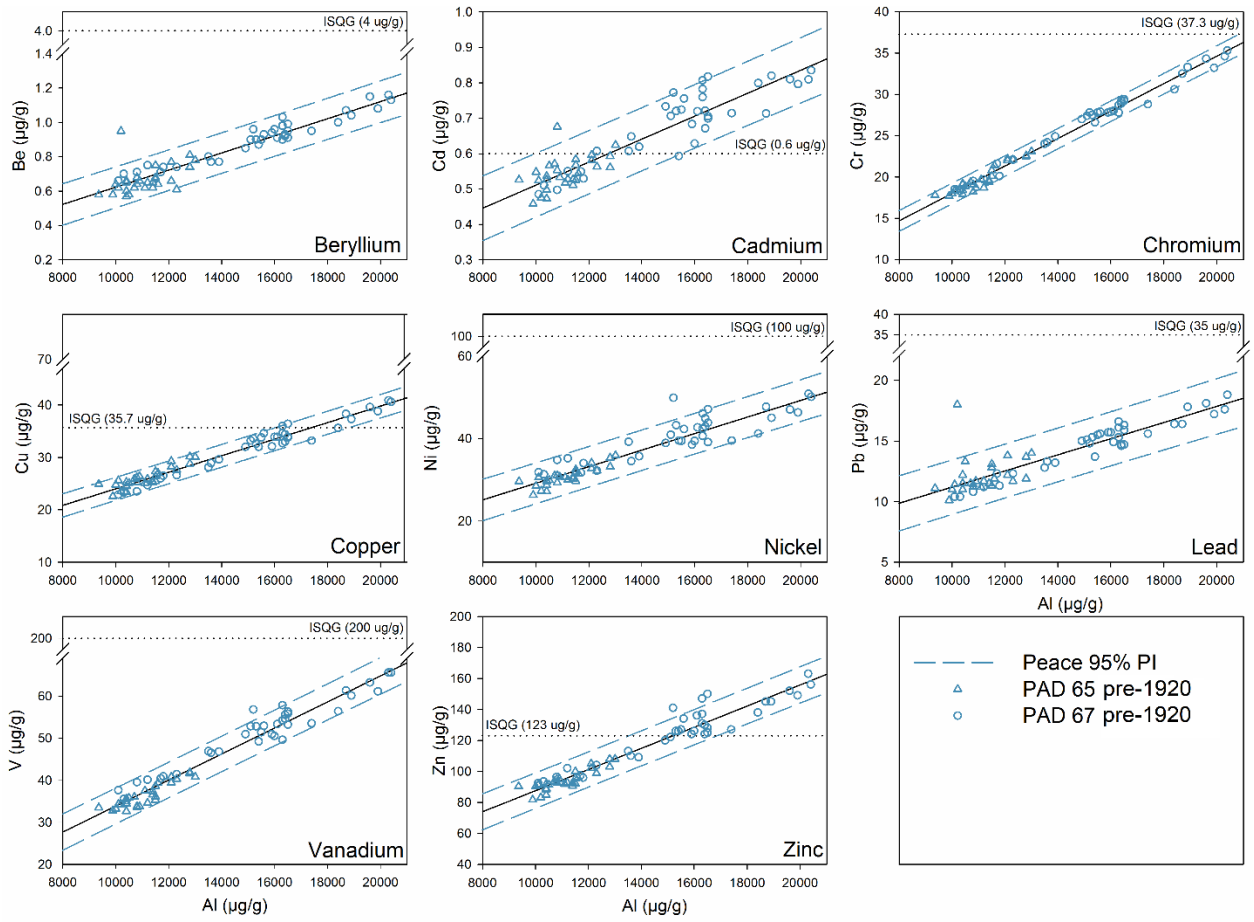

Figure 11: Metal-normalizer relationships from core samples dated as pre-industrial (pre-1920) from PAD 65 and PAD 67.

Assessment of post-1920 metals concentrations on pre-1920 baselines

The post-1920 data from PAD 65 and PAD 67 span similar ranges as the pre-1920 data (Figure 12). As with the pre-1920 baseline data, the data from PAD 65 lie in the lower ranges of metal concentrations, while PAD 67 lies in the upper ranges. The majority of the sediment samples from PAD 65 lie below the upper 95% prediction interval for all metals, consistent with the pre-1920 baseline. Some samples lie above the prediction interval: one of the 26 samples of chromium and zinc (4%), but 27% of copper (seven samples). For PAD 67, the majority of the post-1920 data lie above the 95% PI for cadmium (80% of the samples, 16 of 20 samples), copper (85%, 17 samples), nickel (65%, 13 samples),

and zinc (90%, 18 samples), and one sample from lead (5%). The other metals (beryllium, chromium, lead, and vanadium) show no elevated concentrations with respect to the baselines.

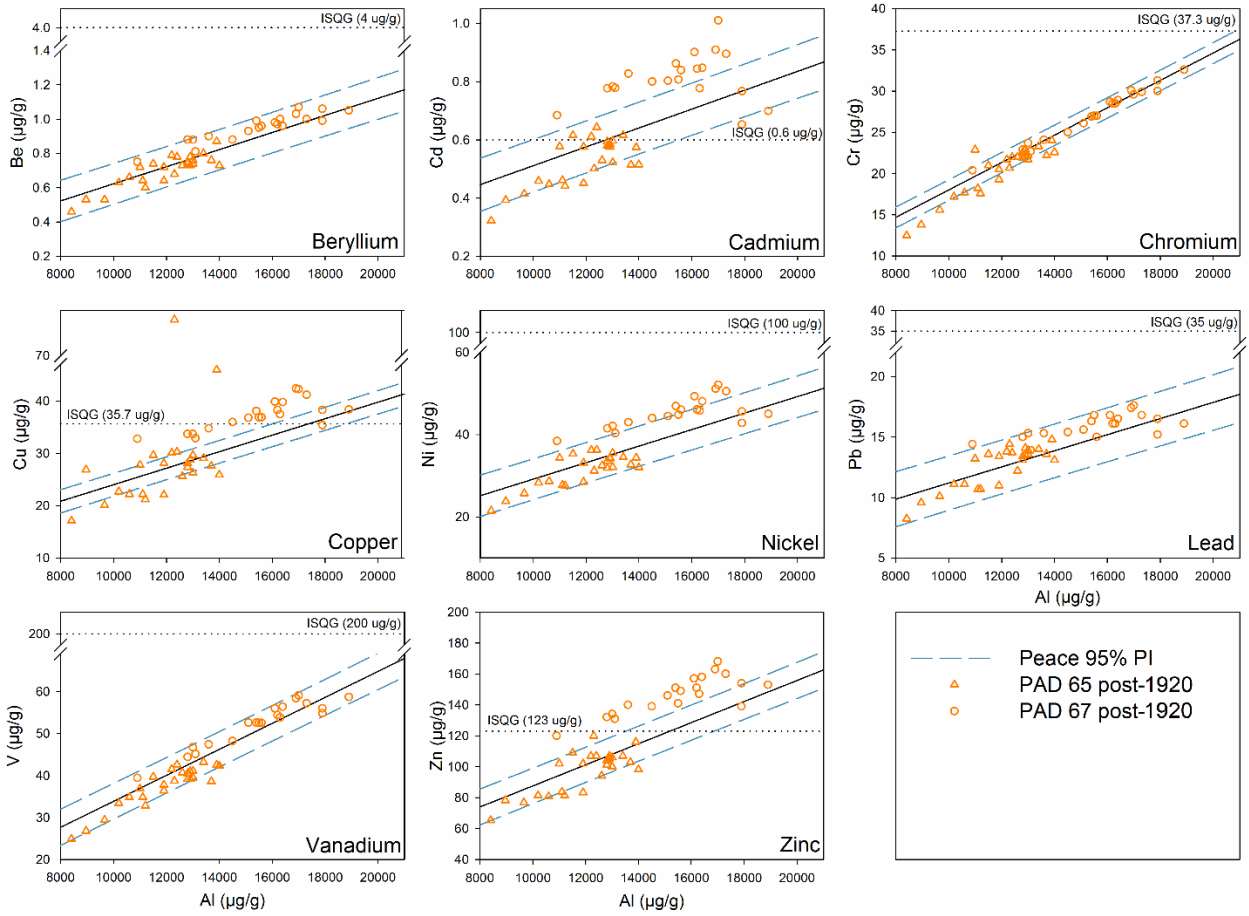

Figure 12: Post-industrial (post-1920) samples plotted on the pre-industrial metal-normalizer relationships from PAD 65 and PAD 67.

Enrichment factors as an indication of anthropogenic influence

At PAD 65, the enrichment factor of all eight metals generally follow a linear trend with some variation about 1.0 (Figure 13). Cd, Cr, Cu, Ni, Pb, and V peak at 1835 (to max 1.2 for Be), followed by a period of slight enrichment until another peak at 1928 (to 1.1 for Be). The enrichment factor decreases, again, to ~1 for all metals except Pb until 1965. After 1965, there is much variation between 0.8 and 1.2. The sample enriched in Zinc at 1750 is likely an erroneous measurement, considering the low EF values of all the other measurements of Zinc. Importantly, besides this value, these enrichment factors are well

below the EF of 1.5 that is considered by Birch (2017) to be threshold between pristine conditions and minimal modification.

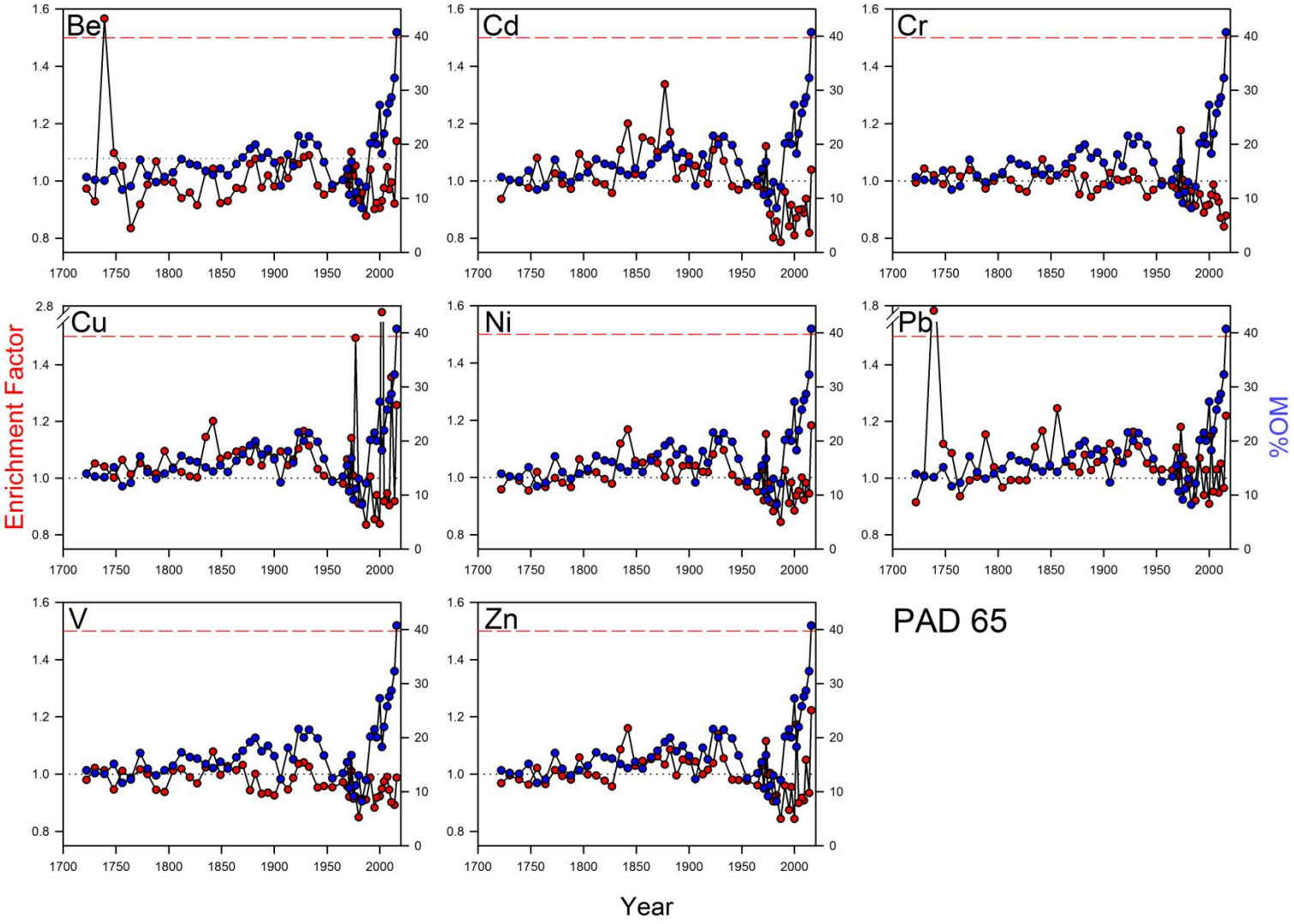

Figure 13: Enrichment factors and organic matter percent over time at PAD 65.The dashed red line indicates the EF of minimum infuence of 1.5, as recommended by Birch (2017).

The enrichment factors at PAD 67 show very similar trends among all metals (Figure 14). There is a peak in metal EF values between ca. 1852 and 1900 (max Ni to 1.21). This is followed by a trough until 1945, and then a rise until present (max copper 1.36). Though it may be tempting to attribute this increase to industrial activity, an examination of the organic matter is necessary to understand the

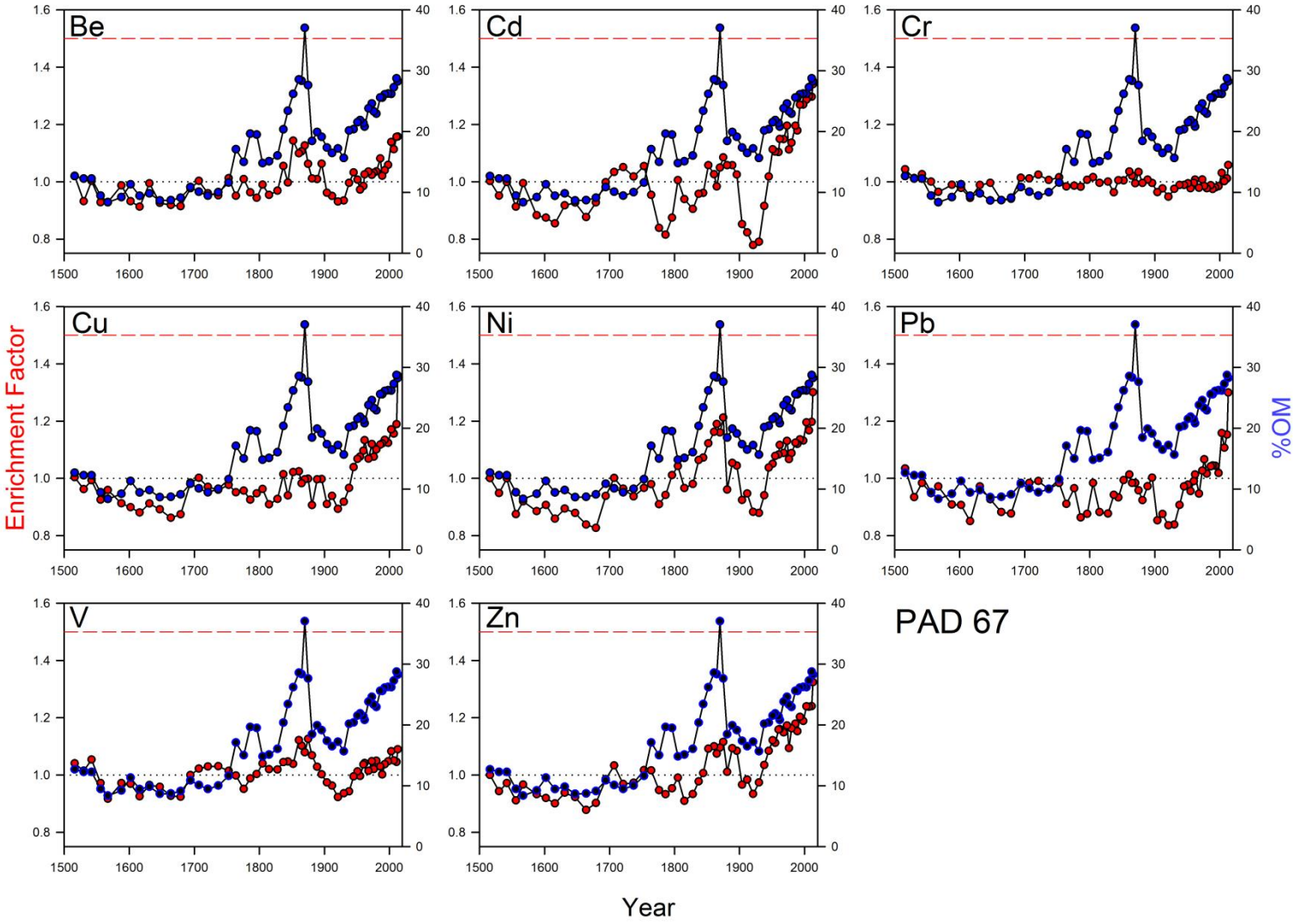

Figure 14: Enrichment factors and organic matter percent over time at PAD 67. The dashed red line indicates the EF of minimum infuence of 1.5, as recommended by Birch (2017).

processes occurring here (Figure 14). It is well known that metals adsorb very readily to organic matter (Elliott & Denneny 1982; Killey et al. 1984; Curtis et al. 1986; Ashworth & Alloway 2008; Boechat et al. 2016), and in this lake the OM% appears to be very closely positively correlated to the EF. It is interesting to note as well that the metals increased during a period of less frequent flooding. As at PAD 65, all enrichment factor measurements lie well below the 1.5 EF threshold of minimal modification (Birch 2017).

Chapter 4: Discussion

The perched lakes of the Peace sector of the PAD are thought to be recharged mainly during ice-jam flood events that occur via overland flow of the Peace River (Prowse & Lalonde 1996). These shallow lakes provide an excellent basis for a paleolimnological project that addresses the two objectives of this study. Because of their dependence on ice-jam floods, the flood frequency of these perched basins may be potentially affected by changes in climate and river regulation that might influence the potential for ice-jams to form on the Peace River in the vicinity of the PAD. Developing an understanding of pre-dam conditions allows for a comparison to post-dam conditions.

These lakes also provide a record of river sediment metal concentrations, as metals associated with organic and inorganic particles from the river are supplied to each lake during ice-jam flood events. Using a dated sediment core can provide a record of changes in metal concentrations through time (Wiklund, Hall, Wolfe, et al. 2012; Kay et al. 2020). This provides an understanding of "baseline" metals concentrations, against which contemporary sediments and river-borne materials can be compared to assess for enrichment due to industrial activity.

Using Lake Sediment Cores to Establish Pre-1968 Baseline Hydrologic Conditions

Within the Peace sector of the PAD, previously published sediment core records from PAD 5, PAD 15, and PAD 54 show drying trends since the early 20th century (see Figure 15,Wolfe et al. 2005; 2006). At PAD 54 and PAD 15, decreases in magnetic susceptibility are associated with reduction in flood frequency and magnitude as the sediment becomes more organic, and contains less magnetic-rich inorganic material. At PAD 5, the cellulose-inferred lake water $\delta^{18}O$ gradually increases since the

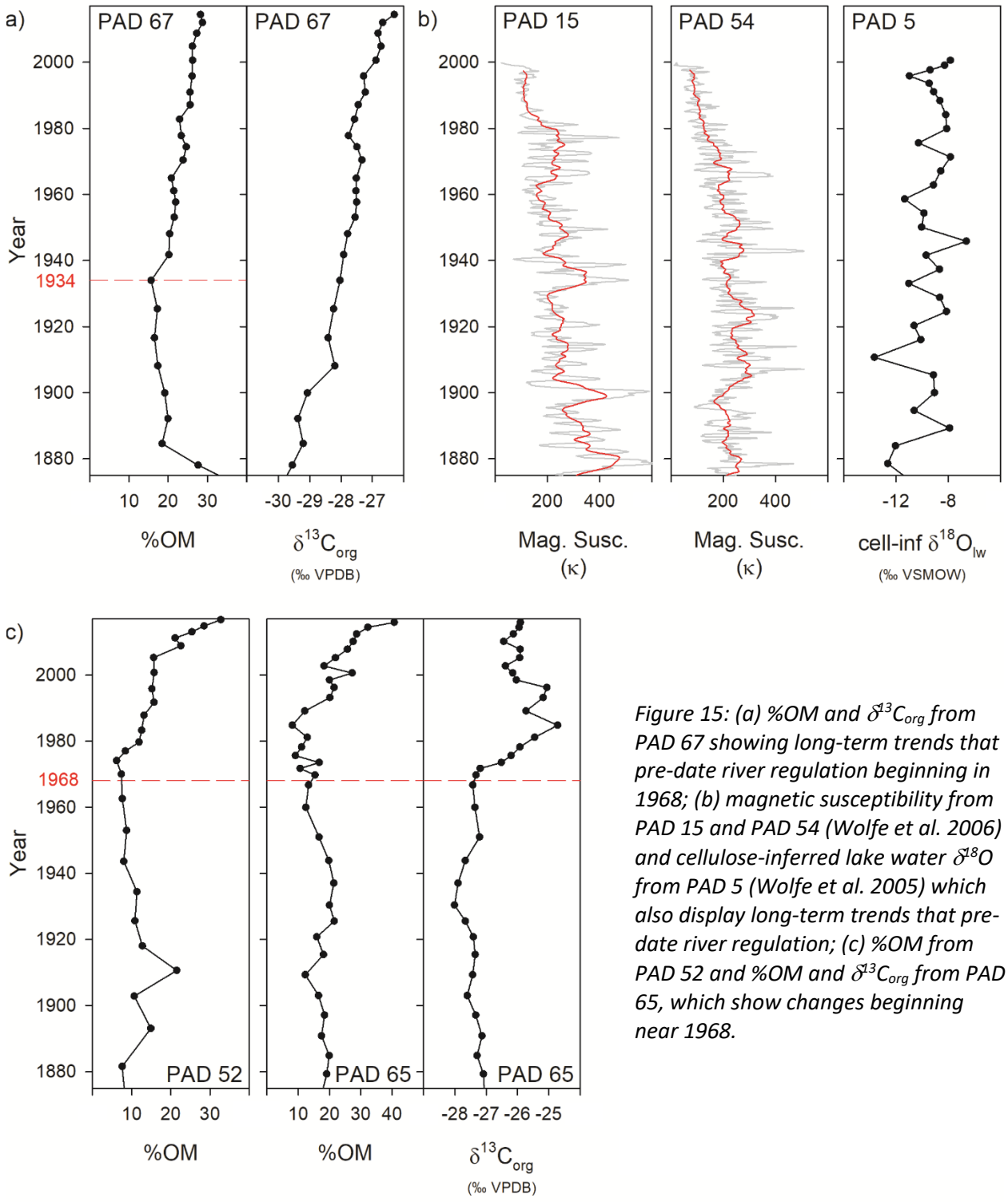

Figure 15: (a) %OM and $\delta^{13}C_{org}$ from PAD 67 showing long-term trends that pre-date river regulation beginning in 1968; (b) magnetic susceptibility from PAD 15 and PAD 54 (Wolfe et al. 2006) and cellulose-inferred lake water $\delta^{18}O$ from PAD 5 (Wolfe et al. 2005) which also display long-term trends that pre-date river regulation; (c) %OM from PAD 52 and %OM and $\delta^{13}C_{org}$ from PAD 65, which show changes beginning near 1968.

1940s, reflecting increasing importance of evaporation to the lake water balance. Here, at PAD 65 and 67, increases in $\delta^{13}C_{org}$ indicates that the increase in OM is due to increases in aquatic productivity.

Declining flood frequency due to a changing climate

At PAD 67 there is no directional change observed around 1968. It may be argued that the lack of response to the construction of the dam is due to the lake's location along the Slave River, below the conjunction of the Peace and Athabasca waters and therefore affected by the Athabasca River, but this is unlikely. The Peace River is estimated to contribute 76.5% of the Slave River discharge in April, when the ice jam floods occur (English et al. 1996), and thus PAD 67 is expected to be susceptible to changes in the Peace River hydrograph. Because the lake is beyond the extent of the PAD, it has been omitted from water sampling and has not been visited since the lake was cored in 2016, and consequently, hydrologic regime cannot be inferred from water chemistry or isotopic analysis. However, satellite imagery and photographs taken during the sampling suggest that the lake is not experiencing extensive drying, and the slow drying trend observed in the paleolimnological record began decades before the construction of the Bennett Dam, likely in step with the records of declining flood frequency at PAD 15 and PAD 54, increasing evaporation at PAD 5, and climate warming (Wolfe et al. 2005; 2006).

Declining flood frequency due to river regulation by the Bennett Dam

In contrast to the paleolimnological data obtained from PAD 67, PAD 52 and PAD 65 show directional shifts in paleolimnological data approximately concurrent with the construction of the dam in 1968. These two lakes display shifts toward less flood-prone conditions after 1968 (+/- 17 years) at PAD 52, and after 1965 (+/- 10 years) at PAD 65, as identified by a transition from Phase 1 to Phase 2 at both lakes. This suggests that these lakes are more sensitive to regulation-driven changes in the hydrologic regime of the Peace River than many other lakes in the PAD where paleolimnological records have been obtained (Figure 16).

Previous research in the PAD includes sediment cores collected from 16 other lakes in the floodplain of the Peace sector of the PAD (See Figure 16). Notably, PAD 52 and PAD 65 are the **first** to show an inferred increase in aquatic productivity that aligns with the timing of the construction of the WAC Bennett Dam. It is possible that these lakes have a sill elevation that is lower than the perched lakes that have been drying since before the installation of the dam, and yet higher than lakes with a low enough sill elevation to still receive ice-jam flooding after the regulation of the Peace River, and are thus situated at a precise elevation and proximity to the Peace River for changes in Peace River hydrology to have affected them. Notably, both these lakes are estimated to have an elevation within one metre of the Peace River during open-water flow conditions. Alternately, fluvial geomorphologic processes may have affected these two lakes in the 1960s, coincident with, but not a result of, the construction of the Bennett Dam. It is worth noting, too, the error values on the dates at both lakes, leaving the possibility that the observed changes occurred 30 years apart, though the peaks in sedimentation rate at both lakes, dated at 1976 at PAD 52 and at 1973 at PAD 65, align very closely with the large flood event of 1974.

Another possible reason for the decrease in flood frequency at PAD 65 and PAD 52 is a decline in open-water flood events. Regulation of the Peace River has substantially influenced the hydrograph during the open-water period (Figure 3). It is possible that these lakes are located at elevations and in close enough proximity to the Peace River to be affected by open-water flood frequency. Although these flood events have not been known to be the main source of floodwaters to perched lakes in the Peace sector of the PAD, recent lake monitoring in the Athabasca sector of the PAD has shown this hydrological process to be important (Neary, PhD in progress). Further studies are required to test this hypothesis.

Considering the number of studied lakes that began drying before 1968, compared to the two that have shown drying at 1968, it is unlikely that the change in the Peace River hydrograph is the

dominant factor in the drying of the perched lakes in the PAD. These two lakes lie within relatively close proximity to the Peace River, and a preliminary "zone of influence" of the Bennett Dam can be drawn (dashed line in Figure 16). This zone is likely only within a few kilometres of sharp bends in the Peace River, where ice jams occur, and at relatively low elevation. Outside this zone, climate appears to be the main driver of lake hydrological change in the Peace sector. Several other lakes have been cored since the analysis of PAD 52 and 65, along a transect from the Peace River (PAD sites 72-74 and 78-82), and their results will better define the apparent limited extent of influence of the dam on lake water balances.

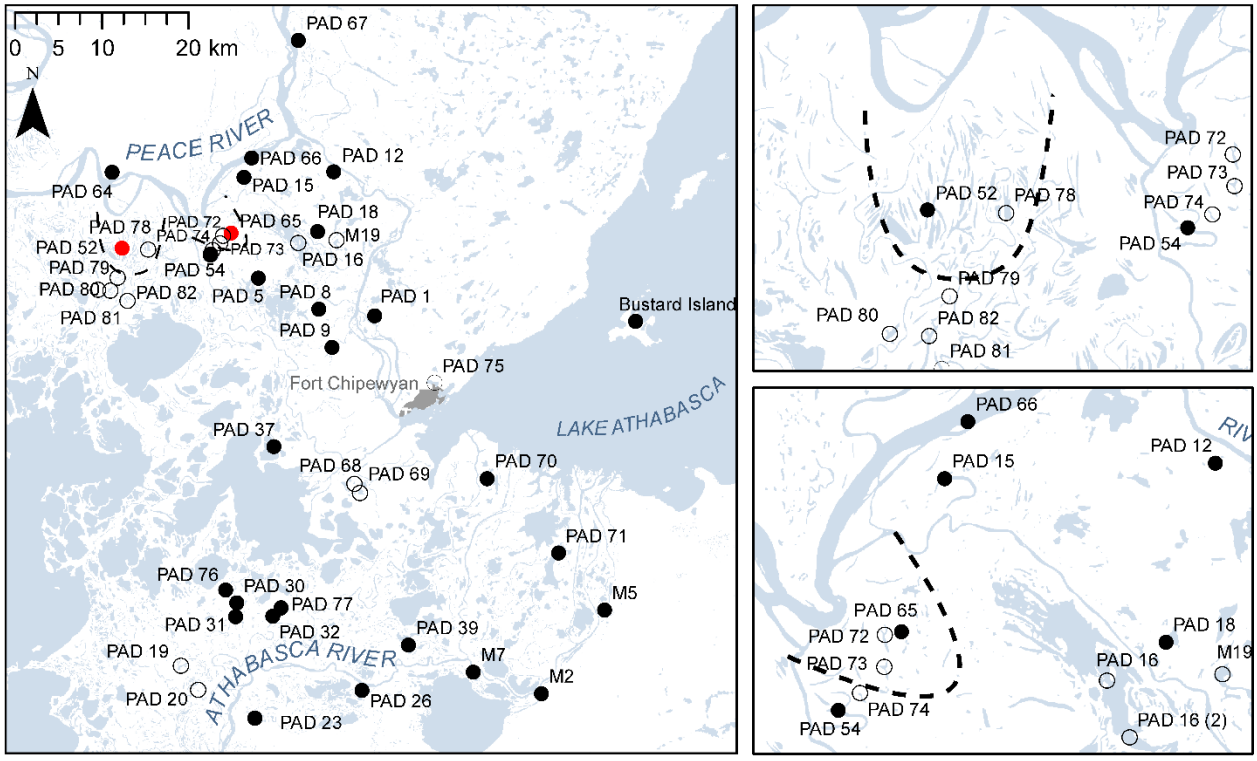

Figure 16: All cored lakes of the Peace-Athabasca Delta by the Hall-Wolfe research group, as of 2020. Lakes symbolized with open circles indicate that analysis is in progress. Note that there are 38 lakes that have been analyzed, and PAD 52 and PAD 65 are the first that show directional change at the time of the constructon of the W. A. C. Bennett Dam. Dashed lines speculate on the potential zone of influence of the Bennett Dam. Figure was created using ArcGIS Desktop version 10.7.1 and assembled using self-generated shapefiles and files from the from the University of Calgary (water bodies: https:// library.ucalgary.ca/c.php?g=255401&p=1705346)

Using lake sediment cores to establish pre-1920 baseline metals concentrations

Lake sediment cores from PAD 65 and PAD 67, two of the perched lakes of this study, act as excellent natural archives of metals carried by the Peace River. The examination of sediment metal concentrations in these sediment cores is the first step in characterising the natural supply of sediment metals to the PAD via the Peace River. The characterisation of the sediment provided to the delta by both the Peace and Athabasca rivers allows for assessment of the influence of each river at any lake in the PAD, for both contemporary sediment deposition (Owca et al. 2020), and the relative influence of each river at any point in the past via the examination of sediment cores.

The metal-normalizer relationships explored here provide a reliable dataset for the assessment of pre-industrial metal concentrations. The pre-industrial data from both lakes fall on the same relationship, suggesting that these data may provide an accurate representation of Be, Cd, Cr, Cu, Ni, Pb, V, and Zn supplied by the Peace River (Figure 11), though these two lakes are only a preliminary assessment of the many lakes in the Peace sector of the PAD. Contemporary normalized metals can be compared to pre-industrial conditions to assess for enrichment of the Peace River. This has been successfully demonstrated in the analysis of surface sediments by Owca et al. (2020), using the baselines developed here. Also, this addresses Recommendation 7 of the UNESCO Reactive Monitoring Mission, to "Establish adequate baseline hydrological information of the Peace and Athabasca River Basins to enhance the reference for monitoring and assessing current and future hydrological conditions" (WHC/IUCN 2017, p. 4).

Post-industrial metals from PAD 67 show increases in cadmium, copper, nickel, and zinc. The majority of data points from these metals lie slightly above the 95%PI. However, calculation of the enrichment factor shows that no metals exceed an EF value of 1.5, considered by Birch (2017) to be the threshold of minimal influence. It is unlikely that these are a result of industrial development for several reasons. Firstly, oil sands pollution can be omitted because vanadium, the metal most associated with

the refinement of bitumen in the Alberta oil sands, is not significantly elevated. Secondly, the metals enrichment in this lake appears to be strongly correlated to OM% in the past century (Figure 14), suggesting an association between the enrichment in Cd, Cu, Ni, and Zn and increased aquatic productivity. This may reflect metals scavenging process by algae, which are known to sequester metals (Gekeler et al. 1988). This has been shown to be especially true of Cd, Cu, Ni, and Zn, the metals found to be especially elevated here at PAD 67 (Behra et al. 2002; Holding et al. 2003; Romera et al. 2007; Abirhire & Kadiri 2011), though the relationship between organic matter and metals is complex.

It is likely that this association with %OM reflects an increase in scavenging and uptake of metals by algae as the productivity of the lake increases and the influence of floodwater decreases. This is similar to findings by Wolfe and Härtling (1997), where copper, chromium, lead, nickel, and zinc were concentrated in association with OM, associated with a changing climate. They reported this effect to not be true for vanadium, which displays the least increase with %OM in the upper sediments of PAD 67. A similar effect has been seen in scavenging of adsorbable organically-bound halogens in the water column, also associated with climate variation (Stern et al. 2005). At PAD 65, on the other hand, %OM appears to cause dilution, where increases in %OM are associated with decreases in EF, and vice versa. This also appears to be true at PAD 67 between 1700 and 1800. Evidently, further research is needed to understand the role of organic matter and its influence on metal deposition in the lakes of the PAD.

Conclusions

This research aimed to enhance knowledge of the potential hydrological effects of the WAC Bennett Dam on perched basins near the Peace River in northern part and vicinity of the Peace-Athabasca Delta. The analysis of dated sediment cores provided data to identify changes in hydrological conditions of three lakes during the past several decades. Research also developed pre-industrial metal-normalizer relationships at two lakes, as a reference of the ratios of metals supplied to the delta by the Peace River, and examination of post-1920 metal concentrations.

Paleohydrological reconstructions

This project identified two lakes (PAD 52, PAD 65), the first of sixteen examined in the Peace sector of the PAD, that displayed directional changes in proxies of flood frequency near the time of the installation of the Bennett Dam. A third lake in this project, PAD 67, was in agreement with the findings at the other perched lakes of the Peace sector, where reduction in flood frequency and lake drying has been identified to having begun decades before the construction of the WAC Bennett Dam (Wolfe et al. 2005; 2006; 2012; 2020). Considering the former, abrupt changes were observed in organic matter content at PAD 52, and organic matter content, C/N ratio, and $\delta^{13}C_{org}$ at PAD 65. These stratigraphic changes are consistent with an increase in aquatic productivity and decreased influx of minerogenic sediment due to declining flood frequency, identified in the stratigraphic record of PAD 52 at 1968 (+/- 17 years), and in the record of PAD 65 at 1965 (+/- 10 years), near in timing to the construction of the Bennet Dam, which was completed in 1968. It is probable that the effects of the dam reconstructed here are spatially limited, since these are the first two of more than 30 lakes in the PAD to show a possible hydrological effect of the dam. This is likely because of the close proximity of PAD 52 and PAD 65 to the Peace River (3.2 and 2.2 km, respectively) and their elevations are within a metre of the river during typical open-water conditions. The effects of a warming climate are also likely having a strong influence on these observed changes, in which decreasing river ice strength and thickness, decreasing spring

runoff, and increased freeze-up elevation are resulting in fewer ice-jam flood events (Prowse & Lalonde 1996; Prowse & Conly 1998; Beltaos et al. 2006; Prowse et al. 2006), and possibly changing flood magnitude as well. It is also possible that the changes reconstructed at these lakes are not a direct result of the Bennett Dam, but rather a consequence of climatic changes, as seen at other lakes in the Peace sector of the PAD over the past century (Wolfe et al. 2005; Wolfe et al. 2006; Wolfe et al. 2012). Ultimately, it is most likely that a combination of factors are causing the changes observed here. An analysis of grain size could be used to better define periods of high and low flood events, and also define flood magnitude, which in turn may explain whether a reduction in open-water floods or ice-jam flood events are the cause of the paleolimnological trends seen here. An analysis of cellulose $\delta^{18}O$ could provide insight to the changes in evaporation of the lakes, better defining and understanding the years of low or high flood frequency.

Metal deposition

In this study, strong linear metal-normalizer relationships were developed at lakes PAD 65 and PAD 67 for eight metals of concern, including beryllium, cadmium, copper, chromium, nickel, lead, vanadium, and zinc. All post-industrial normalized concentrations at PAD 65 plotted within the 95% prediction interval, as did beryllium, chromium, lead, and vanadium at PAD 67. But at PAD 67 the post-1920 data for cadmium, copper, nickel, and zinc plotted above the 95%PI. The calculation of enrichment factors provided a further examination of these post-industrial metals, to quantify levels of enrichment and to observe temporal trends. At PAD 65, there is no enrichment in recent decades, but at PAD 67 there are increases in the enrichment factor of all metals. However, these increases are still below the threshold of “minimal influence” of 1.5 suggested by Birch (2017). Additionally, these increases appear to be strongly correlated with percent organic matter, suggesting that changes in the lake’s hydrologic processes have resulted in metals scavenging by algal matter (Gekeler et al. 1988; Behra et al. 2002; Holding et al. 2003; Romera et al. 2007; Abirhire & Kadiri 2011). However, this relationship with organic

matter is complex, as the opposite trends are seen at PAD 65, where increases in OM occur at times when the enrichment factor decreases, and vice versa.

These results contribute to addressing the concerns of local stakeholders, including the community of Fort Chipewyan, UNESCO, and Wood Buffalo National Park. Wood Buffalo National Park is at risk of being added to the list of World Heritage in Danger, downstream of major industrial activity on two of Canada's largest rivers. These results build on previous sediment cores analysed from the Peace sector of the PAD (Wolfe et al. 2005; 2006), which address Recommendation 7 of the Reactive Monitoring Mission (WHC/IUCN 2017), to establish baseline hydrologic information of the Peace and Athabasca River basins. The contemporary assessment of metal deposition on the metal-normalizer relationships also address Parks Canada's call for further environmental assessment in the WBNP Action Plan (2019).

Recommendations

The sediment cores in this research project expanded on previous studies in the Peace sector of the PAD, but still represent only a small portion of the Peace sector and also raised further questions. Two lakes here display changes in hydrology around the time of the construction of the Bennett Dam. The analysis of sediment cores from adjacent lakes in the Peace sector of the PAD will be useful in better defining the extent of potential influence of the Bennett Dam, and, in light of the construction of the Site C Dam, identify which lakes in the PAD are susceptible to further changes in the hydrology of the Peace River (see Figure 16 for lake sediment core analyses in progress).

The metal-normalizer relationships developed here have been critical in the development of monitoring frameworks for metals in the PAD, carried out by Owca et al. (2020), where contemporary surface sediments have been compared to the natural range of variation of these metals as measured in this study. At this point, only two lakes have been used as the baseline for these metals, and although they comprise a total of ~60 measurements pre-1920, the incorporation of pre-industrial data from a variety of lakes in the Peace sector would further strengthen our understanding of the natural range of

variation of metals in the Peace sector of the PAD. This knowledge would also build our understanding of the natural supply of metals from the Peace River versus the Athabasca River, and the influence of each river in different lakes and regions of the PAD.

References

Abirhire O, Kadiri MO. 2011. Bioaccumulation of heavy metals using microalgae. Asian Journal of Microbiology, Biotechnology and Environmental Sciences. 13(1):91–94.

Appleby PG. 2001. Chronostratigraphic Techniques in Recent Sediments. In: Last WM, Smol JP, editors. Tracking environmental Change Using Lake Sediments Volume 1: Basin Analysis, Coring, and Chronological Techniques. Dordrecht, the Netherlands: Kluwer Academic Publishers; p. 171–203.

Appleby PG, Oldfield F. 1978. The calculation of lead-210 dates assuming a constant rate of supply of unsupported 210Pb to the sediment. Catena. 5(2):1–8.

Ashworth DJ, Alloway BJ. 2008. Influence of dissolved organic matter on the solubility of heavy metals in sewage-sludge-amended soils. Communications in Soil Science and Plant Analysis. 39(3–4):538–550.

Athabasca Chipewyan First Nation. 2003. Athabasca Chipewyan First Nations Traditional Land Use Study. Fort Chipewyan, Alberta: Athabasca Chipewyan First Nation.

Baker LF, Ciborowski JJH, MacKinnon MD. 2012. Petroleum coke and soft tailings sediment in constructed wetlands may contribute to the uptake of trace metals by algae and aquatic invertebrates. Science of the Total Environment. 414:177–186.

Behra R, Landwehrjohann R, Vogel K, Wagner B, Sigg L. 2002. Copper and zinc content of periphyton from two rivers as a function of dissolved metal concentration. Aquatic Sciences. 64(3):300–306.

Beltaos S. 2018a. Frequency of ice-jam flooding of Peace-Athabasca Delta. Canadian Journal of Civil Engineering. 45(1):71–75.

Beltaos S. 2018b. Reply to Discussions by Timoney et al (2018) and Hall et al (2018) on “Frequency of ice-jam flooding of Peace-Athabasca Delta.” Canadian Journal of Civil Engineering. 45:71–75.

Beltaos S, Peters DL. 2020. Naturalized flow regime of the regulated Peace River, Canada, during the spring breakup of the ice cover. Cold Regions Science and Technology. 172(December 2019):103005.

Beltaos S, Prowse TD, Bonsal B, MacKay R, Romolo L, Pietroniro A, Toth B. 2006. Climatic effects on ice-jam flooding of the Peace-Athabasca Delta. Hydrological Processes. 20:4031–4050.

Beltaos S, Prowse TD, Carter T. 2009. Ice regime of the lower Peace River and ice-jam flooding of the Peace-Athabasca Delta. Hydrological Processes. 20:4009–4029.

Bennett RM, Card JR, Hornby DM. 1973. Hydrology of lake athabasca: past, present and future. Hydrological Sciences Bulletin. 18(3):337–345.

Birch GF. 2017. Determination of sediment metal background concentrations and enrichment in marine environments – A critical review. Science of the Total Environment [Internet]. 580:813–831. http://dx.doi.org/10.1016/j.scitotenv.2016.12.028

Boechat CL, Pistóia VC, Ludtke AC, Gianello C, Camargo FA de O. 2016. Solubility of heavy metals/metalloid on multi-metal contaminated soil samples from a gold ore processing area: Effects of humic substances. Revista Brasileira de Ciencia do Solo. 40:1–10.

CCME’s Water Quality Guidelines and Soil Quality Guidelines Task Groups. 2015. Canadian Environmental Quality Guidelines [Internet]. [accessed 2018 Feb 10]. http://ceqg-rcqe.ccme.ca/en/index.html

Chastko PA. 2004. Developing Alberta's oil sands: from Karl Clark to Kyoto. Canada: University of Calgary Press.

Cronmiller JG, Noble BF. 2018. The discontinuity of environmental effects monitoring in the Lower Athabasca region of Alberta , Canada : institutional challenges to long-term monitoring and cumulative effects management. 180(January):169–180.

Curtis GP, Reinhard M, Roberts P V. 1986. Sorption of Hydrophobic Organic Compounds by Sediments. In: Geochemical Processes at Mineral Surfaces. Stanford, CA: American Chemical Society; p. 191–216.

Dean WEJ. 1974. Determination of carbonate and organic matter in calcareous sediments and sedimentary rocks by loss on ignition: comparison with other methods. Journal of Sedimentary Petrology. 44(1):242–248.

Dowdeswell L, Dillon P, Ghoshal S, Andrew M, Rasmussen J, Smol JP, Dowdesw L, Dillon P, Miall A, Smol JP. 2010. A foundation for the future: building an environmental monitoring system for the oil sands. A report submitted to the Minister of Environment.(December):47.

Edwards TWD, Birks SJ, Luckman BH, MacDonald GM. 2008. Climatic and hydrologic variability during the past millennium in the eastern Rocky Mountains and northern Great Plains of western Canada. Quaternary Research. 70(2):188–197.

Elliott HA, Denneny CM. 1982. Soil Adsorption of Cadmium From Solutions Containing Organic Ligands. Journal of Environmental Quality. 11(4):658–663.

English MC, Stone MA, Hill BR, Wolfe PM, Ormson R. 1996. Northern River Basins Study Project Report No. 74: Assessment of Impacts on the Slave River Delta of Peace River Impoundment at Hudson Hope. In: Northern River Basins Study. Edmonton, AB; p. 91.

Farquhar G., Ehleringer JR, K.T H. 1989. Carbon Isotope Discrimination and Photosynthesis. Annual review of Plant Physiology and Plant molecular biology. 40:503–37.

Fogel ML, Cifuentes LA. 1993. Isotope Fractionation during Primary Production. In: Engel MH, Macko SA, editors. Organic Geochemistry. New York: Plenum Press; p. 73–98.

Foster IDL, Mighall TM, Proffitt H, Walling DE, Owens PN. 2006. Post-depositional 137Cs mobility in the sediments of three shallow coastal lagoons, SW England. Journal of Paleolimnology. 35(4):881–895.

Galloway JN, Thornton JD, Norton SA, Volchok HL, McLean RAN. 1985. Trace metals in atmospheric deposition: A review and assessment. Atmospheric Environment. 16(7):1677–1700.

Gekeler W, Grill E, Winnacker EL, Zenk MH. 1988. Algae sequester heavy metals via synthesis of phytochelatin complexes. Archives of Microbiology. 150(2):197–202.

Gobeil C, Macdonald RW, Sundby B. 1997. Diagenetic separation of cadmium and manganese in suboxic continental margin sediments. Geochimica et Cosmochimica Acta. 61(21):4647–4654.

Gosselin P, Hrudey SE, Naeth MA, Plourde A, Van Der Kraak G, Xu Z. 2010. Environmental and health impacts of Canada's oil sands industry. Ottawa.

Hall RI, Wolfe BB, Wiklund JA. 2019. Discussion of "Frequency of ice-jam flooding of Peace-Athabasca Delta." Canadian Journal of Civil Engineering. 46(3):236–238.

Heiri O, Lotter A, Lemcke G. 2001. Loss on Ignition as a Method for Estimating Organic and Carbonate

Content in Sediments : Reproducibility and Comparability of Results. Journal of Paleolimnology. 25:101–110.

Holding KL, Gill RA, Carter J. 2003. The relationship between epilithic periphyton (biofilm) bound metals and metals bound to sediments in freshwater systems. Environmental Geochemistry and Health. 25(1):87–93.

Jasek M. 2019. An Emerging Picture of Peace River Break-up Types that Influence Ice Jam Flooding of the Peace-Athabasca Delta Part 1 : The 2018 Peace River Break-up. (May 2018).

Johnston JW, Köster D, Wolfe BB, Hall RI, Edwards TWD, Endres AL, Martin ME, Wiklund JA, Light C. 2010. Quantifying lake athabasca (Canada) water level during the “Little Ice Age” highstand from palaeolimnological and geophysical analyses of a transgressive barrier-beach complex. Holocene. 20(5):801–811.

Juichang R, Freedman B, Coles C, Zwicker B, Holzbecker J, Chatt A. 1995. Vanadium contamination of lichens and tree foliage in the vicinity of three oil-fired power plants in Eastern Canada. Journal of the Air and Waste Management Association. 45(6):461–464.

Kay ML, Wiklund JA, Remmer CR, Owca TJ, Klemt WH, Neary LK, Brown K, MacDonald E, Thomson K, Vucic JM, et al. 2020. Evaluating temporal patterns of metals concentrations in floodplain lakes of the Athabasca Delta (Canada) relative to pre-industrial baselines. Science of the Total Environment. 704:135309.

Kelly EN, Schindler DW, Hodson P V, Short JW, Radmanovich R, Nielsen CC. 2010. Oil sands development contributes elements toxic at low concentrations to the Athabasca River and its tributaries. :1–6.

Kelly EN, Short JW, Schindler DW, Hodson P V., Ma M, Kwan AK, Fortin BL. 2009. Oil sands development contributes polycyclic aromatic compounds to the Athabasca River and its tributaries. Proceedings of the National Academy of Sciences. 106(52):22346–22351.

Kersten M, Smedes F. 2002. Normalization procedures for sediment contaminants in spatial and temporal trend monitoring. Journal of environmental monitoring : JEM. 4(1):109–115.

Khalaf F, Literathy V, Anderlini V. 1982. Vanadium as a tracer of oil pollution in the sediments of Kuwait. Hydrobiologia. 91–92(1):147–154.

Killey RWD, McHugh JO, Champ DR, Cooper EL, Young JL. 1984. Subsurface Cobalt-60 Migration from a Low-Level Waste Disposal Site. Environmental Science and Technology. 18(3):148–157.

Leng MJ, Lamb AL, Marshall JD, Wolfe BB, Jones MD, Holmes JA, Arrowsmith C. 2005. Isotopes in Lake Sediments. In: Leng MJ, editor. Isotopes in Palaeoenvironmental Research. Dordrecht, the Netherlands: Springer; p. 147–184.

Loring DH. 1991. Normalization of heavy-metal data from estuarine and coastal sediments. ICES Journal of Marine Science. 48(1):101–115.

MacDonald LA, Wiklund JA, Elmes MC, Wolfe BB, Hall RI. 2016. Paleolimnological assessment of riverine and atmospheric pathways and sources of metal deposition at a floodplain lake (Slave River Delta, Northwest Territories, Canada). Science of the Total Environment. 544:811–823.

Meko DM. 2006. Tree-Ring Inferences on Water-Level Fluctuations of Lake Athabasca. Canadian Water Resources Journal. 31(4):229–248.

Meyers PA. 1994. Preservation of elemental and isotopic source identification of sedimentary organic matter. Chemical Geology. 114:289–302.

Meyers PA, Ishiwatari R. 1993. Lacustrine organic geochemistry-an overview of indicators of organic matter sources and diagenesis in lake sediments. Organic Geochemistry. 20(7):867–900.

Meyers PA, Leenheer MJ, Eaoie BJ, Maule SJ. 1984. Organic geochemistry of suspended and settling particulate matter in Lake Michigan. Geochimica et Cosmochimica Acta. 48(3):443–452.

Meyers PA, Teranes JL. 2001. Sediment Organic Matter. In: Last WM, Smol JP, editors. Tracking Environmental Change Using Lake Sediments Volume 2: Physical and Geochemical Methods. Dordrecht, the Netherlands: Kluwer Academic Publishers; p. 239–269.

Mikisew Cree First Nation. 2014. Petition to the World Heritage Committee. Fort McMurray, AB.

Mizutani H, Wada E. 1982. Effect of high atmospheric CO2 concentration on δ13C of algae. Origins of Life. 12(4):377–390.

O'Leary MH. 1981. Carbon isotope fractionation in plants. Phytochemistry. 20(4):553–567.

Oldfield F, Appleby PG. 1984. Empirical testing of 210Pb-dating models for lake sediments. In: Haworth EY, Lund JWG, editors. Lake Sediments and Environmental History. Minneapolis, MN: University of Minnesota Press; p. 93–124.

Owca TJ, Kay ML, Faber JA, Remmer CR, Zabel N, Wiklund JA, Wolfe BB, Hall RI. 2020. Use of pre-industrial baselines to monitor anthropogenic enrichment of metals concentrations in recently deposited sediment of floodplain lakes in the Peace-Athabasca Delta (Alberta, Canada). Environmental Monitoring and Assessment. 192(2).

Parks Canada. 2019. Wood Buffalo National Park World Heritage Site Action Plan [Internet]. Gatineau, QC: Library and Archives Canada - Cataloguing in Publication. https://www.pc.gc.ca/en/pn-np/nt/woodbuffalo/info/action

Peace-Athabasca Delta Ecological Monitoring Program. Traditional Use in the Peace-Athabasca Delta [Internet]. [accessed 2020 Feb 24]. http://www.pademp.com/delta-way-of-life/traditional-use/

Peace-Athabasca Delta Implementation Committee. 1987. Peace-Athabasca Delta water management works evaluation: final report. [place unknown].

Peace-Athabasca Delta Project Group. 1972. Peace-Athabasca Delta: A Canadian Resource. Ottawa, ON: Queen's Printer.

Peace-Athabasca Delta Project Group. 1973. Peace-Athabasca Delta Project, technical report and appendices. Alberta.

Peace-Athabasca Delta Technical Studies. 1996. Peace-Athabasca Delta Technical Studies : Final Report. Macmillan S, editor. Alberta.

Peters DL, Prowse TD. 2001. Regulation effects on the lower Peace River, Canada. Hydrological Processes. 15(16):3181–3194.

Peters DL, Prowse TD, Marsh P, Lafleur PM, Buttle JM. 2006. Persistence of water within perched basins of the Peace-Athabasca Delta, Northern Canada. Wetlands Ecology and Management. 14(3):221–243.

Peters DL, Prowse TD, Pietroniro A, Leconte R. 2006. Flood hydrology of the Peace-Athabasca Delta,

northern Canada. Hydrological Processes. 20(19):4073–4096.

Peterson M. 1995. PAD Flood History Study final report. Fort Chipewyan, Alberta.

Prowse TD, Beltaos S, Gardner JT, Gibson JJ, Granger RJ, Leconte R, Peters DL, Pietroniro A, Romolo LA, Toth B. 2006. Climate change, flow regulation and land-use effects on the hydrology of the Peace-Athabasca-Slave system; Findings from the Northern Rivers Ecosystem Initiative. Environmental Monitoring and Assessment. 113(1–3):167–197.

Prowse TD, Conly FM. 1998. Effects of climatic variability and snow regulation on ice-jam fooding of a northern delta. Hydrological Processes. 12:1589–1610.

Prowse TD, Conly FM. 2000. Multiple-hydrologic stressors of a northern Delta ecosystem. Journal of Aquatic Ecosystem Stress and Recovery. 8(1):17–26.

Prowse TD, Conly FM, Church M, English MC. 2002. A review of hydroecological results of the Northern River Basins Study, Canada. Part 1. Peace and Slave rivers. River Research and Applications. 18(5):429–446.

Prowse TD, Lalonde V. 1996. Open-water and ice-jam flooding of a Northern Delta. Nordic Hydrology. 27:85–100.

Remmer CR, Owca T, Neary L, Wiklund JA, Kay ML, Wolfe BB, Hall RI. 2020. Delineating extent and magnitude of river flooding to lakes across a northern delta using water isotope tracers. Hydrological Processes.(January 2020):303–320.

Romera E, González F, Ballester A, Blázquez ML, Muñoz JA. 2007. Comparative study of biosorption of heavy metals using different types of algae. Bioresource Technology. 98(17):3344–3353.

Sinnatamby RN, Yi Y, Sokal MA, Clogg-Wright KP, Asada T, Vardy SR, Karst-Riddoch TL, Last WM, Johnston JW, Hall RI, et al. 2010. Historical and paleolimnological evidence for expansion of Lake Athabasca (Canada) during the Little Ice Age. Journal of Paleolimnology. 43(4):705–717.

Smyntek PM, Maberly SC, Grey J. 2012. Dissolved carbon dioxide concentration controls baseline stable carbon isotope signatures of a lake food web. Limnology and Oceanography. 57(5):1292–1302.

Stern GA, Braekevelt E, Helm PA, Bidleman TF, Outridge PM, Lockhart WL, McNeeley R, Rosenberg B, Ikonomou MG, Hamilton P, et al. 2005. Modern and historical fluxes of halogenated organic contaminants to a lake in the Canadian arctic, as determined from annually laminated sediment cores. Science of the Total Environment. 342(1–3):223–243.

Talbot MR. 2001. Nitrogen isotopes in palaeolimnology. In: Smol JP, Last WM, editors. Tracking Environmental Change Using Lake Sediments Volume 2: Physical and Geochemical Methods. Dordrecht, Netherlands: Springer Netherlands; p. 401–439.

Timoney KP. 2002. A Dying Delta? A Case Study of a Wetland Paradigm. Wetlands. 22(2):282–300.

Timoney KP. 2013. The Peace-Athabasca Delta: Portrait of a Dynamic Ecosystem. Edmonton, Alberta, Canada: The University of Alberta Press.

Timoney KP, Peterson G, Fargey P, Peterson M, McCanny S, Wein R. 1997. Spring ice-jam flooding of the Peace-Athabasca Delta: Evidence of a climatic oscillation. Climatic Change. 35(4):463–483.

Timoney KP, Smith JD, Lamontagne JR, Jasek M, Hall RI, Wolfe BB, Wiklund JA, Timoney KP, Smith JD,

Lamontagne JR, Jasek M. 2018. Discussion of “Frequency of ice-jam flooding of Peace-Athabasca Delta.” Canadian Journal of Civil Engineering. 00(1–4):0000.

WBNP (Wood Buffalo National Park). 2016. Wood Buffalo National Park World Heritage Site Action Plan.

WHC/IUCN. 2017. International Union for Conservation of Nature - IUCN Reactive Monitoring Mission to. (January).

Wiklund JA, Hall RI, Wolfe BB. 2012. Timescales of hydrolimnological change in floodplain lakes of the Peace-Athabasca Delta, northern Alberta, Canada. Ecohydrology. 5:351–367.

Wiklund JA, Hall RI, Wolfe BB, Edwards TWD, Farwell AJ, Dixon DG. 2012. Has Alberta oil sands development increased far-field delivery of airborne contaminants to the Peace-Athabasca Delta? Science of the Total Environment. 433:379–382.

Wiklund JA, Hall RI, Wolfe BB, Edwards TWD, Farwell AJ, Dixon DG. 2014. Use of pre-industrial floodplain lake sediments to establish baseline river metal concentrations downstream of Alberta oil sands: a new approach for detecting pollution of rivers. Environmental Research Letters. 9(12):124019.

Wolfe AP, Härtling JW. 1997. Early Holocene Trace Metal Enrichment in Organic Lake Sediments, Baffin Island , Arctic Canada. Arctic and Alpine research [Internet]. 29(1):24–31. https://www.jstor.org/stable/1551833

Wolfe BB, Edwards TWD, Elgood RJ, Beuning KRM. 2001. Carbon and oxygen isotope analysis of lake sediment cellulose: methods and applications. In: Smol JP, Last WM, editors. Tracking Environmental Change Using Lake Sediments Volume 2: Physical and Chemical Techniques. Vol. 2. Dordrecht, the Netherlands: Kluwer Academic Publishers; p. 373–400.

Wolfe BB, Edwards TWD, Hall RI, Johnston JW. 2011. A 5200-year record of freshwater availability for regions in western North America fed by high-elevation runoff. Geophysical Research Letters. 38(11):2–6.

Wolfe BB, Hall RI, Edwards TWD, Jarvis SR, Sinnatamby RN, Yi Y, Johnston JW. 2008. Climate-driven shifts in quantity and seasonality of river discharge over the past 1000 years from the hydrographic apex of North America. Geophysical Research Letters. 35(24):1–5.

Wolfe BB, Hall RI, Edwards TWD, Johnston JW. 2012. Developing temporal hydroecological perspectives to inform stewardship of a northern floodplain landscape subject to multiple stressors: paleolimnological investigations of the Peace–Athabasca Delta. Environmental Reviews. 20:191–210.

Wolfe BB, Hall RI, Last WM, Edwards TWD, English MC, Karst-Riddoch TL, Paterson A, Palmini R. 2006. Reconstruction of multi-century flood histories from oxbow lake sediments, Peace-Athabasca Delta, Canada. Hydrological Processes. 20:4131–4153.

Wolfe BB, Hall RI, Wiklund JA, Kay ML. 2020. Past variation in Lower Peace River ice-jam flood frequency. Environmental Reviews. 9(December 2019):1–9.

Wolfe BB, Karst-Riddoch TL, Hall RI, Edwards TWD, English MC, Palmini R, McGowan S, Leavitt PR, Vardy SR. 2007. Classification of hydrological regimes of northern floodplain basins (Peace–Athabasca Delta, Canada) from analysis of stable isotopes d18O, d2H and water chemistry. Hydrological Processes. 21:151–168.

Wolfe BB, Karst-Riddoch TL, Vardy SR, Falcone MD, Hall RI, Edwards TWD. 2005. Impacts of climate and

river flooding on the hydro-ecology of a floodplain basin, Peace-Athabasca Delta, Canada since A.D. 1700. Quaternary Research. 64(2):147–162.

Wrona FJ. 2017. Oil Sands Monitoring Program Report 2016-17. Alberta, Canada.

Appendix A: Loss on Ignition and C&N isotope and elemental data

Table A1: PAD 52 Hammer Core 1 (working core)

Depth	Year	%H_2O	%OM	%MM	%$CaCO_3$
0	2016	92.43	32.76	57.14	22.95
1	2014	90.44	28.51	64.88	15.03
2	2012	92.42	25.37	69.40	11.87
3	2010	90.72	21.12	70.04	20.08
4	2008	88.17	22.58	69.90	17.10
5	2003	78.58	15.64	76.36	18.19
6	1999	77.42	15.77	75.68	19.42
7	1993	79.69	15.20	76.86	18.05
8	1990	77.81	15.72	76.94	16.66
8	1985	72.53	13.15	79.96	15.67
9	1981	71.68	12.58	80.22	16.36
10	1978	65.21	11.90	81.90	14.10
11	1976	57.26	8.41	85.99	12.74
12	1972	44.50	6.18	89.33	10.19
13	1968	50.30	7.40	88.42	9.50
14	1958	48.18	7.64	89.36	6.81
15	1948	46.28	8.73	86.48	10.88
16	1939	46.26	8.01	87.62	9.94
17	1930	49.03	11.37	83.85	10.86
18	1921	48.61	10.84	84.07	11.57
19	1915	48.64	12.74	82.19	11.54
20	1906	66.04	21.51	72.23	14.23
21	1899	47.24	10.70	84.48	10.96
22	1887	53.89	14.93	76.41	19.68
23	1876	37.26	7.61	88.03	9.90
24	1866	41.69	8.42	86.10	12.45
25	1855	44.82	12.37	82.15	12.45
26	1845	42.84	9.87	84.57	12.66
27	1832	41.49	8.56	86.08	12.19
28	1821	39.34	7.82	87.56	10.51
29	1811	40.92	8.26	87.78	9.00
30	1803	40.10	8.61	87.19	9.53
31	1794	42.97	10.30	86.34	7.62
32	1783	46.60	10.26	85.29	10.13
33	1773	44.48	10.07	86.33	8.18
34	1766	47.17	10.87	85.26	8.80
35	2016	50.83	11.04	85.43	8.02

Table A2: PAD 52 Hammer Core 2

Depth	%H_2O	%OM	%MM	%$CaCO_3$
0	87.03	22.46	71.23	14.34
1	85.20	21.10	74.19	10.69
2	79.71	20.21	75.49	9.77
3	71.55	13.42	81.73	11.02
4	69.37	13.49	81.89	10.51
5	60.95	11.22	84.21	10.39
6	59.94	11.22	83.99	10.88
7	57.30	11.13	83.59	12.01
8	54.93	11.28	83.12	12.72
8	55.71	10.73	84.21	11.49
9	54.43	10.63	84.08	12.03
10	57.39	11.37	83.85	10.88
11	49.41	9.08	87.29	8.24
12	63.34	13.29	79.85	15.60
13	57.44	11.89	82.58	12.56
14	57.52	11.85	82.43	13.00
15	49.36	8.62	87.49	8.85
16	47.13	8.81	87.48	8.42
17	46.32	8.91	87.44	8.30
18	46.77	10.46	86.36	7.22
19	43.91	9.12	87.39	7.93
20	51.33	11.45	85.20	7.62
21	52.19	12.21	83.87	8.91
22	51.74	13.00	81.71	12.03
23	44.01	9.24	87.70	6.97
24	45.82	12.04	83.99	9.01
25	59.12	16.71	76.45	15.56
26	49.15	11.73	84.45	8.68
27	43.54	8.94	87.34	8.47
28	42.61	8.78	88.24	6.78
29	43.41	9.64	87.61	6.27
30	44.10	10.17	87.19	6.00
31	44.29	9.38	88.14	5.62
32	45.43	9.80	87.20	6.82
33	45.31	9.11	88.14	6.25
34	40.93	8.25	89.41	5.30
35				

36	48.91	10.12	86.86	6.85
37	45.88	10.03	86.52	7.85
38	47.86	10.77	86.67	5.82
39	47.47	10.14	86.91	6.70

Table A3: PAD 64 Hammer Core 1

Depth	$\%H_2O$	%OM	%MM	$\%CaCO_3$
0	87.36	12.52	85.13	5.34
1	72.23	7.70	88.99	7.52
2	72.07	11.44	85.05	7.97
3	80.94	17.89	78.39	8.46
4	67.20	9.96	86.87	7.21
5	68.57	10.08	86.65	7.44
6	65.70	8.07	88.31	8.21
7	65.39	8.77	87.72	7.97
8	51.96	7.23	89.53	7.37
9	56.94	6.76	89.78	7.84
10	59.69	7.63	89.26	7.07
11	68.96	10.48	85.67	8.74
12	70.52	11.29	84.54	9.47
13	77.16	13.20	83.22	8.13
14	68.05	10.72	86.01	7.43
15	62.73	7.02	89.56	7.79
16	64.15	6.95	88.64	10.03
17	50.93	5.91	90.46	8.24
18	41.90	5.81	91.01	7.22
19	38.94	5.04	91.47	7.94
20	40.04	5.31	91.02	8.34
21	45.46	5.97	90.76	7.45
22	51.51	5.85	90.81	7.58
23	42.11	6.22	90.24	8.05
24	49.11	5.56	90.95	7.93
25	54.72	6.92	90.39	6.11
26	46.25	6.15	90.57	7.44
27	42.68	5.19	90.97	8.73
28	51.37	6.36	90.44	7.27
29	46.83	6.32	90.33	7.61
30	47.13	6.05	91.00	6.71
31	42.99	5.36	91.35	7.47
32	30.09	3.70	92.85	7.85

33	35.95	4.61	91.87	8.00
34	49.17	6.18	90.39	7.81
35	42.41	5.57	91.32	7.07
36	52.03	6.48	90.14	7.69
37	52.94	7.38	89.42	7.28
38	55.62	6.95	89.57	7.90
39	45.35	6.61	90.30	7.02
40	51.55	6.01	90.41	8.14
41	44.50	5.44	91.17	7.70
42	40.50	5.73	90.60	8.34
43	42.38	5.68	91.02	7.50
44	35.91	4.11	92.15	8.50
45	39.46	4.72	91.73	8.08
46	45.54	5.88	91.29	6.44
47	45.24	5.48	91.31	7.30
48	50.62	5.92	90.43	8.31
49	54.29	7.13	89.85	6.86
50	54.90	6.85	90.27	6.54
51	50.65	6.45	90.54	6.84
52	46.93	5.16	91.11	8.49
53	53.03	6.70	90.16	7.14
54	56.15	6.73	90.18	7.03
55	53.79	6.81	90.17	6.86
56	47.89	5.49	91.06	7.83
57	42.41	5.18	91.37	7.85
58	44.02	5.26	91.52	7.31

Table A4: PAD 64 Hammer Core 2 (working core)

Depth	%H_2O	%OM	%MM	%$CaCO_3$
0	81.89	10.32	86.13	8.06
1	69.93	10.32	86.62	6.96
2	77.81	13.15	83.60	7.37
3	65.82	9.66	87.33	6.84
4	63.39	8.98	88.08	6.68
5	66.77	9.72	87.03	7.41
6	62.98	9.45	87.14	7.76
7	44.07	6.35	90.73	6.65
8	45.91	6.60	90.14	7.41
9	56.84	7.76	89.10	7.14
10	66.45	10.58	86.65	6.31

11	66.82	10.96	85.57	7.88
12	76.50	13.15	83.35	7.96
13	65.93	8.57	88.31	7.07
14	56.92	7.70	89.37	6.65
15	58.68	7.74	89.06	7.26
16	54.03	6.65	90.07	7.45
17	45.93	6.12	90.68	7.28
18	40.74	4.95	91.17	8.81
19	38.97	4.75	91.48	8.56
20	41.94	5.77	90.45	8.61
21	54.04	7.24	89.82	6.66
22	47.36	6.30	90.49	7.29
23	44.61	6.32	90.38	7.50
24	52.77	6.74	89.96	7.51
25	54.40	7.28	89.56	7.18
26	46.98	6.89	89.92	7.25
27	42.82	5.55	91.28	7.20
28	44.68	6.16	90.31	8.03
29	47.02	5.88	90.88	7.38
30	48.89	6.33	90.54	7.11
31	49.42	6.28	90.75	6.74
32	34.36	4.97	91.57	7.85
33	41.11	5.39	91.15	7.86
34	51.04	6.27	90.77	6.71
35	39.21	5.38	91.33	7.46
36	45.89	5.99	90.82	7.25
37	55.66	7.70	88.99	7.52
38	57.45	7.32	89.40	7.44
39	40.65	5.48	90.92	8.18
40	48.90	6.31	90.10	8.15
41	46.84	6.42	90.07	7.97
42	46.66	5.89	89.42	10.66
43	38.39	5.61	90.95	7.82
44	39.24	5.05	91.27	8.36
45	39.48	5.43	91.19	7.66
46	42.00	5.27	91.10	8.24
47	46.86	6.15	90.41	7.83
48	51.40	7.02	89.49	7.93
49	50.44	7.34	89.73	6.67
50	50.95	7.60	89.65	6.25
51	51.18	7.45	89.14	7.77

52	52.88	7.42	89.64	6.67
53	47.14	6.87	90.07	6.95
54	52.96	6.90	89.92	7.23
55	49.89	6.69	89.96	7.60
56	50.95	6.92	89.91	7.21
57	45.35	6.07	90.61	7.54
58	38.23	4.96	91.54	7.93

Table A5: PAD 65 Hammer Core 1 (working core)

Depth	Year	%H_2O	%OM	%MM	%$CaCO_3$	C/N	%C_{org}	%N	$\delta^{13}C_{org}$	$\delta^{15}N$
0	2016	94.79	40.68	50.57	19.88	9.4731	16.9389	1.7881	-25.9034	-2.0971
1	2014	92.18	32.25	58.49	21.06	9.7205	17.1989	1.7694	-25.9441	-1.3645
2	2011	87.09	28.64	66.31	11.49	9.6271	13.9455	1.4486	-26.1325	-1.5299
3	2009	85.04	27.53	65.86	15.03	9.8109	13.2505	1.3506	-26.4470	-1.4720
4	2007	82.60	25.74	67.54	15.27	10.6926	13.5815	1.2702	-25.9106	-1.0276
5	2004	79.08	21.92	71.31	15.39	10.2292	9.7146	0.9497	-25.9269	-0.8908
6	2002	77.54	18.26	75.27	14.72	10.0343	8.4506	0.8422	-26.3859	-0.6666
7	2000	82.32	27.23	66.33	14.64	9.4639	11.6421	1.2302	-26.1493	-1.4880
8	1997	83.85	20.00	71.93	18.35	8.8283	11.3154	1.2817	-26.0345	-0.8265
9	1995	83.40	21.48	73.42	11.58	9.0991	11.2487	1.2362	-25.0619	-1.2910
10	1991	80.79	20.15	72.51	16.69	9.3449	10.1995	1.0915	-25.1804	-0.8210
11	1987	66.56	12.11	81.89	13.63	9.8686	5.2811	0.5351	-25.7238	-0.2787
12	1983	53.11	8.17	88.10	8.47	10.6983	4.5418	0.4245	-24.7166	-0.3560
13	1980	65.67	12.95	80.75	14.32	10.2751	5.1126	0.4976	-25.4515	0.0438
14	1977	64.30	11.10	83.19	12.99	9.6978	4.4476	0.4586	-25.9211	-0.8924
15	1975	60.48	9.14	84.99	13.35	9.6940	4.4761	0.4617	-26.2033	-0.3680
16	1973	55.64	16.71	77.98	12.08	10.2903	4.5365	0.4408	-26.5179	-0.1061
17	1971	61.98	10.63	84.80	10.39	11.1876	6.5306	0.5837	-27.1902	-0.7296
18	1969	59.08	15.41	80.03	10.36	11.4957	7.5933	0.6605	-27.3240	-0.9001
19	1965	60.01	13.36	81.44	11.82	11.7628	8.5494	0.7268	-27.4281	-0.7327
20	1955	57.51	12.45	83.71	8.75	11.7307	7.6437	0.6516	-27.3576	-0.5016
21	1947	62.17	16.65	79.21	9.40	11.9711	8.4915	0.7093	-27.2115	-0.8136
22	1941	68.16	19.81	76.32	8.78	12.0004	9.1995	0.7666	-27.6688	-0.5495
23	1933	64.53	21.42	75.35	7.34	12.2828	10.4441	0.8503	-27.8983	-0.6343
24	1928	67.81	19.99	76.43	8.13	12.1867	10.6471	0.8737	-28.0119	-0.6766
25	1923	68.98	21.54	75.08	7.69	12.4076	10.0857	0.8129	-27.6622	-0.9685
26	1918	61.63	15.94	79.86	9.53	12.1939	8.1317	0.6669	-27.4094	-0.5854
27	1913	64.53	18.09	78.12	8.61	12.1581	7.2577	0.5969	-27.3509	-0.5271
28	1906	50.86	12.32	83.46	9.58	12.0053	7.3496	0.6122	-27.4299	-0.3359
29	1900	59.94	16.54	79.32	9.40	12.3346	7.6205	0.6178	-27.6030	-0.5379

30	1894	60.67	18.44	78.08	7.91	12.6447	9.5541	0.7556	-27.3358	-0.3003
31	1888	61.34	17.45	78.79	8.55	12.0900	9.2435	0.7646	-27.1338	-0.4975
32	1882	64.35	19.92	76.02	9.23	12.5081	10.4662	0.8368	-27.2931	-0.7356
33	1877	62.25	19.13	77.25	8.23	12.2811	9.5346	0.7764	-27.0904	-0.4919
34	1870	58.75	17.52	78.07	10.03	12.3720	8.7189	0.7047	-27.0593	-0.5601
35	1864	60.16	16.32	79.22	10.13	12.4287	7.5546	0.6078	-27.2378	-0.3033
36	1856	53.56	14.24	80.97	10.89	12.0685	7.0010	0.5801	-27.1186	-0.7411
37	1849	54.25	15.50	79.60	11.12	11.9896	7.6762	0.6402	-27.2192	-0.4455
38	1842	54.33	14.33	80.07	12.73	12.3232	7.9909	0.6484	-27.0592	-0.5276
39	1835	54.50	15.07	79.04	13.39	11.9811	7.8347	0.6539	-27.0688	-0.4340
40	1827	53.29	16.06	78.91	11.43	11.9559	8.0310	0.6717	-27.1292	-0.3430
41	1820	54.45	16.36	78.57	11.52	12.0141	7.6339	0.6354	-27.1245	-0.6615
42	1812	55.34	17.21	77.43	12.17	12.2748	7.9476	0.6475	-27.1486	-0.4480
43	1804	54.29	14.76	80.00	11.90	12.2129	7.2074	0.5901	-27.1168	-0.0085
44	1796	51.70	13.94	80.49	12.66	12.2191	6.6696	0.5458	-26.8906	-0.1000
45	1788	52.82	12.98	82.14	11.10	12.3302	6.6506	0.5394	-27.1179	-0.3964
46	1780	51.16	14.20	81.10	10.69	12.0776	6.8941	0.5708	-27.0167	-0.1503
47	1773	58.83	17.10	78.11	10.88	12.4079	7.1587	0.5769	-26.9821	-0.3100
48	1764	49.38	12.22	83.23	10.35	12.2702	6.7423	0.5495	-27.2270	0.2996
49	1756	49.40	11.58	83.96	10.15	12.2668	6.2910	0.5128	-27.0869	-0.1538
50	1748	51.55	15.10	80.91	9.08	12.0571	6.1237	0.5079	-27.0579	0.0778
51	1739	51.76	13.26	82.28	10.14	12.2984	5.7877	0.4706	-26.9638	-0.3945
52	1730	52.11	13.41	82.04	10.35	11.9199	5.3648	0.4501	-26.8513	0.2292
53	1722	52.79	13.89	81.58	10.30	12.2973	6.7165	0.5462	-26.8213	-0.1308

Table A6: PAD 65 Hammer Core 2

Depth	%H_2O	%OM	%MM	%$CaCO_3$
0	96.97	31.82	63.64	10.33
1	90.91	27.65	63.71	19.63
2	88.78	27.65	65.35	15.91
3	89.64	28.41	65.15	14.63
4	88.03	25.13	68.47	14.56
5	67.43	12.55	84.64	6.37
6	83.06	22.62	71.55	13.26
7	79.06	20.61	74.14	11.93
8	76.91	21.20	75.18	8.23
9	78.17	23.77	72.80	7.78
10	77.40	22.65	73.09	9.69
11	75.41	21.46	73.17	12.20
12	75.70	21.89	74.38	8.48

13	71.68	20.97	74.16	11.06
14	74.74	19.36	75.21	12.37
15	55.66	8.05	87.46	10.19
16	71.57	16.79	79.00	9.58
17	73.23	16.33	78.16	12.54
18	73.86	17.17	76.75	13.82
19	73.84	17.52	76.47	13.67
20	71.61	17.29	75.11	17.28
21	74.58	14.67	80.30	11.42
22	68.05	14.34	79.53	13.93
23	71.24	19.33	76.81	8.78
24	66.65	16.66	77.79	12.62
25	74.95	21.07	75.47	7.86
26	70.33	19.93	76.97	7.04
27	59.01	16.25	80.22	8.02
28	58.68	14.02	82.84	7.13
29	49.44	12.27	84.90	6.45
30	52.45	13.97	82.78	7.38
31	59.96	18.78	77.81	7.75
32	54.25	13.39	82.59	9.14
33	54.17	16.16	80.79	6.93
34	55.56	14.83	81.27	8.86
35	54.24	14.35	82.13	8.00
36	61.32	18.40	78.02	8.13
37	65.32	21.68	74.31	9.10
38	65.52	20.86	75.34	8.65
39	56.76	15.37	80.26	9.92
40	54.37	13.79	81.00	11.85
41	58.96	13.79	81.06	11.70
42	51.65	14.80	80.42	10.89
43	56.47	17.52	77.52	11.29
44	49.28	12.15	83.18	10.61
45	53.07	14.34	81.66	9.09
46	53.10	15.34	80.87	8.62
47	46.70	11.65	84.25	9.31
48	29.86	6.41	89.98	8.22
49	61.09	22.10	74.20	8.39
50	51.57	14.67	81.61	8.45
51	48.13	12.51	82.77	10.72
52	52.01	17.16	79.60	7.35
53	51.94	14.86	81.15	9.08

54	49.60	12.24	83.82	8.97
55	53.43	14.91	81.04	9.20
56	40.84	9.66	86.05	9.75
57	48.74	16.95	82.81	0.54

Table A7: PAD 66 Hammer Core 1

Depth	$\%H_2O$	%OM	%MM	$\%CaCO_3$
0	84.07	8.79	87.90	7.51
1	52.44	6.61	90.06	7.56
2	31.82	4.61	92.37	6.86
3	36.18	6.69	90.66	6.04
4	38.23	6.82	90.41	6.31
5	34.89	6.86	90.02	7.10
6	33.41	6.93	90.13	6.68
7	32.27	6.68	90.49	6.45
8	29.75	5.59	90.98	7.79
9	29.67	5.80	90.87	7.56
10	33.47	7.05	89.83	7.09
11	33.34	6.50	90.12	7.69
12	35.47	7.30	89.66	6.91
13	41.37	7.23	89.44	7.56
14	35.12	7.15	89.70	7.15
15	33.51	6.79	90.02	7.24
16	33.09	6.86	89.65	7.93
17	33.82	6.74	89.81	7.83
18	34.63	8.63	88.56	6.40
19	29.93	6.55	89.61	8.73
20	28.37	6.00	90.85	7.16
21	27.84	5.81	90.74	7.84
22	28.05	5.09	91.47	7.83
23	27.40	5.15	91.63	7.33
24	28.65	5.63	91.35	6.87
25	31.52	5.96	91.26	6.31
26	27.51	5.33	91.78	6.58
27	28.66	6.01	91.09	6.58
28	28.71	6.34	90.72	6.70
29	29.05	6.59	90.43	6.78
30				
31	27.91	5.80	90.50	8.42
32	28.10	5.98	90.29	8.48

33	27.06	6.27	90.29	7.83
34	27.61	5.80	90.40	8.64
35	27.69	6.11	89.82	9.24
36	28.58	5.92	90.45	8.27

Table A8: PAD 66 Hammer Core 2 (working core)

Depth	$\%H_2O$	%OM	%MM	$\%CaCO_3$
0	51.66	4.61	92.00	7.71
1	33.43	4.58	92.72	6.13
2	34.59	6.38	90.73	6.57
3	35.11	6.42	90.63	6.71
4	32.93	5.97	91.05	6.78
5	31.23	5.68	91.13	7.25
6	30.94	5.49	91.32	7.23
7	30.89	5.20	91.51	7.47
8	32.70	6.45	89.65	8.87
9	32.41	6.12	90.03	8.74
10	34.43	6.40	90.46	7.13
11	33.91	6.62	90.06	7.53
12	32.69	5.81	90.78	7.74
13	31.14	5.93	90.82	7.39
14	31.86	5.70	90.93	7.66
15	28.50	4.71	91.67	8.23
16	34.49	6.40	89.20	10.00
17	31.43	5.48	90.37	9.45
18	29.82	4.51	92.11	7.67
19	28.86	5.27	91.60	7.12
20	27.93	4.82	92.13	6.93
21	27.88	4.69	92.15	7.18
22	27.40	4.35	92.40	7.39
23	28.91	5.09	92.06	6.48
24	28.16	4.88	92.08	6.91
25	27.57	4.80	92.08	7.08
26	30.12	5.37	91.64	6.81
27	31.27	6.07	90.92	6.86
28	26.04	4.58	92.43	6.78
29	25.64	4.30	92.56	7.12
30	29.59	5.37	91.32	7.54
31	28.93	6.01	90.39	8.20
32	27.87	5.84	90.47	8.37

33	29.00	5.83	90.49	8.37
34	29.74	6.18	90.06	8.53
35	30.79	5.86	90.18	8.99
36	28.87	5.94	89.90	9.46
37	29.54	6.50	89.16	9.87
38	30.28	5.55	90.42	9.14

Table A9: PAD 67 Hammer Core 1

Depth	$\%H_2O$	%OM	%MM	$\%CaCO_3$
0	84.37	26.88	69.82	7.51
1	80.61	25.63	70.52	8.75
2	79.49	25.58	71.25	7.21
3	78.24	25.80	70.74	7.87
4	75.53	24.05	72.33	8.23
5	72.02	23.63	73.17	7.26
6	72.87	23.54	73.10	7.64
7	70.87	21.93	75.17	6.59
8	69.03	22.42	74.03	8.07
9	66.41	21.65	75.07	7.44
10	67.10	22.40	74.47	7.12
11	64.08	20.17	76.91	6.64
12	60.71	18.73	78.43	6.44
13	58.87	17.44	79.73	6.44
14	59.66	17.10	80.23	6.07
15	59.77	18.74	75.73	12.56
16	61.03	20.29	76.78	6.65
17	61.20	19.00	78.39	5.93
18	60.48	18.85	78.02	7.12
19	58.74	17.84	79.14	6.87
20	60.08	18.11	79.40	5.65
21	61.70	18.43	78.75	6.41
22	62.92	21.26	76.22	5.72
23	60.32	19.87	77.12	6.84
24	60.71	19.44	77.98	5.85
25	58.88	17.92	79.22	6.52
26	56.41	17.03	79.95	6.85
27	55.13	16.05	81.23	6.18
28	54.13	15.82	81.57	5.94
29	56.52	18.37	79.02	5.93
30	55.01	16.12	81.00	6.54

31	60.66	19.55	77.69	6.28
32	59.34	20.33	76.71	6.71
33	58.62	20.10	77.00	6.57
34	54.56	17.26	79.69	6.94
35	46.87	12.57	83.89	8.05
36	38.24	8.81	87.79	7.73
37	40.71	11.01	84.83	9.43
38	43.24	12.50	83.57	8.94
39	42.28	11.60	83.03	12.20
40	37.68	9.51	85.83	10.59
41	31.30	7.10	89.21	8.40
42	36.25	9.50	86.23	9.70
43	32.80	9.05	86.25	10.69
44	37.76	9.58	87.11	7.52
45	39.96	10.37	86.41	7.33
46	44.11	13.04	83.96	6.80
47	41.02	11.11		
48	36.63	8.75	88.24	6.84
49	34.03	7.36	88.65	9.07
50	37.44	10.51		
51	40.63	11.17	85.21	8.21
52	41.23	11.26	84.60	9.42
53	36.68	9.50	86.16	9.87
54	39.42	10.92	85.22	8.77
55	42.39	12.13	83.49	9.95
56	50.31	17.41	79.02	8.11

Table A10: PAD 67 Hammer Core 2 (working core)

Depth	Year	%H_2O	%OM	%MM	%$CaCO_3$	C/N	%C_{org}	%N	$\delta^{13}C_{org}$	$\delta^{15}N$
0	2013	87.75	28.25	67.86	8.85	9.0989	13.8067	1.5174	-26.3028	-0.9482
1	2011	81.38	28.74	68.59	6.07	9.6158	12.8255	1.3338	-26.6722	-0.9919
2	2007	78.26	27.28	70.07	6.01	9.9586	12.3437	1.2395	-26.8192	-0.6383
3	2003	78.10	26.18	70.74	7.00	10.2423	12.8121	1.2509	-26.7277	-0.5600
4	1998	77.14	26.24	70.72	6.91	9.8279	13.1369	1.3367	-26.8867	-0.5833
5	1993	76.01	26.11	71.26	5.97	9.9550	12.4687	1.2525	-27.2815	-0.7891
6	1989	75.04	25.56	71.51	6.67	10.1825	11.8402	1.1628	-27.2237	-0.5965
7	1986	74.51	25.59	71.84	5.85	9.9478	10.5954	1.0651	-27.4510	-0.5485
8	1980	72.70	22.93	73.80	7.44	10.4419	10.6748	1.0223	-27.5681	-0.5212
9	1976	69.91	23.32	74.37	5.25	10.6883	10.5173	0.9840	-27.7652	-0.3355
10	1973	69.46	24.61	72.64	6.25	10.5963	10.5062	0.9915	-27.4924	-0.4727

11	1968	71.09	23.81	73.81	5.41	10.3870	10.2530	0.9871	-27.3299	-0.4819
12	1962	66.89	20.82	76.06	7.09	10.3397	10.0554	0.9725	-27.5127	-0.1222
13	1960	68.37	21.41	75.48	7.07	10.2270	9.8956	0.9676	-27.5235	-0.4723
14	1955	67.57	21.88	74.76	7.64	10.8544	10.4224	0.9602	-27.4995	-0.6124
15	1951	65.01	21.53	76.03	5.57	10.2940	9.4015	0.9133	-27.5525	-0.0187
16	1945	67.41	20.37	76.49	7.12	10.6157	9.0042	0.8482	-27.7903	-0.3267
17	1938	64.14	20.16	77.80	4.62	10.6927	8.0901	0.7566	-27.9163	0.2226
18	1930	56.31	15.65	81.61	6.23	10.4455	6.6329	0.6350	-28.0345	0.0486
19	1921	57.52	17.21	80.24	5.80	10.4942	7.0867	0.6753	-28.2394	0.1389
20	1912	57.12	16.47	80.64	6.56	11.2347	7.5688	0.6737	-28.4114	-0.0300
21	1904	58.06	17.35	80.14	5.70	11.1525	7.5781	0.6795	-28.2008	0.0918
22	1896	59.27	19.12	78.29	5.88	11.9545	7.7441	0.6478	-29.0703	0.5236
23	1889	63.99	19.92	77.19	6.56	12.3906	8.5210	0.6877	-29.3779	0.5217
24	1881	61.36	18.45	78.57	6.77	12.4865	7.7404	0.6199	-29.2080	0.5027
25	1875	69.63	27.63	69.58	6.34	13.7736	13.7929	1.0014	-29.5522	0.6172
26	1870	71.30	37.03	60.84	4.85	12.5975	17.2611	1.3702	-29.8612	0.2984
27	1865	68.99	28.35	69.02	5.98	13.8023	16.3102	1.1817	-29.5195	0.0696
28	1861	67.44	28.57	69.10	5.30	12.2360	11.6144	0.9492	-28.8773	0.5002
29	1852	63.53	26.19	71.23	5.88	12.8244	11.4958	0.8964	-28.7635	0.5852
30	1844	63.79	23.42	73.45	7.12	13.1218	11.8687	0.9045	-28.8174	0.3120
31	1837	59.17	20.37	77.34	5.21	13.0098	10.6433	0.8181	-28.9085	0.5402
32	1828	53.28	16.06	80.30	8.28	12.2639	6.7047	0.5467	-28.3670	0.5541
33	1815	48.06	15.10	82.25	6.01	12.0088	6.4007	0.5330	-28.4544	0.2182
34	1805	48.72	14.80	82.24	6.73	12.7674	6.7961	0.5323	-28.4722	0.0650
35	1796	57.49	19.50	77.67	6.42	14.4530	10.6143	0.7344	-28.9492	-0.0622
36	1786	54.32	19.65	77.60	6.25	11.6903	7.7799	0.6655	-27.8867	-0.0925
37	1776	48.97	15.01	82.32	6.05	12.2087	5.8333	0.4778	-29.4923	0.4758
38	1764	49.48	17.10	80.15	6.25	11.5650	6.2763	0.5427	-28.1843	0.3138
39	1753	41.88	11.61	83.84	10.34	11.4380	5.0636	0.4427	-26.7784	0.2882
40	1737	37.83	10.03	85.47	10.24	11.5909	4.0742	0.3515	-26.5315	-0.0552
41	1721	37.23	9.46	86.80	8.49	11.5720	3.8905	0.3362	-26.4955	0.5138
42	1707	40.52	10.10	85.29	10.46	11.8038	4.3922	0.3721	-26.5954	0.3227
43	1694	39.48	10.87	85.73	7.73	11.4868	3.6999	0.3221	-26.8368	0.5309
44	1679	36.18	9.11	87.49	7.72	11.2461	3.1399	0.2792	-26.8260	1.0447
45	1664	36.55	8.71	87.53	8.53	11.3828	3.2475	0.2853	-26.7793	0.9481
46	1647	36.17	8.67	87.73	8.17	11.8563	3.1590	0.2664	-26.8658	0.0862
47	1631	37.94	9.82	87.37	6.38	11.9424	3.3941	0.2842	-26.6990	0.6008
48	1616	37.74	9.43	87.64	6.67	11.4182	3.3444	0.2929	-26.9819	0.4702
49	1602	38.31	11.32	86.17	5.71	11.6632	3.7299	0.3198	-26.8507	0.5859
50	1588	38.30	9.20	87.30	7.95	11.5364	3.7574	0.3257	-27.1227	0.6327
51	1567	35.69	8.37	88.25	7.67	11.9863	2.7928	0.2330	-26.6157	1.1774

52	1556	37.94	9.44	86.76	8.63	12.6240	4.1735	0.3306	-26.9087	0.4151
53	1542	41.97	12.25	83.32	10.08	12.6392	5.9771	0.4729	-26.8712	0.0781
54	1530	42.15	12.26	83.27	10.16	12.7489	5.0817	0.3986	-26.8079	0.6866
55	1516	42.55	12.69	83.03	9.74	12.5062	5.2301	0.4182	-26.5773	0.1909

Appendix B: Radioisotope and CRS-inferred ^{210}Pb chronology

Table B1: PAD 52 Hammer Core 1. Interpolated and extrapolated values highlighted in grey.

CRS Raw Date	Date Error	Total ^{210}Pb (dpm/g)	Total ^{210}Pb (Bq/kg)	^{210}Pb Error (Bq/kg)	^{226}Ra Activity (Bq/kg)	Total dry mass sedimentation (g/cm^2 yr)	Organic matter sed. (g/cm^2 yr)	inorganic matter sed. (g/cm^2 yr)	^{137}Cs (Bq/kg)	^{137}Cs Error
2015.87	0.62	8.87	147.79	12.98	25.11	0.053	0.017	0.030	3.73	1.23
2013.89	1.09	9.96	166.02	14.93	24.92	0.043	0.012	0.028	2.16	1.24
2012.33	1.47	8.13	135.43	11.65	30.69	0.055	0.014	0.038	3.25	1.08
2010.19	2.03	8.48	141.26	11.61	30.88	0.050	0.010	0.035	3.33	1.07
2007.62	2.76	8.38	139.70	10.10	33.90	0.048	0.011	0.034	3.88	0.94
2002.93	4.25	7.72	128.72	10.10	35.80	0.051	0.008	0.039	2.50	0.91
1998.58	5.79	7.06	117.63	10.16	42.34	0.054	0.009	0.041	5.78	1.02
1993.08	8.00	6.56	109.37	13.68	30.43	0.045	0.007	0.035	4.69	1.33
1990.35	9.21	4.14	68.95	6.06	40.87	0.107	0.015	0.084	4.15	0.62
1985.27	11.68	4.58	76.34	7.93	38.08	0.072	0.009	0.058	4.46	0.81
1981.25	13.75	3.35	55.76	6.20	35.25	0.115	0.014	0.094	5.69	0.68
1978.15	14.98	3.22	53.62	7.81	43.02	0.196	0.017	0.169	4.41	0.85
1975.84	15.34	2.99	49.86	5.41	44.12	0.329	0.020	0.294	4.92	0.59
1972.38	15.98	3.19	53.24	6.79	45.07	0.215	0.016	0.190	8.88	0.82
1967.65	16.89	2.69	44.75	5.76	35.24	0.166	0.013	0.148	8.42	0.72
1957.56	20.68	3.01	50.22	6.22	32.51	0.077	0.007	0.066	8.57	0.75
1948.42	21.07	2.78	46.42	5.27	35.96	0.095	0.008	0.083	5.67	0.60
1938.79		2.98	49.65	6.12	29.93				3.11	0.62
1930.03		2.77	46.18	5.62	41.22				1.04	0.50
1921.13		2.44	40.61	6.18	31.50				-0.21	4.06
1914.94		2.50	41.68							
1906.27		2.57	42.77	6.06	35.27				-0.11	0.53
1899.36		2.68	44.63							
1886.78		2.79	46.55	5.94	37.36				-0.06	0.23
1876.36		2.78	46.38							
1866.22		2.77	46.22	5.75	43.81				-0.55	1.00
1855.04		2.84	47.27							
1844.90		2.90	48.33	6.21	44.98				-0.37	1.85
1831.92		2.64	43.96	5.06	39.48					
1820.61		2.54	42.38	5.90	46.79				-0.52	1.12
1811.29		2.64	44.01							
1802.88		2.51	41.91	6.07	34.21				-1.07	0.82
1793.66		2.64	44.01							
1783.41		2.77	46.19	5.66	34.45				-0.22	6.15
1772.55		2.96	49.33							
1766.40		3.16	52.62	6.65	35.00				-0.61	1.27

Table B2: PAD 64 Hammer Core 2

^{137}Cs Date	Date Error	Total ^{210}Pb (dpm/g)	Total ^{210}Pb (Bq/kg)	^{210}Pb Error (Bq/kg)	^{226}Ra Activity (Bq/kg)	^{137}Cs (Bq/kg)	^{137}Cs Error
2016.14	0.12	5.21	86.81	0.46	68.41	0.79	1.39
2015.11	0.39	5.11	85.12	0.38	62.24	-0.10	0.59
2014.36	0.58	5.69	94.82	0.44	54.88	0.52	1.35
2013.16	0.88	5.42	90.35	0.61	59.98	-0.40	0.99
2012.04	1.16	3.66	60.97	0.43	67.14	0.42	1.44
2010.92	1.45						
2009.39	1.84						
2007.05	2.43						
2004.87	2.98	3.17	52.78	0.28	54.96	-0.07	0.43
2003.30	3.38						
2002.13	3.68						
2001.02	3.96						
2000.30	4.14	6.37	106.17	0.37	42.11	7.22	1.10
1999.09	4.45						
1997.44	4.87						
1995.95	5.25						
1994.24	5.68	3.06	50.95	0.31	51.55	2.46	0.94
1992.00	6.25						
1989.37	6.91						
1986.66	7.60						
1984.03	8.27	3.29	54.75	0.27	47.87	0.21	1.11
1982.24	8.72						
1980.11	9.27						
1977.64	9.89						
1975.91	10.33	3.22	53.68	0.29	46.09	6.33	0.88
1974.16	10.77						
1972.00	11.32						
1969.53	11.95						
1967.27	12.52	3.03	50.52	0.30	46.03	8.11	0.92
1965.06	13.08						
1963.00	13.61						
1960.89	14.14						
1957.34	15.04	2.54	42.39	0.26	47.36	6.03	0.78

1955.18	15.59						
1953.37	16.05						
1950.76	16.71						
1948.70	17.23	3.77	62.80	0.30	47.15	6.94	0.90
1946.98	17.67						
1945.43	18.06						
1942.91	18.70						
1940.83	19.23	3.08	51.39	0.30	41.53	0.18	1.31
1938.70	19.77						
1936.32	20.37						
1933.69	21.04						
1930.95	21.74						
1928.16	22.44						
1925.59	23.10						
1923.45	23.64						
1921.52	24.13	2.98	49.71	0.27	43.47	-0.64	0.71
1919.62	24.61						
1917.72	25.09						
1915.76	25.59						
1913.98	26.04						
1911.72	26.61						
1909.88	27.08						
1907.90	27.58						
1905.96	28.08						
1903.50	28.70						
1900.38	29.49						

Table B3: PAD 65 Hammer Core 1. Interpolated and extrapolated values highlighted in grey.

CRS Raw Date	Date Error	Total ^{210}Pb (dpm/g)	Total ^{210}Pb (Bq/kg)	^{210}Pb Error (Bq/kg)	^{226}Ra Activity (Bq/kg)	Total dry mass sedimentation (g/cm^2 yr)	Organic matter sed. (g/cm^2 yr)	inorganic matter sed. (g/cm^2 yr)	^{137}Cs (Bq/kg)	^{137}Cs Error
2015.50	0.31	10.74	179.06	15.73	44.87	0.052	0.021	0.031	5.93	2.59
2013.51	0.72	10.73	178.80	16.03	43.47	0.050	0.014	0.036	5.21	2.52
2011.39	1.01	8.45	140.80	9.19	35.23	0.061	0.022	0.038	6.40	1.13
2009.00	1.45	7.31	121.78			0.071	0.020	0.051		
2006.61	1.85	6.27	104.55	7.19	38.35	0.084	0.023	0.061	5.79	0.98
2003.86	2.42	5.28	87.99			0.104	0.027	0.077		
2001.61	2.85	4.40	73.27	5.71	36.90	0.130	0.029	0.102	6.97	0.87

1999.61	3.26	4.63	77.12			0.111	0.020	0.090		
1997.37	3.73	4.87	81.10			0.095	0.026	0.069		
1995.07	4.24	5.11	85.21			0.081	0.016	0.065		
1991.27	5.14	5.37	89.47	6.26	37.71	0.070	0.015	0.055	10.64	0.95
1986.98	6.19	4.49	74.82			0.097	0.020	0.077		
1982.63	7.16	3.71	61.87	7.05	42.51	0.144	0.017	0.127	8.86	1.44
1979.66	7.81	3.41	56.89			0.148	0.012	0.136		
1976.75	8.65	3.13	52.19	3.84	38.36	0.161	0.021	0.140	20.25	0.77
1974.52	9.10	3.09	51.56			0.217	0.024	0.193		
1972.58	9.45	3.06	50.94	4.38	45.00	0.317	0.029	0.288	23.70	0.97
1970.86	9.57	2.86	47.71			0.281	0.029	0.251		
1968.61	9.97	2.68	44.63	4.08	37.88	0.251	0.058	0.193	9.57	0.79
1964.82	10.72	2.90	48.30			0.130	0.014	0.116		
1955.05	14.10	3.13	52.16	4.46	32.38	0.071	0.011	0.060	10.50	0.81
1946.85	16.19	3.07	51.25			0.066	0.009	0.057		
1940.84	18.32	3.02	50.34			0.067	0.008	0.058		
1933.19	17.98	2.97	49.44			0.073	0.012	0.061		
1927.59	19.48	2.91	48.56	4.10	41.95	0.079	0.016	0.063	4.08	0.70
1923.44		2.87	47.84							
1918.07		2.83	47.13							
1912.77		2.79	46.42							
1905.79		2.74	45.72	4.24	41.85				1.10	0.60
1900.22		2.71	45.20							
1893.90		2.68	44.68	3.59	44.45				-0.32	1.94
1887.70		2.65	44.23							
1881.95		2.63	43.77							
1876.59		2.60	43.32							
1870.06		2.57	42.88	3.73	37.66				-0.96	0.82
1864.02		2.55	42.46							
1856.31		2.52	42.04							
1848.70		2.50	41.63							
1841.84		2.47	41.22	3.72	31.57				-1.04	0.80
1834.72		2.33	38.81							
1826.82		2.19	36.49							
1819.62		2.06	34.27							
1812.37		1.93	32.14	3.54	31.44				-0.98	0.82
1804.48		2.10	34.99							
1796.02		2.28	38.00							

1787.95		2.47	41.19							
1780.30		2.67	44.54	4.29	41.75				-0.17	3.18
1772.87		2.49	41.43							
1764.33		2.31	38.47	3.45	50.97				0.03	0.08
1755.64		2.28	37.93							
1747.84		2.24	37.39	3.40	38.10				-0.03	0.09
1738.79		2.24	37.28							
1730.31		2.23	37.16	3.41	36.77				-0.45	1.17

Table B4: PAD 67 Hammer Core 2. Interpolated and extrapolated values highlighted in grey.

CRS Raw Date	Date Error	Total ^{210}Pb (dpm/g)	Total ^{210}Pb (Bq/kg)	^{210}Pb Error (Bq/kg)	^{226}Ra Activity (Bq/kg)	Total dry mass sedimentation (g/cm^2 yr)	Organic matter sed. (g/cm^2 yr)	inorganic matter sed. (g/cm^2 yr)	^{137}Cs (Bq/kg)	^{137}Cs Error
2014.43	0.71	7.70	128.25	10.23	40.58	0.074	0.021	0.053	12.49	1.13
2012.02	1.5	6.37	106.20	9.64	44.45	0.098	0.028	0.070	13.57	1.18
2008.78	2.36	6.67	111.12	10.41	35.51	0.074	0.020	0.054	13.32	1.24
2004.84	3.34	6.57	109.55	10.59	33.40	0.065	0.017	0.048	10.92	1.22
2000.59	4.51	6.52	108.60	9.47	40.27	0.064	0.017	0.047	11.60	1.12
1995.80	6.08	6.41	106.85	9.81	43.91	0.060	0.016	0.045	12.86	1.18
1990.91	7.61	5.53	92.09	10.10	48.45	0.074	0.019	0.055	11.95	1.27
1987.14	8.64	4.60	76.65	9.28	49.59	0.103	0.026	0.077	11.81	1.21
1982.76	10.95	4.90	81.65	8.58	44.35	0.068	0.016	0.053	12.79	1.12
1977.77	12.64	4.12	68.61	8.41	46.84	0.098	0.023	0.075	13.23	1.14
1974.37	13.47	3.96	66.03	8.44	53.40	0.148	0.036	0.112	13.67	1.16
1970.42	15.85	4.50	75.05	8.46	52.18	0.075	0.018	0.057	11.84	1.12
1964.92	18.71	3.94	65.59	8.56	46.35	0.076	0.016	0.060	11.89	1.14
1961.05	18.67	3.78	62.95	9.09	57.01	0.206	0.044	0.162	11.94	1.23
1957.67	20.56	4.02	67.05	6.92	55.18	0.097	0.021	0.076	10.57	0.93
1953.09	21.82	3.69	61.57	7.98	52.16	0.105	0.023	0.082	11.85	1.08
1948.07	21.34	3.42	57.00	10.43		0.087	0.018	0.070		
1941.77		3.16	52.68	6.73	42.33				8.24	0.89
1933.97		3.06	50.98	9.51						
1925.35		2.96	49.32	6.72	53.34				6.51	0.87
1916.60		2.92	48.63	9.12						
1908.11		2.88	47.95	6.16	45.20				1.45	0.78
1899.89		3.02	50.26	8.69						
1892.12		3.16	52.64	6.13	50.46				0.08	0.80
1884.61		2.72	45.30	9.02						

1878.07		2.32	38.67	6.62	49.08				-0.19	0.85
1872.60		2.57	42.78	9.02						
1867.36		2.83	47.17	6.14	43.19				0.15	0.84
1862.94										
1856.68										
1848.42										
1840.62										
1832.18										
1821.18										
1809.86										
1800.38										
1791.08										
1780.96										
1769.77										
1758.28										
1744.92										
1728.88										
1713.89										
1700.50										
1686.35										
1671.28										
1655.19										
1638.98										
1623.60										
1608.83										
1594.70										
1577.39										
1561.34										
1548.52										
1535.64										
1522.82										

Appendix C: Raw Metals concentrations

Table C1: PAD 65 Hammer Core 1. All metals concentrations in µg/g and sample depth in centimetres.

Depth	Al	Be	Cd	Cr	Cu	Pb	Li	Ni	Ti	V	Zn	Zr
0	6500	0.44	0.316	10.1	18.1	8.06	9.9	20.8	9.7	21.3	66.1	1.9
1	8410	0.46	0.322	12.5	17.1	8.25	10.9	21.5	19.5	24.9	65.3	2
2	8960	0.53	0.393	13.8	26.9	9.57	12.8	23.8	24.5	26.8	78.2	2.3
3	11100	0.64	0.461	18.2	22.2	10.7	14.8	27.7	27.6	34.8	83.8	3.9
4	10600	0.66	0.447	17.7	22.2	11.1	14.6	28.7	30.3	34.8	80.8	3.4
5	12600	0.73	0.53	22	25.6	12.2	17.2	32.5	32.8	40.7	94.2	4.9
6	12300	0.68	0.501	20.7	74	14.4	16.4	31.2	26.5	38.7	120	5.3
7	11900	0.64	0.451	19.3	22.1	11	15	28.5	23.9	36.4	83.4	3.7
8	9660	0.53	0.414	15.6	20.1	10.1	12.6	25.7	21.7	29.4	76.7	3.5
9	11200	0.6	0.441	17.6	21.2	10.7	14	27.6	22.6	32.8	81.4	3.9
10	10200	0.63	0.459	17.2	22.7	11.1	14.8	28.3	24.3	33.4	81.4	3.2
11	14000	0.73	0.515	22.6	25.9	13.1	17.9	32	32.6	42.3	98.2	3.4
12	13000	0.74	0.522	22.2	26.3	13.6	18.2	32.1	26.9	39.4	100	5.8
13	13700	0.76	0.514	22.2	27.6	13.6	18.7	32.7	14.5	38.6	103	5.3
14	13900	0.87	0.574	24	46	14.8	21	34.4	19.2	42.5	116	5.7
15	12900	0.78	0.576	22.9	28.8	14.1	18.9	34.2	34.2	39.1	107	5
16	11000	0.72	0.577	22.9	27.8	13.2	17	34.3	20.5	36.9	102	5.6
17	12800	0.75	0.58	21.9	27.4	13.1	17.7	31.9	22.9	39.1	101	6.3
18	11900	0.72	0.576	20.5	28.1	13.4	16.7	33.1	19.6	37.8	102	6.8
19	13400	0.8	0.616	23.3	29.1	14	18.9	34.5	34.1	43.2	107	7.2
20	12800	0.74	0.594	22.6	28.1	13.4	18.3	33.6	30.7	40.5	104	6.5
21	12900	0.73	0.585	22.1	28.8	13.5	17.5	34.4	25	41	105	7
22	13000	0.76	0.597	21.7	29.7	13.9	17.1	35.5	22.2	41.1	106	7.7
23	12200	0.79	0.611	21.7	30.1	13.8	17.7	36.2	21.8	41.5	107	7.7
24	11500	0.74	0.616	21	29.7	13.6	17	35.3	20.8	39.7	109	7.6
25	12400	0.78	0.643	22	30.3	13.7	17.8	36.3	28.2	42.6	107	7.2
26	12800	0.81	0.593	22.6	30.2	13.7	19	35.3	29.6	41.9	108	7.3
27	13000	0.78	0.624	23.1	30.1	14	19	35.9	29.5	40.8	108	7.3
28	12100	0.77	0.596	22	29.3	13.8	18.1	34.1	28.4	39.4	105	7
29	11500	0.67	0.584	20.1	27.3	12.8	16.3	32.5	24.9	35.3	99.9	6.8
30	10900	0.66	0.533	18.7	26.4	11.7	15.4	30.7	19.5	33.8	95.2	6.9
31	11200	0.65	0.528	18.7	25.9	11.7	15.5	30	23.5	34.6	92.7	6.9
32	10000	0.64	0.548	18	24.8	11	15.4	28.5	27.2	33.2	90.3	6.5
33	10800	0.68	0.676	18.2	25.3	11.2	16.2	29.3	19.8	33.8	92.8	6.9
34	10400	0.6	0.536	19.2	25.3	11	13	29.6	26	35.6	91.8	7.2
35	10700	0.62	0.571	19.4	25.9	11.5	13.5	31	28.3	36	93.6	7.3
36	10500	0.58	0.566	18.9	25.1	13.3	12.7	29.9	26.1	35.8	91.3	6.9

37	10400	0.57	0.498	18.4	24.6	11	12.3	29.8	21.7	34.4	89	6.9
38	9360	0.58	0.526	17.8	24.9	11.1	12	29.6	25.3	33.5	90.3	6.9
39	10100	0.62	0.524	18.3	25.6	11.4	13.1	30.6	23.5	34.3	91.2	7.2
40	11400	0.62	0.511	19.4	25.3	11.5	13	30.2	33.4	36.6	90.7	6.9
41	11400	0.65	0.527	19.6	25.4	11.5	14	30.7	29.8	37.4	92.6	7
42	11100	0.62	0.517	19.7	25.1	11.2	13.3	30.6	34.8	37.5	91.8	6.8
43	11500	0.68	0.568	20.8	26.4	11.3	14.5	31.8	34.1	38.6	95.5	4.9
44	10800	0.64	0.553	19.1	26.2	11.4	14.3	31.1	16.9	33.6	95	6.4
45	10400	0.66	0.473	17.9	23.4	12.2	14.7	27.2	29.8	32.6	84.8	6.7
46	9890	0.58	0.458	17.7	22.6	10.1	12.9	26.3	31.9	32.8	81.7	6
47	12100	0.66	0.581	22.2	28.2	12.2	14.6	32.7	36.4	40.8	102	7.4
48	12300	0.61	0.563	22.1	27.6	11.7	13.8	32.2	33.2	40.3	98.7	7.2
49	10400	0.65	0.526	19.1	24.5	11.5	14.8	28.7	30.5	34.9	88.3	6.8
50	11500	0.75	0.525	20.1	25.5	13.1	17.1	29.7	33.2	36.1	92.1	7.8
51	10200	0.95	0.475	18.4	23.5	18	20.3	27.3	38.5	34.3	83.2	10.8
52	11600	0.64	0.544	21.4	27	11.9	13.8	31.5	39.6	39.3	96	7.1
53	12800	0.74	0.561	22.5	28.8	11.9	16.4	33.2	36.4	41.6	103	7.4

Table C2: PAD 66 Hammer Core 2. All metals concentrations in µg/g and sample depth in centimetres.

Depth	Al	Be	Cd	Cr	Cu	Pb	Li	Ni	Ti	V	Zn	Zr
0	8840	0.52	0.529	16.8	19.8	9.97	11.2	26.6	40.6	29.6	82.9	3.7
1	8360	0.47	0.467	16.6	18.1	9.46	9.4	25.2	38.3	29.7	80.1	3.8
2	12500	0.74	0.563	22.4	27.1	12.8	15.2	32.9	27.7	39.9	107	5.5
3	12500	0.77	0.584	23	28.5	13.7	15.9	34.5	24.8	39.5	112	5.4
4	13000	0.76	0.551	22.8	28.2	13.9	16.5	33.2	33.7	40.9	107	6.3
5	12000	0.68	0.547	21.5	27.3	13.1	14.2	32.3	35.4	37.9	104	6.3
6	12300	0.67	0.524	22.4	28.5	13.2	14.9	33.5	38.1	39	106	6.5
7	12300	0.73	0.615	21.9	27.4	13	14.8	33.8	30.2	40.2	108	5.1
8	11200	0.64	0.569	20.3	25.6	13.2	13.6	31.4	28.2	36.9	104	4.5
9	13300	0.77	0.548	22.8	27.7	14	16.2	35.2	32.4	40.3	109	6.4
10	15500	0.89	0.527	25.9	29.7	15.1	18.6	37.4	22.8	45.1	114	6.7
11	14600	0.9	0.525	25	29.5	14.8	17.9	35.1	24.9	42.2	111	6.5
12	12900	0.77	0.64	23.6	28	14.3	15.9	34.9	26.9	42.9	118	5.2
13	13200	0.75	0.568	23.2	29.4	14.4	16.6	35	24.4	41.3	111	5.8
14	11800	0.69	0.52	21.1	26.1	13.3	15	32.6	32.1	37.8	103	5.9
15	9240	0.53	0.54	17.4	20.3	10	11.1	25.7	45.5	32.1	84.6	4.4
16	11500	0.66	0.548	20.8	24.1	12.4	13.5	30.2	31.8	38	99.5	4.6
17	11000	0.67	0.591	20.9	24.8	13.2	13.9	31.6	37.6	38.5	102	4.8
18	12700	0.68	0.545	22	25.9	13	15	31.9	47.2	40	103	6.4
19	10300	0.57	0.524	18.4	22.8	11.5	12.2	27.8	50	33.3	90.9	5.7

20	10100	0.56	0.551	18	22.9	11.2	11	28.1	43.3	32.6	89.9	5.8
21	10015	0.61	0.553	18.7	24	11.6	12.7	29.3	51.8	33.9	91.0	6.5
22	9890	0.54	0.533	18.2	21.8	10.8	11.8	27.2	33.6	32.3	88.6	5.8
23	12300	0.69	0.555	21.4	25.4	11.8	14.4	31.3	45.1	39.3	100	6.4
24	12300	0.68	0.525	22	25.1	12.5	14.6	31.7	50.3	40.7	103	6
25	11400	0.62	0.54	20.7	22.5	11.2	13.5	29	45.7	37.5	94.9	5.7
26	13100	0.71	0.566	22.7	25.1	12.8	15.2	32.4	37.4	42.8	104	4.7
27	12900	0.69	0.594	22.4	26.9	12.9	14.6	33.7	34	40.9	112	5
28	11300	0.62	0.568	20.9	23.9	11.9	13.7	30.4	41.5	37.8	98.6	5.7
29	11100	0.61	0.581	21	23.9	11	13	30.7	49.4	37.8	98.6	5.3
30	14200	0.83	0.713	25.1	29.5	14.6	16.5	39.1	34.7	46.9	123	4.9
31	13500	0.7	0.705	23.9	28.7	14.2	14.6	36.5	31.7	44.5	118	4.2
32	13150	0.71	0.703	23.5	28.2	14.0	14.7	35.6	33.8	44.2	115.5	4
33	12700	0.72	0.728	23.5	30	14.5	14.1	38.7	27.6	43.7	123	3.7
34	11300	0.71	0.719	21.1	27.3	13.6	13.8	34.9	25.3	38.4	114	3.4
35	12300	0.78	0.666	21.5	27.5	14.2	14.8	34.1	23.6	39.7	112	3.7
36	14100	0.8	0.722	23.6	35.1	15.5	15.3	36.6	24.1	43.8	118	4.2
37	13400	0.77	0.716	22.7	28.5	14.4	14.3	34.5	29.2	42	114	4
38	14400	0.84	0.677	23.7	28.1	15	15.5	34.9	37.8	43.7	110	4.8

Table C3: PAD 67 Hammer Core 2. All metals concentrations in µg/g and sample depth in centimetres.

Depth	Al	Be	Cd	Cr	Cu	Pb	Li	Ni	Ti	V	Zn	Zr
0	10900	0.75	0.684	20.4	32.8	14.4	15.7	38.4	30	39.4	120	4.5
1	12800	0.88	0.777	22.9	33.7	15	19.7	41.5	25.2	44.4	132	6.5
2	13600	0.9	0.827	24.1	34.8	15.3	19.2	43	27.2	47.4	140	6.8
3	13000	0.88	0.783	23.7	33.7	15.3	19.5	42.1	29.4	46.7	134	6.4
4	17000	1.07	1.01	29.6	42.3	17.6	23.4	52.1	39.9	59.1	168	8.1
5	13100	0.81	0.778	22.7	32.9	13.9	16.8	40.3	25.7	45.1	131	6.6
6	14500	0.88	0.8	25	36	15.4	19	44	27	48.2	139	7.5
7	15400	0.99	0.862	26.9	38.1	16.3	22.3	46.9	26.1	52.6	151	8.3
8	15100	0.93	0.803	26.1	36.8	15.6	21.6	44.5	32.9	52.6	146	8
9	15500	0.95	0.807	27	36.9	16.8	22.4	44.8	31.9	52.5	141	7.5
10	16100	0.98	0.901	28.7	39.9	16.8	22.5	49.3	29	56	157	8.3
11	15600	0.96	0.839	27	36.9	15	22.6	46	29.2	52.5	149	8.4
12	16900	1.03	0.909	30.1	42.4	17.4	23.8	51.1	30	58.4	163	9.1
13	16400	0.96	0.847	28.9	39.8	16.5	22	48.1	32	56.4	158	8.4
14	17300	1	0.895	29.9	41.2	16.8	22.8	50.5	29.1	57.2	160	8.9
15	16200	0.97	0.844	28.5	38.3	16.1	23.8	46.1	36.1	54.4	151	8.5
16	16300	1	0.777	28.5	37.5	16.1	23.7	45.8	33.4	53.8	147	8.4

17	17900	1.06	0.767	31.3	38.3	16.5	25.9	45.6	28.4	56	154	8.9
18	18900	1.05	0.699	32.6	38.4	16.1	26.1	45	40.4	58.7	153	8.8
19	17900	0.99	0.652	30	35.4	15.2	24.7	42.8	35.2	54.8	139	8.6
20	15400	0.87	0.593	26.6	32	13.7	20.7	39.5	30	49.2	126	7.5
21	20300	1.16	0.809	34.6	40.9	17.6	27.6	50.8	39.8	65.6	163	10
22	16300	1.03	0.782	28.7	36	16.6	24.4	46.1	27.8	54.2	147	7.5
23	16500	0.99	0.817	29.4	36.4	16.3	23.1	47.1	23.1	56.3	150	8.4
24	16300	0.98	0.807	28.7	32.7	15.3	23.6	42.4	28.5	57.8	137	6.3
25	15200	0.96	0.772	27.8	33.6	14.8	21.2	49.9	31.7	56.8	141	8.7
26	11200	0.75	0.55	19.7	24.7	11.2	15.8	35.2	27.1	40.1	102	6.7
27	10800	0.71	0.497	19.5	23.5	10.8	15.3	34.8	36.2	39.5	96.5	6.5
28	10100	0.66	0.485	18.5	22.9	10.4	14.6	31.8	33.6	37.6	92.4	6.4
29	10300	0.7	0.51	18.3	23.3	10.4	16.1	31.3	24	35.5	93.5	6.3
30	13500	0.8	0.607	24	28.1	12.8	17.7	39.2	43.7	46.9	113	7.7
31	11800	0.74	0.529	20.1	26.5	11.3	16.9	34	32.3	40.9	95.9	7
32	16500	0.95	0.699	29.2	33.9	14.7	24.5	43.8	45.7	55.8	128	9.2
33	16400	0.93	0.721	28.9	33	14.7	22.9	42.9	52.1	55.5	124	8.3
34	15300	0.9	0.72	27.5	32.6	15.3	22.4	43.2	39.1	52.8	126	9.1
35	16400	0.92	0.671	29.2	34.4	14.6	22.3	44.9	36.1	54.6	130	9.5
36	18700	1.07	0.713	32.5	38.3	16.4	25.9	47.7	34.4	61.3	145	9.8
37	16000	0.96	0.628	27.9	33.9	15.7	24.1	39.4	24	50.5	126	9.5
38	16100	0.91	0.719	28	33.9	14.9	23.5	42.7	27.5	53.3	136	8.3
39	12300	0.74	0.607	22.1	26.6	12.3	17.5	32.2	35.1	41.4	104	6.9
40	13600	0.77	0.648	24.2	28.9	13.3	19.6	34.5	52.6	46.5	110	7.2
41	14900	0.85	0.733	27	32	15	20.8	38.9	46.5	50.9	120	7.8
42	15600	0.93	0.755	27.9	34.6	15.6	24.2	42.3	37.6	52.9	134	8.5
43	15500	0.9	0.724	27.8	33.8	15.5	21.7	39.4	38.6	51.4	127	7.3
44	18400	1	0.799	30.6	35.6	16.4	24.9	41.2	42.9	56.4	138	7.5
45	17400	0.95	0.714	28.8	33.2	15.6	23.9	39.5	41.6	53.5	127	7.8
46	18900	1.04	0.82	33.3	37.3	17.8	25.6	45	48	60.1	145	8.5
47	15900	0.94	0.683	27.8	32.1	15.7	22.3	38.5	32.4	50.9	124	8.6
48	19900	1.08	0.796	33.2	38.8	17.2	26.5	46.3	43.3	61.1	149	9.1
49	20400	1.13	0.835	35.3	40.6	18.8	28.3	50.1	42.8	65.6	156	10.4
50	19600	1.15	0.81	34.3	39.6	18.1	27.9	47	43.4	63.2	152	10
51	16300	0.9	0.759	27.8	34.6	16.1	22.2	40.6	37.6	49.6	131	6.9
52	16500	0.91	0.705	29.2	33.8	15.9	23.2	39.1	59.9	53.2	125	9.5
53	15100	0.9	0.706	27.4	33.2	15.1	20.9	40.9	51.9	52.8	122	9.7
54	13900	0.77	0.619	24.9	29.6	13.2	19.7	35.7	47.7	46.8	109	8.6
55	11700	0.71	0.549	21.6	26	12.3	17.3	31.7	39.6	40.4	97.3	7.7

Appendix D: Metals Enrichment factors

Table D1: PAD 65 Hammer Core 1

Depth	PbEF	NiEF	VEF	ZnEF	BeEF	CdEF	CrEF	CuEF
0	1.22	1.18	0.99	1.22	1.14	1.04	0.88	1.26
1	0.97	0.94	0.89	0.93	0.92	0.82	0.84	0.92
2	1.05	0.98	0.90	1.05	0.99	0.94	0.87	1.36
3	0.95	0.92	0.94	0.91	0.97	0.89	0.93	0.90
4	1.03	1.00	0.99	0.92	1.05	0.90	0.94	0.95
5	0.95	0.95	0.97	0.90	0.97	0.90	0.99	0.92
6	1.15	0.94	0.95	1.17	0.93	0.87	0.95	2.72
7	0.91	0.88	0.92	0.84	0.90	0.81	0.92	0.84
8	1.03	0.98	0.92	0.95	0.92	0.92	0.91	0.94
9	0.94	0.91	0.88	0.87	0.90	0.84	0.89	0.85
10	1.07	1.02	0.99	0.96	1.04	0.96	0.95	1.01
11	0.92	0.84	0.91	0.84	0.88	0.79	0.91	0.84
12	1.03	0.91	0.91	0.92	0.96	0.86	0.97	0.91
13	0.98	0.88	0.85	0.90	0.93	0.80	0.92	0.91
14	1.05	0.91	0.92	1.00	1.05	0.88	0.98	1.49
15	1.08	0.98	0.91	1.00	1.02	0.95	1.00	1.01
16	1.18	1.15	1.01	1.11	1.10	1.12	1.18	1.14
17	1.01	0.92	0.92	0.95	0.99	0.97	0.97	0.97
18	1.11	1.03	0.96	1.03	1.02	1.03	0.97	1.07
19	1.03	0.95	0.97	0.96	1.00	0.98	0.98	0.98
20	1.03	0.97	0.95	0.98	0.97	0.99	1.00	0.99
21	1.03	0.98	0.96	0.98	0.95	0.97	0.97	1.01
22	1.05	1.01	0.95	0.98	0.98	0.98	0.94	1.03
23	1.11	1.10	1.02	1.05	1.09	1.07	1.01	1.11
24	1.16	1.13	1.04	1.14	1.08	1.14	1.03	1.17
25	1.09	1.08	1.04	1.04	1.06	1.11	1.00	1.10
26	1.05	1.02	0.99	1.01	1.06	0.99	1.00	1.07
27	1.06	1.02	0.95	1.00	1.01	1.03	1.00	1.05
28	1.12	1.04	0.98	1.04	1.07	1.05	1.03	1.09
29	1.09	1.04	0.92	1.04	0.98	1.08	0.99	1.07
30	1.06	1.04	0.93	1.05	1.02	1.04	0.97	1.09
31	1.03	0.99	0.93	1.00	0.98	1.01	0.94	1.04
32	1.08	1.05	1.00	1.09	1.08	1.17	1.02	1.12
33	1.02	1.00	0.94	1.03	1.06	1.34	0.95	1.06
34	1.04	1.05	1.03	1.06	0.97	1.10	1.04	1.10
35	1.06	1.07	1.01	1.05	0.97	1.14	1.02	1.09
36	1.25	1.05	1.03	1.05	0.93	1.15	1.02	1.08

37	1.04	1.06	1.00	1.03	0.92	1.02	1.00	1.07
38	1.17	1.17	1.08	1.16	1.04	1.20	1.07	1.20
39	1.11	1.12	1.02	1.09	1.03	1.11	1.02	1.14
40	0.99	0.98	0.97	0.96	0.91	0.96	0.96	1.00
41	0.99	0.99	0.99	0.98	0.96	0.99	0.97	1.01
42	0.99	1.02	1.02	0.99	0.94	0.99	1.00	1.02
43	0.97	1.02	1.01	1.00	0.99	1.05	1.02	1.04
44	1.04	1.06	0.94	1.06	1.00	1.09	1.00	1.10
45	1.15	0.97	0.94	0.98	1.07	0.97	0.97	1.02
46	1.00	0.98	1.00	0.99	0.99	0.99	1.01	1.03
47	0.99	1.00	1.02	1.01	0.92	1.03	1.04	1.05
48	0.94	0.97	0.99	0.96	0.83	0.98	1.02	1.01
49	1.09	1.02	1.01	1.02	1.05	1.08	1.04	1.06
50	1.12	0.95	0.95	0.96	1.10	0.97	0.99	1.00
51	1.74	0.99	1.01	0.98	1.57	0.99	1.02	1.04
52	1.01	1.00	1.02	1.00	0.93	1.00	1.04	1.05
53	0.91	0.96	0.98	0.97	0.97	0.94	0.99	1.02

Table D2: PAD 67 Hammer Core 2

Depth	PbEF	NiEF	VEF	ZnEF	BeEF	CdEF	CrEF	CuEF
0	1.30	1.30	1.09	1.32	1.16	1.34	1.06	1.36
1	1.15	1.20	1.05	1.24	1.16	1.30	1.01	1.19
2	1.11	1.17	1.05	1.24	1.11	1.30	1.00	1.16
3	1.16	1.20	1.08	1.24	1.14	1.29	1.03	1.17
4	1.02	1.13	1.05	1.19	1.06	1.27	0.98	1.12
5	1.04	1.14	1.04	1.20	1.04	1.27	0.98	1.13
6	1.04	1.12	1.00	1.15	1.02	1.18	0.97	1.12
7	1.04	1.12	1.03	1.18	1.08	1.20	0.99	1.12
8	1.02	1.09	1.05	1.16	1.04	1.14	0.98	1.10
9	1.07	1.07	1.02	1.09	1.03	1.11	0.98	1.08
10	1.03	1.13	1.05	1.17	1.02	1.20	1.01	1.12
11	0.95	1.09	1.01	1.15	1.03	1.15	0.98	1.07
12	1.01	1.12	1.04	1.16	1.02	1.15	1.01	1.13
13	0.99	1.08	1.04	1.16	0.98	1.10	1.00	1.10
14	0.96	1.08	1.00	1.11	0.97	1.10	0.98	1.08
15	0.98	1.05	1.01	1.12	1.01	1.11	0.99	1.07
16	0.97	1.04	0.99	1.08	1.03	1.02	0.99	1.04
17	0.91	0.94	0.94	1.03	1.00	0.92	0.99	0.97
18	0.84	0.88	0.94	0.97	0.93	0.79	0.97	0.92
19	0.84	0.88	0.92	0.93	0.93	0.78	0.95	0.89

20	0.88	0.95	0.96	0.98	0.95	0.82	0.98	0.94
21	0.85	0.92	0.97	0.97	0.96	0.85	0.96	0.91
22	1.00	1.04	1.00	1.08	1.06	1.02	1.00	1.00
23	0.97	1.05	1.03	1.09	1.01	1.06	1.01	1.00
24	0.92	0.96	1.07	1.01	1.01	1.06	1.00	0.91
25	0.96	1.21	1.13	1.12	1.06	1.08	1.03	1.00
26	0.98	1.16	1.08	1.10	1.13	1.05	0.99	1.00
27	0.98	1.19	1.10	1.07	1.11	0.98	1.02	0.98
28	1.01	1.16	1.12	1.10	1.10	1.03	1.04	1.02
29	0.99	1.12	1.04	1.09	1.14	1.06	1.00	1.02
30	0.93	1.07	1.05	1.01	1.00	0.96	1.00	0.94
31	0.94	1.06	1.04	0.98	1.05	0.96	0.96	1.01
32	0.88	0.98	1.02	0.93	0.97	0.90	1.00	0.93
33	0.88	0.97	1.02	0.91	0.95	0.94	1.00	0.91
34	0.98	1.04	1.04	0.99	0.99	1.01	1.02	0.96
35	0.88	1.01	1.00	0.95	0.94	0.87	1.01	0.95
36	0.86	0.94	0.99	0.93	0.96	0.81	0.98	0.93
37	0.97	0.91	0.95	0.95	1.01	0.84	0.99	0.96
38	0.91	0.98	1.00	1.02	0.95	0.95	0.98	0.95
39	0.98	0.97	1.01	1.02	1.01	1.05	1.02	0.98
40	0.96	0.94	1.03	0.97	0.95	1.02	1.01	0.96
41	0.99	0.96	1.03	0.97	0.96	1.05	1.02	0.97
42	0.98	1.00	1.02	1.03	1.00	1.03	1.01	1.00
43	0.98	0.94	1.00	0.99	0.98	1.00	1.01	0.98
44	0.88	0.83	0.92	0.90	0.91	0.93	0.94	0.87
45	0.88	0.84	0.93	0.88	0.92	0.88	0.94	0.86
46	0.93	0.88	0.96	0.92	0.93	0.93	1.00	0.89
47	0.97	0.89	0.96	0.94	0.99	0.92	0.99	0.91
48	0.85	0.86	0.93	0.90	0.91	0.85	0.94	0.88
49	0.91	0.91	0.97	0.92	0.93	0.87	0.98	0.90
50	0.91	0.89	0.97	0.93	0.99	0.88	0.99	0.91
51	0.97	0.92	0.92	0.97	0.93	0.99	0.96	0.96
52	0.95	0.87	0.97	0.91	0.93	0.91	1.00	0.93
53	0.98	1.00	1.05	0.97	1.00	1.00	1.03	0.99
54	0.93	0.95	1.01	0.94	0.93	0.95	1.01	0.96
55	1.03	1.00	1.04	1.00	1.02	1.00	1.04	1.00